Investigating the role of nuclear myosin I in the low serum induced repositioning of chromosome 10 in interphase nuclei

Thesis submitted for the degree of

Master of Philosophy

at Brunel University, West London

by

Manelle Amira

Division of Bioscience

School of Health Sciences and Social Care

Brunel University, West London

September 2009

Abstract

The nucleus of mammalian cells has been proven to be highly organised. A recent study on interphase chromosome positioning has identified low serum induced rapid chromosome repositioning. Chromosome 10 initially localised at an intermediate position in normal proliferating human dermal fibroblasts (HDF) was found to relocate to the nuclear periphery 15 minutes after the cells have been incubated in low serum. Whereas chromosome X has remained in a peripheral position. The relocation of chromosome 10 has been shown to be dependant on both actin and myosin functions. In this project we have further investigated the possible role of nuclear myosin I in chromosome 10 repositioning. Using siRNA to block the expression of the nuclear myosin I (NMI) we were able to identify this nuclear myosin as necessary for the rapid repositioning of chromosome 10. Furthermore, using image analysis software we investigated the effect of the NMI knock down on the overall nuclear size and shape. The analysis has revealed that while the nuclear size of normal proliferating cells remained unchanged after the low serum incubation both in cells expressing the NMI and NMI depleted cells, the knock down of the NMI seems to have affected the nuclear shape when the cells were subjected to the serum incubation. On the other hand, the analysis of the chromosome territories area has revealed significant differences in the chromosome territories sizes before and after the low serum incubation, in normal proliferating HDF cells .

Acknowledgements

I would first of all like to express my sincere thanks to my supervisors; Dr. Joanna Bridger, not only for her advice and guidance during this research, but for all her encouragement and support, Dr. Amanda Harvey for her support and valuable input throughout this project.

I would like to acknowledge The School of health sciences and social care for proving funding for this project's consumables.

My thanks also go to Ishita Mehta for her FISH images and help, Lauren, Ed and Raj for their help and friendliness. As it is impossible to acknowledge everyone, I would like to thank all those who have contributed, in any way, to this research.

My deepest gratitude goes to my loving husband for his patience and support, all my family and friends for their constant encouragement, love and for the never failing confidence they have in me.

Finally and above all, I shall express all praises to God, as it was with his help, that I was able to complete this work.

List of Abbreviations

2D	Two dimentional
2DD	Human dermal fibroblast cell line
2G2	Anti actin antibody 1999 Gonsior, S.M. et al
ATP	Adenosine triphosphate
BAF	BRG-associated factor
BAP	Brm-associated protein
C02	Carbon dioxide
cm	Centimeter
CT	Chromosome territory
Cy3	Cyanine 3
DAPI	4, 6-Diamidino-2-phenylindole
DFC	Dense fibrillar component
D-MEM	Delbeco's modified Eagles Medium
DNA	Deoxyribonucleic acid
EDTA	Ethylenediamenetetra- acetic acid
Exp6	Exportin 6
FC	Fibrillar centre
FISH	Fluorescence in situ hybridisation
FRAP	Fluorescence recovery after photo bleaching
G1	Gap phase 1
GC	Granular centre
HDF	Human dermal fibroblast
hnPNP	Hetero nuclear ribonucleoproteins

KCl	Potassium Chloride
KDa	Kilo Dalton
MDa	Mega Dalton
NCS	Newborn calf serum
NES	Nuclear export signal
NLS	Nuclear Localisation Signal
NMI	Nuclear myosin I
NuA4	Nucleosomal acetyltransferase of histone 4
PHA	Phytohemagglutinin
rDNA	Ribosomal DNA
RNA	Ribonucleic acid
rpm	Rotations per minute
S	DNA synthesis phase of the cell cycle
siRNA	Small interfering RNA
snRNP	Small nuclear ribonucleoprotein
SSC	Sodium Saline Citrate
SWI/SNF	The switch mating type/sucrose non-fermenting
WSTF	Williams Syndrome Transcription Factor

Contents

List of Figures

List of Tables

Chapter 1

Introduction

1.1 Architecture of the nucleus

The eukaryotic cell nucleus, figure 1.1 houses most of the genetic material of the cell. It accommodates all the materials and structures necessary for genome replication and DNA repair, timely control of gene expression and processing of transcripts. To perform these functions efficiently, the nucleus is extremely well organised with several individual nuclear structures providing architecture to maintain the nuclear integrity and participate in nuclear processes (Foster & Bridger 2005).

1.1.1 Nuclear envelope

The nuclear envelope (NE) surrounds the nucleus, and consists of two sheets of membrane with a lumen, with the inner and outer membranes connecting only at the nuclear pores (Voeltz, et al., 2002). It serves in the transit of materials between the nucleus and cytoplasm (Stoffler, et al., 1999). The nuclear pore complexes are highly complex structures that selectively regulate the transit of larger molecules in both directions, they allow the free passage of small molecules, whereas, above 50 kilodaltons molecular weight, only "nuclear" proteins are allowed in the nucleus (Laskey, 1987).

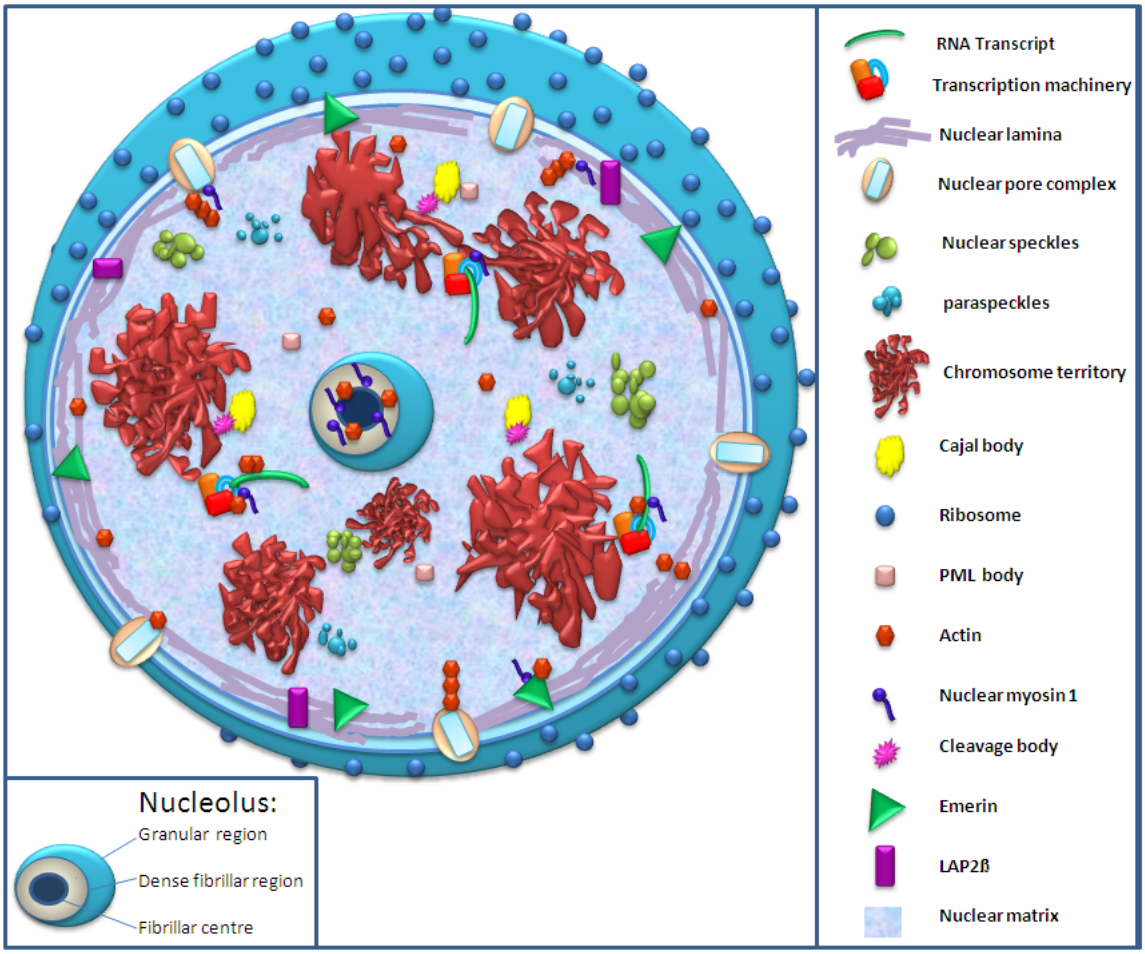

Figure 1.1: **Cartoon showing the nuclear architecture**
This cartoon representation of the nucleus shows some of the actin and myosin identified locations and interactions, inluding; transcription machinery, nuclear pore complex, nucleolus, emerin and nuclear lamina.

1.1.2 Chromatin and Chromosomes

Different patterns of interphase chromosome organization have been identified in functionally distinct cell types (Manuelidis & Borden 1988). In the nucleus of mammalian cell, the chromatin exists in the form of chromosome territories that can be visualized by fluorescence in situ hybridization (FISH) using whole-chromosome DNA probes (Misteli & Spector 1998). In these chromosome territories, chromosomal sub-domains have been shown to occupy distinct non random sub-nuclear localization depending on the cell's cycle (Manuelidis, 1984). Chromosomes occupy distinct territories in the cell nucleus with pre-

ferred nuclear locations (Cremer, et al., 2006). Using radial distance measurements Cremer's group has suggested that chromosomes have a probalistic three-dimentional position (Bolzer, et al., 2005) rather than a determinate one as previously concluded by Bickmore group in their studies on chromosome 18 and 19 positioning (Croft, et al., 1999). Cremer et al, found that small chromosomes were distributed significantly closer to the center of the nucleus or prometaphase rosette, while large chromosomes were located closer to the nuclear or rosette rim. This arrangement was confirmed in two cell types with flat-ellipsoidal cell nuclei (human fibroblast and amniotic fluid cell nuclei). in the same study Cremer's group, had reported that gene-poor chromatin domains, formed a layer beneath the nuclear envelope, while gene-enriched domain are found in the nuclear interior (Bolzer, et al., 2005).

Measurements of the chromosome HSA18 and 19 territories, showed areas of HSA18 signals were significantly smaller than those of chromosome 19 despite that their DNA content being 85 Mb and 67 Mb respectively (Croft, et al., 1999). To address whether the spatial organization of the genome affects the gene expression, or whether it is just a reflection of it, Bikemore's group in 2007, have actively induced the rearrangement of some chromosmes to the nuclear periphery by tethering them to the inner nuclear membrane (INM). The repositioning of chromosome 4 and 11 to the nuclear periphery resulted in a down- regulation of some of their active genes, but not all of them, with the expression of genes closer to the tethering point being the most affected (Finlan, et al., 2008).

Cremer, et al., (2000) have proposed a modular and dynamic model for chromosome territory based on three nuclear compartments; an "open" higher-order chromatin compartment, a "closed" chromatin compartment, and an interchromatin domain (ICD) compartment (Zirbel, et al., 1993). While the "open" chromatin compartments contain active genes , "closed" chromatin compartments comprise inactive genes, and the (ICD) includes macromolecular complexes necessary for DNA replication, transcription, splicing, and repair. Only

Genes in "open" compartments would have access to transcription and splicing complexes located in the ICD compartment (Cremer, et al., 2000)

1.1.3 Nuclear bodies

PML nuclear bodies (PML-NBs)

The promyelocytic leukaemia protein (PML) nuclear bodies (NBs), previously known as nuclear domains-10, Kremer bodies and PML oncogenic domains are punctate nuclear structures that are interspersed between chromatin (Melnick & Licht 1999). PML-NBs are present in most mammalian cell nuclei as discrete nuclear foci, 0.2-1.0 μm wide. Depending on the cell type, cell-cycle phase and differentiation stage their number varies between 1 - 30 bodies per nucleus (Dellaire & Bazett-Jones 2004). Despite their uniform appearance, PML-NBs are structurally and functionally heterogeneous and are dynamic structures. Although the main role of PML-NBs seems to be tumour-suppressive (Salomoni & Pandolfi 2002), they have been implicated to have a role in regulating many cellular functions, from inhibiting cell proliferation, to inducing apoptosis and cellular senescence. Along with, maintaining genomic stability and antiviral responses (reviewed by Bernardi & Pandolfi 2007).

Cajal bodies

Cajal bodies are dynamic nuclear bodies of 0.2-1.0 μm in diameter, previously called coiled bodies thought to play a role in small nuclear ribonucleoprotein (snRNP) biogenesis and in the trafficking of snRNPs and snoRNPs (Spector, 2001). The number of cajal bodies present in nuclei is variable during different stages of the cell cycle (Zimber, et al., 2004). They have been shown to associate with histone loci as well as U1, U2 and U3 gene clusters (Matera, 1999). Adjacent to cajal bodies, are found Gems, (gemini of cajal bodies) (Spector, 2001) they are characterized by the presence of the survival of motor neurons gene product (SMN) and an associated factor, Gemin2 (Matera, 1999).

Nuclear speckles

Nuclear speckles consist of regions in which splicing factors are concentrated (spector, 1993). By immunofluorescence microscopy using anti-splicing-factor antibodies, speckles can be visualised as irregularly shaped nuclear domain. They are dynamic structures and their shape, size and number is variable even within the same cell type, their number depends on the levels of gene expression and metabolic and environmental signals. In interphase mammalian nucleus the number of speckles, usually varies between 25-50 (Lamond & Spector 2003). Also known as splicing factor compartments (SFCs), by light microscopy, they appear as irregularly shaped entities with a diameter of 1-2 μm and correspond to interchromatin granule clusters (IGCs) under electron microscope (Vecerova, et al., 2004).

Paraspeckles

Paraspeckles are a relatively newly identified subnuclear body between 0.5-1.0 μm in size. These foci were named paraspeckles because they were observed in the interchromatin space near to, the nuclear speckles but distinct from them (Fox, et al., 2002). They are restricted to mammalian nuclei and their numbers vary both within cell populations and depending on cell type (Bond & Fox 2009). Paraspeckles proteins are defined by their co-localisation with a member of the mammalian DBHS (*Drosophila melanogaster* behavior human splicing) protein family in a subnuclear foci. But recent studies have reported that they are formed around a long nuclear noncoding RNA (ncRNA) and contain a small number of proteins involved in transcription and/or RNA processing. They have been suggested to have a role in controlling gene expression by trapping adenosine to inosine (A to I) hyperedited RNA within the nucleus (reviewed by Bond and Fox 2009).

1.1.4 Nuclear matrix

The nuclear matrix was revealed (Rando, et al., 2000); after extracting most the DNA and the histones, to comprise inner filaments organized in a three-dimensional anastomosed network and bounded by the nuclear lamina connected to the cytoskeletal framework. The filaments range in diameter from 3 to 22 nm. The proteins of the nuclear matrix are very different from those of the cytoskeleton and chromatin. Although some researchers view the nuclear matrix as a functionally defined organelle in the nucleus, many other researchers prefer to refer to it as a biochemical fraction (Rando, et al., 2000). The matrix is thought to function in some ways as a nuclear homologue of the cytoplasmic cytoskeleton, providing an organisational scaffold upon which nuclear events might take place.

1.2 Nuclear motors

Introduction

Active transport in the cell is mostly driven by molecular motors. There are three classes of molecular motors: the kinesin families that move toward the plus-end of microtubules, the dynein families that move toward the minus-end of microtubules, and the unconventional myosin motors that move along actin filaments (reviewed by Mallik and Gross, 2004). While, the discovery in the nucleus of actin (reviewed by Bettinger et al., 2004) and more recently of a nuclear isoform of the myosin I (Nowak, et al., 1997) has opened a whole new horizon of our understanding of some of the fundamental nuclear processes involving this nuclear motor, more studies are needed to fully understand, many of the functions allocated to the actin-myosin complex.

1.2.1 Nuclear actin

There are at least six actin genes in mammals encoding for six isoforms (α, γ and β). These are alpha-skeletal (ACTA1), alpha-cardiac (ACTC1), alpha-smooth muscle (ACTA2), gamma-smooth muscle (ACTG2), beta-cytoplasmic (ACTB) and gamma-cytoplasmic isoactin (ACTG1) (Vandekerckhove & Weber 1987). The α actin isoforms are present in various muscle cells and are involved in contractile structures, while γ actin and β actin isoforms are present in all cell types (Bettinger, et al., 2004). β actin is a globular protein that is separated into two lobes by a cleft that forms the ATP-binding site as illustrated in figure 1.2.

ATP-bound actin monomers (globular or G-actin) can assemble into filaments (filamentous or F-actin), which results in the hydrolysis of ATP (Bettinger, et al., 2004). Actin filaments are composed of two strands that twist around one another to form a double right-handed helix as shown in figure 1.3.

Figure 1.2: **Cartoon representation of a globular actin molecule**
In the cleft region, ATP binding is shown in red and Mg+ in yellow, the different molecule regions are noted 1 to 4.

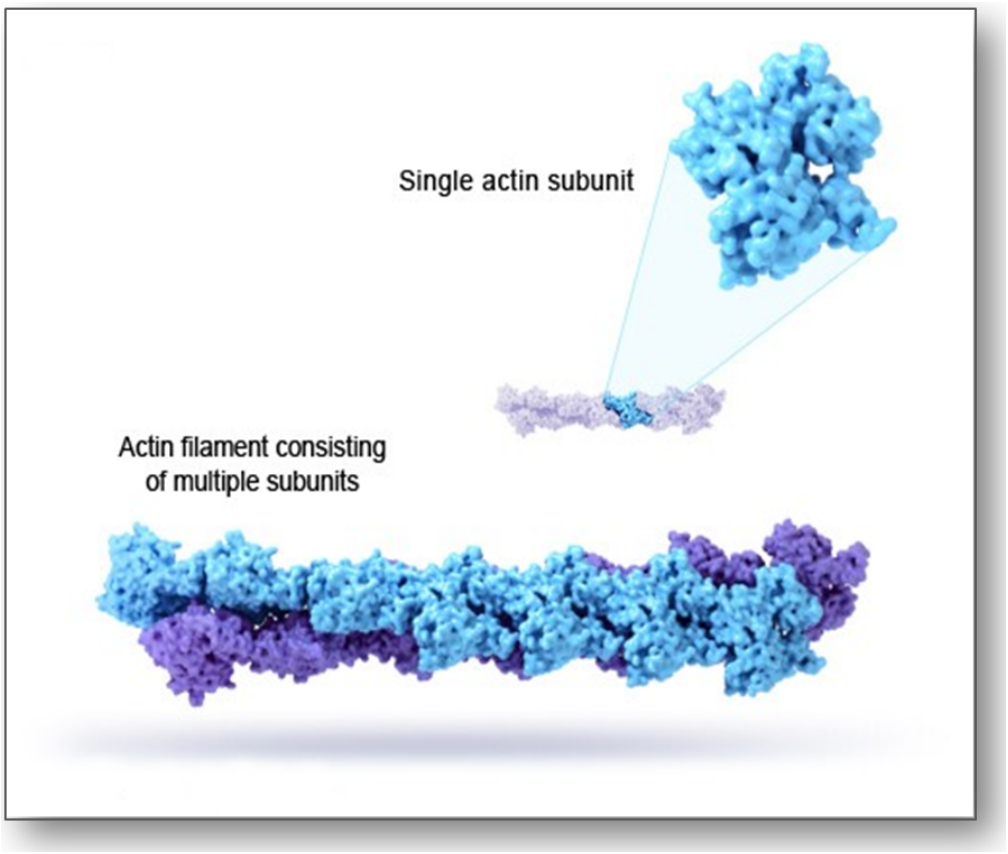

Figure 1.3: **Double helix strand of F actin.**
(Available at www.daviddarling.info/images/actin.filament.jpg). Light blue: G actin molecule. Actin filaments are formed by the twist of two strands (blue and purple) one another around to form a double right-handed helix.

Actin in the nucleus

Actin was first revealed in the nucleus in the late sixties (lane, 1969), but the low amounts of nuclear actin relative to cytoplasm, the inability to detect nuclear actin using conventional staining methods, and the lack of a specific function for actin in this compartment led to scepticism (reviewed by Pederson & Aebi 2002 and Bettinger, et al., 2004). Gonsior, et al., (1999) presented undisputed evidence of actin presence in the nucleus using a particular anti-actin monoclonal antibody (2G2) directed against parts of the cleft region of the actin molecule. Immunofluorescence studies revealed a distinctive focal pattern of nuclear staining in differentiated myogenic cells, as well as a fibrillar structures in nuclei of *Xenopus* oocytes (Gonsior, et al., 1999). At present, although the presence of actin in the nucleus is undisputed, the molecular conformation and role in nuclear processes of this molecule is yet to be completely uncovered (reviewed by Pederson & Aebi 2002, Bettinger, et al., 2004 and Vartiainen, 2008). McDonald, et al., (2006) reported that the actin pool in the nucleus contains monomeric, oligomeric and polymeric populations that presented as both rapidly and slowly moving kinetic populations and that the only significant difference between the cytoplasmic and nuclear actin is the bundling of cytoplasmic actin that generates the stress fibers in the cytoplasm. They also suggested that around 20% of the total nuclear actin pool has properties of polymeric actin that turns over rapidly. Moreover, Hu, et al., (2004) have previously reported that beta actin is associated with and is necessary for the function of the RNA polymerase III and it has been suggested that the monomeric actin is the form of actin required for pol III transcription. On the other hand, different studies have suggested that nuclear actin does not form long F-actin filaments, but can undertake a shorter, potentially novel conformations that are distinct from those found in conventional actin filaments in the cytoplasm (Pederson & Aebi 2002, 2005 and Jockusch, et al., 2006). In the nucleoli of resting cells, actin was found to predominantly localised to fibrillar centres (FCs). After transcriptional activation of phytohemagglutinin

(PHA) stimulated human lymphocytes, actin was found to accumulate in the dense fibrillar component (DFC) and in the granular component of the nucleolus, but FCs remained the main site of actin localisation. Moreover, in the nucleoplasm of transcriptionally active cells, both actin and NMI colocalised with nucleoplasmic transcription sites at the decondensed chromatin, after they were mostly localised in condensed chromatin (Kysela, et al., 2005).

Actin transport into and out of the nucleus

Thanks to its small size, actin can easily enter the nucleus by diffusion, however the low concentration of nuclear actin compared to the cytoplasm suggests the involvement of an active form in actin transport through the nuclear pore complex (NPC) (reviewed by Vartiainen, 2008). Wada, et al.,(1998) reported that actin sequence contains two functional leucine-rich type nuclear export signal (NES) sequences. The rapid export of injected monomeric actin into the nucleus was prevented by leptomycin B (LMB), a specific inhibitor of NES-dependent nuclear export and the disruption of these NES resulted in a nuclear accumulation of the actin. This was supported by the fact that the export receptor Exportin 6 (EXP6), was found to mediate nuclear export of profilin-actin complexes. Profilin was found to highly enhance the primary actin contact with the exportin 6, and was considered as a cofactor of actin export (Stuven, et al., 2003). Furthermore, EXP6 was found to recognise and specifically remove actin from the nucleus (Jockusch, et al., 2006). On the other hand there is evidence that many proteins that binds actin such as cofilin (Lida, et al., 1992 and Pendleton, et al., 2003) CapG (De Corte, et al., 2004) and MAL (Vartiainen, et al., 2007) contain a nuclear localization signal (NLS) and may transport actin in a complex ('piggy-back' it) into the nucleus (Jockusch, et al., 2006, Yahara, et al., 1996 and reviewed by Vartiainen, 2008).

Actin binding proteins

In the cell, the majority of actin molecules are bound to individual partners and consequently locked in a specific conformation, these induced conformational states eventually lead to distinct forms of monomeric, oligomeric or polymeric actin but the exact conformation of the actin bound to these proteins is only known in a few cases, since actin-binding proteins might trigger the formation of different forms of actin. Many of the proteins reacting with conventional actin forms in the cytoplasm are also found in the nucleus (Jockusch, et al., 2006), these include F-actin-binding proteins such as gelsolin (Nishimura, et al., 2003), CapG (De Corte, et al., 2004), myopodin (Weins, et al., 2001) and cofilin (Lida, et al,. 1992), as well as the G-actin-binding proteins profilin (Skare, et al., 2003) and thymosin $\beta 4$ (Huff, et al., 2004).

A list of actin binding proteins shown to be present in the nucleus, as reported by Pederson and Aebi, (2005) is shown in table 1.1, the original table has been slightly modified by adding functions to some proteins (Profilin I, CapG) initially listed as unknown in the original table , the respective references are also provided.

Protein	Function	Reference
Profilin I	Monomer binding protein that promotes nucleotide exchange	(Skare, et al., 2003), (Stuven et al., 2003)
Thymosinβ4	G-actin sequestering peptide in the nucleus	(Huff, et al., 2004)
Myosin I	RNA polymerase I transcription	(Fomproix & Percipalle 2004), (Philimonenko, et al., 2004), (Pestic-Dragovich, et al., 2000)
Filamin	Androgen receptor action	Ozanne et al(2000)
Supervillin	Androgen receptor action	(Ting, et al., 2002)
Gelsolin	Androgen receptor action	(Nishimura, et al., 2003)
CapG	Binds pointed ends of F-actin	(De Corte, et al., 2004), (Onoda, et al., 1993)
Emerin	Cortical network at the inner nuclear membrane	(Holaska, et al., 2004)
Band 4.1	Nuclear pore-attached filament association	(Kiseleva, et al., 2004)
Tropomodulin	Unknown	(Kong & Kedes 2004)
NUANCE	Linkage to cytoplasmic actin filaments	(Zhen, et al., 2002), (Libotte, et al., 2005)
hnRNP U	RNA polymerase II transcription	(Kukalev, et al., 2005)
DNA helicase II/ RNA helicase A	RNA polymerase II transcription and RNA processing	(Zhang, et al., 2002)
Zyxin	Promotes actin polymerization	(Nix and Beckerle 1997), (Fradeliziet, et al., 2001)
Myopodin	Filamentous actin bundling protein	(Weins, et al., 2001)
Nrf2	Forms a complex with actin that translocates to the nucleus upon oxidative stress	(Onoda, et al., 1993)
Lamin A	nuclear lamina protein	(Sasseville, et al., 1998), (Shumaker, et al., 2003)

Table 1.1: Actin-binding proteins in the nucleus
(adapted from Pederson & Aebi 2005)

Nuclear complexes that contain actin

Actin has been found to be a component in many nuclear complexes, hence involved in many nuclear processes, a list of those complexes along with a brief description of each complex as reported by Bettinger, et al., (2004) is provided in table 1.2.

This plethora of actin binding proteins in the nucleus suggests that actin is multifunctional in this compartment. Whether actin takes one or many unconventional forms in the nucleus, and which form for which job is yet to be identified. One actin binding protein recently identified in the nucleus is the nuclear myosin I (Pestic-Dragovich, et al., 2000) this molecule has been the focus of our study as there are strong indications that it may be implicated in chromosome repositioning.

The complex	Function
BAF complex	Actin is required for the optimal ATPase activity of the BAF (BRG-associated factor) complex, a mammalian chromatin-remodelling complex that is related to the yeast SWI/SNF complex
BAP complex	Actin co-purifies with Brm, a SWI2/SNF2-related helicase that functions as the catalytic subunit of the BAP(Brm-associated protein) complex, a Drosophila melanogaster chromatin-remodelling complex
Ino80 complex	Actin co-purifies with INO80, which is the ATPase subunit of the Ino80 complex, a Saccharomyces cerevisiae SWI/SNF-like complex that is involved in transcription and DNA processing
NuA4 complex	Actin co-purifies with the NuA4 (nucleosomal acetyltransferase of H4) complex, that modifies histones H4 a structural component of the nucleosome and H2A
Nuclear DNA helicase-II(NDHII)	(NDHII) binds actin and hnRNP C24.it unwinds double-stranded DNA and has been seen to stimulate translation and have a role in RNA transport
p400 complex	Actin co-purifies with p400 complex the mammalian SWI/SNF-like ,which binds to the adenovirus E1A oncoprotein, and is involved in the oncogenic transformation of cells by E1A.The p400 is also found in the TIP60 complex
PBAF complex	Actin co-purifies with BAF180, a protein that is found in the PBAF(polybromo BRG1-associated factors) complex which localizes to the kinetochores of mitotic chromosomes complex
Pre-mRNP particles	Actin binds to the heterogeneous nuclear ribonucleoproteins (hnRNPs); hrp36, DBP40 and hrp65. pre-mRNA molecules associate with the hnRNP to form ribonucleoprotein complexes that are known as pre-mRNP particles
TIP60 complex	Actin co-purifies with Tat interactive protein TIP60, a histone acetylase of the mammalian TIP60 complex, which also has ATPase and DNA-helicase activity

Table 1.2: Nuclear complexes that contain actin
(as described by Bettinger, et al.,2004)

1.2.2 Nuclear Myosin I

Introduction

According to an analysis of the draft human genome conducted by Cheney et al., (2001) the human genome includes around 40 myosin genes, This family can be divided in two major families; the conventional myosins or Class II myosins consisting of 15 genes, mainly involved in muscle contraction and the unconventional myosins family which constitute around two thirds of the human myosins genes. Myosin superfamily members are characterised by the presence in their heavy chain of a conserved catalytic domain (80 KDa), that is followed in most myosins, by one or more IQ (calmodulin-binding) motifs in addition to a C-terminal tail and /or an N-terminal extension, these are thought to confer class-specific properties such as kinase activity and membrane binding. In spite of the high relative conservation of motor domains among the myosin classes, significant differences are found in biochemical and enzymatic properties of these motor domains. These differences confer to each class of myosin specific characteristics, hence different roles (Cheney et al 2001).

Nuclear myosin I is a member of the myosin I family (Pestic-Dragovich, et al., 2000), members of this family was were first described by Pollard and Korn in 1973 in Acanthamoeba. Single headed, the myosin I was first thought to be a proteolytic form of the myosin II, figure 1.4. It was in 1987 that Hammer et al, finally provided undoubted evidence of its individuality by cloning the myosin I gene.

In mammalian cells, myosin I was found to be abundant in the brush border where it may mediate membrane trafficking, it has an important role in function of the hair cell, it has also been implicated in traction-mediated cytofission and contractile vacuole function in *Dictyostelium* (Hoffman et al 2006). Another role of myosin I as a molecular tension sensor has also recently been reported (Laakso, et al., 2008).

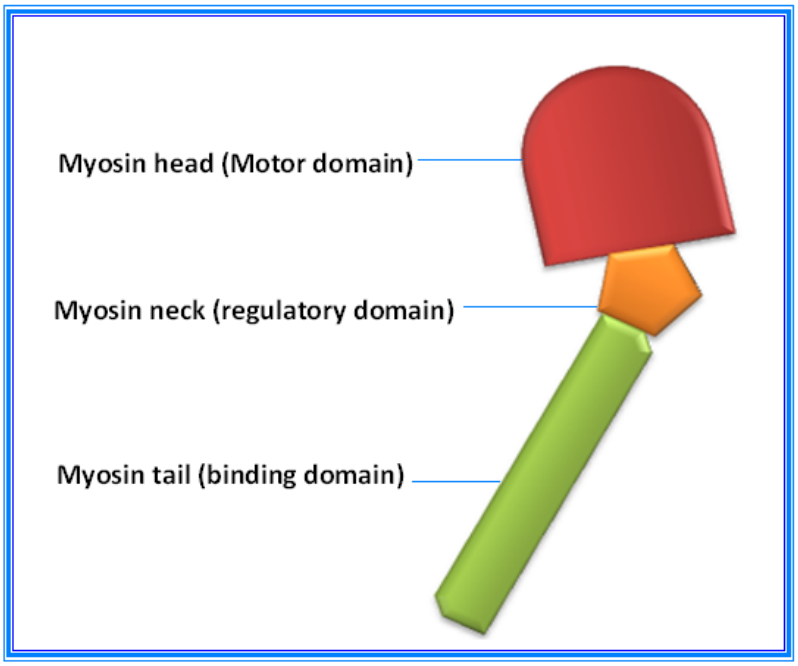

Figure 1.4: **Cartoon of myosin I.**
Schematic representation of the myosin I molecule with the different regions of the molecule; Red: the head region or the motor domain, orange: the neck region comprising the regulatory domain and green: the tail region or the binding domain.

The relatively recent discovery of new members of the unconventional myosin I subfamily in human cells together with the fact that homologous in other species have been given different but yet close similar names, has given rise to much confusion in the literature. For this reason a group of leading scientists in the field had come together in 2001 to recommend the adoption of a common nomenclature based on the Human Genome Organization (HUGO) names system. Names and corresponding coding genes for the myosin I family members are shown in table 1.3.

Human gene	Human synonyms	Mouse gene	Mouse synonyms	Rat synonyms
MYO1A	Brush border myosin I (AF009961) "myosin-IA" (L29137)	Myo1a		
MYO1B	"myosin IB" (L29138)	Myo1b	myosin I (P46735), MIHC L (X69987)	myr 1 (X68199),MI-130K
MYO1C	Nuclear myosin I	Myo1c	myosin-I (X98507)	myr 2 (X74800); MI-110K
MYO1D		Myo1d	myosin-I (C45438)	myr 4 (X71997)
MYO1E	"myosin IC" (U14391)	Myo1e		myr 3 (X74815)
MYO1F	"myosin ID" (U57053),"myosin IE" (X98411)	Myo1f	myosin-If (X97650)	
MYO1G		Myo1g		
MYO1H		Myo1h		

Table 1.3: Reconciliation of myosin I names in the literature (adapted from Berg, et al., 2001)

The Nuclear Myosin I (NMI)

Since the mid-seventies, many studies have suggested the nuclear presence of a myosin or a myosin-like protein but no conclusive evidence was provided (Hofmann, et al., 2006 and references therein). It was in 1997, that presence of a myosin I isoform in the nucleus was first demonstrated (Nowak, et al., 1997), then confirmed to be a myosin I b (Pestic-Dragovich et al., 2000). Nuclear myosin I is a 120 kD monomeric single headed actin based motor molecule pertaining to the Myosin-I subclass of the Myosin superfamily. Members of this myosin class have a single globular motor domain, followed by a neck region and a relatively short (30-40 kD) tail domain. This latter domain is highly basic and binds to acidic phospholipids (Gillespie, et al., 2002). Like all

biochemically characterized unconventional myosins, Myosin I binds calmodulin in its light chain neck region (Barylko, et al., 1992). The human nuclear myosin I (NMI) is encoded by the MYO1C gene, it is slightly shorter than its cytoplasmic homologue and contains a unique 16-amino acid N-terminal extension that is necessary for its nuclear localisation. Although this extension was not found to include a known nuclear localisation signal (NLS) sequence, removing it resulted in retention of the NMI in the cytoplasm (Pestic-Dragovich, et al., 2000). The localization of myosin I to the nucleus has been shown to predate the origin of the vertebrates, as NMI has been present in the last common ancestor of vertebrates and tunicates. Thus, a functional role for NMI appears to have been present at an early stage of animal evolution prior to the rise of both the myosin IC isoform and the vertebrates (Hofmann, et al., 2009). NMI has been found to be expressed in all mouse tissues with the exception of terminal stages of spermiogenesis cell nuclei and has a minimum life span of 16 hours (Kahle at al., 2006). Despite its ubiquitous expression, the NMI level is considerably variable in different tissues, suggesting a tissue specific roles for this myosin. With the highest level in lung cell nuclei, higher levels of the NMI have also been registered in cell nuclei of kidney, skin, small intestines, liver, spleen, testis, and heart tissues. Whereas, lower levels have been detected in brain, skeletal muscle and pancreas (Kahle, et al., 2007).

The level and distribution of NMI in the cell nucleus has been shown to be dependent on the transcriptional state of the cell (Kysela, et al., 2005); transcriptional activation in phytohemagglutinin (PHA) stimulated human lymphocytes was followed by an increase of NMI level and a redistribution of its initial nuclear localization. While NMI was located mainly to the dense fibrillar component (DFC) in nucleoli of resting cells a post-transcriptional activation condensation of the NMI in the DFC and in the granular component of the nucleolus was observed. Furthermore, in transcriptionally active cells, both actin and NMI colocalized with nucleoplasmic transcription sites at the decondensed chromatin, after they were mostly localized in condensed chromatin (Kysela,

et al., 2005). Expression of NMI has also been found to be affected by serum variations, with a lower expression level in serum starved cells that increases after serum stimulation (Kahle, et al., 2007).

1.2.3 Other myosins in the nucleus

The discovery of the nuclear myosin I (Nowak et al 1997) has given rise to the possibility of the presence of other members of the myosin superfamily in the nucleus, effectively many studies have reported the presence of several other myosins in the nucleus, figure1.5.

Myosin V

The phospho-ser1650 myosin Va , a myosin V paralog has been found to localise at the nucleus(Pranchevicius, et al., 2008); immunofluorescence studies had shown the exclusive colocalization of the phospho-ser1650 myosin Va with a splicing factor at the nuclear speckles(SC35). Inhibition of transcription in HeLa cells by actinomycin D has resulted in a dissociation of a fraction of phosphoser1650 MVa from SC35 and a redistribution of the phospho-ser1650 MVa to nucleoli, suggesting a novel role for myosin Va in nuclear compartmentalization(Pranchevicius, et al., 2008).

Myosin VI

The myosin VI is the only identified myosin that moves toward the minus end of actin filaments (wells, et al., 1999). Analysis of myosin VI sequence revealed the presence of five putative monopartite nuclear localization signals (MNLS) and one putative bipartite nuclear localization signal (BNLS), mainly localized in the tail region. Moreover, an immunofluorescence study demonstrated the nuclear localization of the myosin VI (Vreugde, et al., 2006). MyosinVI is a processive moving myosin, it is present both as monomers and as dimers, the processive walking of myosin VI on actin filaments has been shown to require dimerization of the molecule, whereas the protein can also function as a nonpro-

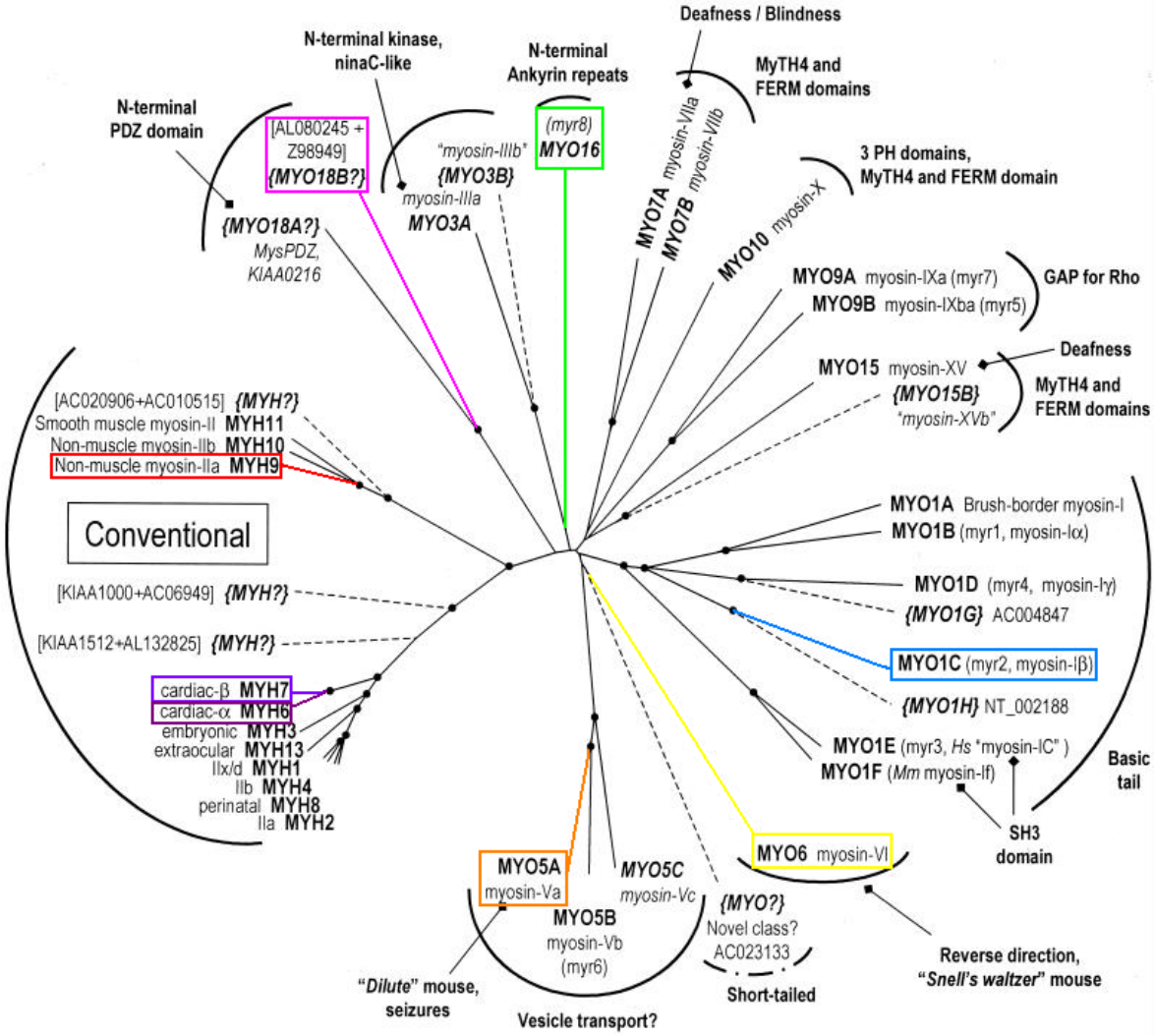

Figure 1.5: **Identified nuclear myosins**
(unrooted phylogenetic tree of the myosin superfamily in humans) solid lines indicate myosins known from cDNA sequences and dashed lines indicate putative myosins predicted from genomic sequence, myosins identified to be present in the nucleus are highlighted in colored boxes.
(adapted from Berg at al 2001)

cessive monomer (Ye, et al., 2009). Myosin VI has been reported to be highly expressed in the nucleus of mammalian cells and modulates RNAPII-dependent transcription; it has been found to be present in the RNAPII complex and to specifically associates with RNAPII at active genes as well as colocalise with nascent transcripts (Vreugd, et al., 2006).

Myosin XVIB

Myosin XVIB, is a founding member of the of the class XVI myosins which are characterized by the presence six ankyrin repeats at the N-terminal that may function as sites for protein-protein interaction (Berg, et al., 2001). The nuclear transition of the myosin XVIB, is found to be dependent on the monopartite nuclear localization signals located in the N-terminal portion of the Myo16b-tail. Several leucine-rich nuclear export signals (NES) have been also identified suggesting a controlled nuclear localization of the myosin16 b (Cameron, et al., 2007). Myosin 16XVIB has been suggested to slow progression through S-phase and its overexpression suppresses cell proliferation (Cameron, et al., 2007).

1.2.4 Functions of the Actin- Nuclear Myosin I complex

The actin-NMI complex has been implicated in many nuclear processes from transport to transcription, in some cases they have been shown to work in concert, whereas in other occasions they have been shown to have distinct roles;

Chromatin remodeling

The WSTF (Williams Syndrome Transcription Factor)-SNF2h chromatin remodeling complex has been reported to interact with the NMI during active transcription (Cavelln, et al., 2006) Purification of cellular NM1 showed that a fraction of NM1 was associated with a 2-3 MDa complex, termed B-WICH, containing WSTF, SNF2h which bound both Pol I and rDNA . Interaction of NM1 with WSTF was suggested to recruit the WICH and WINAC complex to active genes to modify chromatin and activate transcription (Percipalle, et al., 2006).

Transcription

Both actin and NMI cooperate in Pol I transcription activation (Ye, et al., 2008); antibodies to actin inhibit transcription in cell-free transcription assay and both actin and NMI are required to rescue transcription in nuclear extract treated with anti-actin antibody. While, the complex formed by(Pol I, TIF-IA, actin, and NM1) remained preserved in the presence of ADP, the presence of ATP, prevented the association of actin with the transcription machinery and the association of NMI with Pol I was reduced indicateing that ATP binding and hydrolysis lead to detachment of actin from the Pol I/TIF-IA complex and dissociation of actin-NMI complex. Whilest, the actin-dependent motor activity of NMI was identified to be required for transcription elongation and not for the recruitment of Pol I to rDNA, the tail domain seems to have a role in earlier steps of transcription (Ye, et al., 2008). Actin was shown to co-localise with RNA polymerase II and to be recruited to the promoter region of the interferon-gamma-inducible MHC2TA gene as well as the interferon-alpha-

inducible G1P3 gene. It was also established to be part of the pre-initiation complexes of which the formation was prevented by the actin depletion, suggesting that it plays a crucial role in the initiation of transcription by RNA polymerase II (Hofmann et al 2004). Similarly, NMI has been found to co-localise and co-immunoprecipitate with RNA polymerase II. NMI Antibodies to its NH2-terminal extension inhibit transcription by RNA polymerase II in HeLa nuclear extracts (Pestic-Dragovich, et al., 2000). Similar findings were reported by Hofmann, et al., (2006) they showed that antibodies to NMI inhibit transcription both in vitro and in vivo, and this inhibition was found to be in a concentration dependent manner. Antibodies to NMI inhibited the production of the first 15 nucleotides RNA indicating that NMI is involved at the initiation or pre-initiation state of transcription by RNA polymerase II (Hofmann, et al., 2006). Furthermore, transcriptional activation in human lymphocytes has been found to induce a dramatic increase of cellular levels of NMI (the western blot showed about 15 fold after 24 h and 28 fold after 48 h increase in NMI protein levels), while the levels of actin remained unchanged (Kysel, et al., 2005). It appears that NMI is required for transcription initiation and for a post-initiation steps; as NMI has been found to be part of a multiprotein complex containing the chromatin remodeling complex WICH (Percipalle, et al., 2006). On the other hand, beta actin also has a role in RNA polymerase III transcription (Hu, et al., 2004); beta actin has been shown to associate with highly purified pol III and is essential for basal transcription. In addition, actin was localized at the promoter region of an active U6 gene. The dissociation of actin and the polymerase III resulted in an inactive transcription (Hu, et al., 2004). Nuclear myosin I was also found to be associated with the RNA polymerase III genes 5 S rRNA genes and 7SL and was found in complex including WSTF-SNF2h-NMI that is believed to form a platform in transcription while providing chromatin remodeling (Cavelln, et al., 2006)

Nuclear transport

A recent role of the nuclear myosin I and actin has been identified by Parcipalle's group; using Immunoelectron microscopy, they showed NM1 localization at the NPC basket of Xenopus oocyte membrane, decorates pore-linked filaments rich in actin. They also found that NMI coprecipitate with CRM1, and Nup153 as well as same 18S and 28S rRNAs, suggesting a role of the NMI in preribosomal subunits for maturation and their transport to the NPC (Obrdlik, et al., 2009).

Maintaining the nuclear shape and organisation

The co-localisation of nuclear actin spots and p80 coilin-positive cajal bodies staining, that resisted nuclear extraction to reveal the nuclear matrix, and the redistribution of actin to the nuclear periphery identified as a result of Adenovirus 5 infection has led to the conclusion that actin may play an important role in the organization or function of the cajal body (Gedge, et al., 2005). Another role of the nuclear myosin I-containing complexes in sensing and regulating the mechanical tension at the nuclear envelope has been suggested by Holaska and Wilson, (2007). They found that emerin scaffolds a variety of multiprotein complexes at the nuclear envelope that have distinct functions, including nuclear myosin I-containing complexes, they proposed a model where emerin-and-lamin A-anchored NMI might pull actin filaments towards, or along, the nuclear envelope. Together with emerin-promoted actin polymerization at the inner membrane, emerin-bound NMI has the potential to both sense and regulate the mechanical stiffness of the peripheral nuclear lamina network, hence contribute to maintaining the nuclear shape and architecture (Holaska & Wilson 2007).

Chromatin reorganisation and chromosome movement

A fundamental role for the actin-myosin complex in chromatin movement was identified by Chang, et al., (2006). They have demonstrated the migration of a chromosome site from the nuclear periphery to the interior in cells during

interphase, 1-2 hours after transcriptional activation of this site has been targeted. This chromosomal repositioning has been identified to exist throughout a large fraction of the cell cycle (G1 /early S) and depends on NMI and actin polymerization .

Using 4D imaging analysis, Dundr and colleagues, (2007) revealed rapid and directed long-range chromosomal movements of U2 genes during interphase. followed by a stable association between cajal bodies (CBs) and U2 genes. The interaction of CBs and U2 genes was inhibited by the overexpression of a nonpolymerisable actin mutant, which also inhibited the repositioning within the chromosome 7 territory of the U2 locus (Dundr, et al., 2007)

A role of actin and NMI in nuclear reorganisation and interchromosomal interaction has been also identified. Chromosome 21 and chromosome 2, initially localized independently in the nucleus before 17β-estradiol (E2) treatment were found to became intimately localised after The E2 treatment with interchromosomal kissing, this chromosomal rearrangement and kissing was abolished by the inhibition of actin polymerization or the siRNA depletion of the NMI (Hu, et al., 2008).

1.3 Aims of the project

While other studies have reported a role of the nuclear myosin I in chromosome movement, they have been focusing on a gene or a chromosome region. In this project the role of the nuclear myosin I in the repositioning of a whole chromosome territory has been investigated using chromosome positioning and image analysis tools. This project is aiming to:

1. Confirm chromosome 10 repositioning to the nuclear periphery after the cells were incubated in low serum, using IPlab spectrum software.

2. Design siRNA constructs to target the respective nuclear myosin I encoding gene.

3. Repeat the chromosome positioning study using images of nuclei where the nuclear myosin I gene has been silenced by siRNA in order to investigate the effect of the NMI depletion on low serum induced chromosome 10 repositioning.

4. Conduct a comparative study of the nuclear shape and size before and after the low serum incubation.

5. Repeat the comparison of the nuclear size and shape after the siRNA knockdown of the NMI gene.

In order to achieve the above a number of laboratory techniques and image analysis tools have been used, as detailed in the following chapter.

Chapter 2

Methods and Materials

In this chapter all methods and tools used during this project will be described; They can be divided in two categories. The first set is laboratory based, and the second is computer based. The laboratory based methods section will describe techniques used to prepare the cells for the study. Tissue culture permits the generation of enough cells to carry out the experiments. The low serum assay was used to induce the chromosome repositioning. Fluorescence in situ hybridisation (FISH), enabled us to probe the chromosomes in order to study their position in the nucleus before and after the low serum incubation of the cells, pre and post siRNA knock-down of the nuclear myosin 1 gene. FISH images, captured in each experiment are subsequently used in the second part of this Chapter. The computer based methods section will illustrate all the tools utilised to identify all known myosins in the nucleus, design siRNA constructs for the gene knockdown and carry out further analysis on the images generated from the first part of the project. Among which, the IP-Lab program has provided us with raw data relating to a chromosome's position in the nucleus; combined with the Microsoft Excel, these data was put into charts for easy interpretation. Other image analysis tools, including Paint Shop Pro XI and Scion Image were used to investigate eventual effects of the low serum assay and the NMI gene silencing on the nuclear size and shape and the studied chromosomes territories.

2.1 Laboratory based methods

2.1.1 Tissue culture

Human dermal fibroblasts (HDFs) 2DD (Bridger, et al., 1993) have been cultured in Dulbeco's Modified Eagles Medium (DMEM) with the following additives: 10% new born calf serum (NCS), 1% penicillin, 1 % streptomycin, L-glutamine. The cells were cultured in 75 mm flasks and incubated in 5% CO_2 incubator at 37°C temperature. They were harvested and passaged twice weekly. To harvest cells, the media and the necessary reagents are pre-heated to 37°C in a water bath before use. In the sterile hood, first the old media was removed and the flasks were washed with versene (0.197g of EDTA in 1 litre of 1 X PBS). To facilitate the detachment of the cells from the bottom of the flasks, the cells were incubated in 5 ml diluted solution of trypsin: versene (1:10, v:v) for up to five minutes. Meanwhile the cells detachment was checked closely using a microscope. As soon as all the cells were detached from the flask's bottom, the trypsin solution was neutralized by adding an equal amount of the D-MEM medium to the flasks. The resulting suspension was then transferred to centrifuge tubes and centrifuged at 1000 (rpm) for 5 minutes. The supernatant was removed and the pellet of cells was re-suspended in a known volume of fresh medium (5 to 10 ml). To determine the number of cells in the suspension, the haemocytometer was used to count the cells in a drop of the suspension then the total number of the cells in this was calculated using the following equation: Number of cells counted on the haemocytometer (CC), divided by number of haemocytometer's large squares where the cells have been counted (SH), the result is multiplied by the total volume of the suspension (V) then by 10^4 , the final result equals the total number of the cells in the suspension (TC).

$$(\mathrm{CC} \div \mathrm{SH}) \times \mathrm{V} \times 10^4 = \mathrm{TC}$$

The total volume of the cells suspension was then distributed in new flasks at a density of 5×10^5 cells per flask. The volume in each flask was toped to 20 ml using fresh media and the cells were incubated at 37°C in the incubator.

2.1.2 Low serum assay

Normal proliferating 2DD were incubated in a low serum medium (0.5% NCS DMEM) for 15 min to induce the chromosome movement as follows: In the sterile hood the old media was first removed and the cultures were washed twice with serum free fresh media. 20 ml of low serum (0.5% NCS) medium was added to each flask and the cells were replaced in the incubator for 15 minute then immediately harvested as described above (all the media and the reagents used are preheated to 37°C). After centrifugation the supernatant was removed and the cells were fixed in a 3:1 methanol: acetic acid solution as described below in the FISH section.

2.1.3 Immuno-fluorescence in situ hybridisation (Immuno-FISH)

Fixation

Fixation was performed using the methanol: acetic acid solution. Firstly, the cells were harvested using trypsin as described in the previous section, then after centrifugation most of the supernatant was removed and the cells were re-suspended in the remaining media. A hypotonic solution (0.075 M KCl) was added to the cells at room temperature for 15 min. Then, the samples were centrifuged for five at 800 (rpm) for 5 minutes, most of the supernatant was removed and the cells re-suspended in the residual solution. A fixative mixture of methanol:acetic acid (75%:25% respectively) was freshly prepared and put on ice, then was added drop wise to the sample with constant taping of the tube to prevent the cells from clumping. The sample was stored at 4°C for at least 1 hour or overnight. The sample was then centrifuged at 800 (rpm) for five minutes, the supernatant was removed and the fixing procedure was repeated four to five times. A drop of the sample was observed under the microscope to check that most the cytoplasm has been eliminated.

Slide preparation and denaturation

The fixed cells were centrifuged at 1000 (rpm) for 5 minutes, the supernatant discarded and the pellet of cells re-suspended in a small volume of fresh ice cold methanol:acetic acid (3:1) solution to obtain a milky suspension. The cells were dropped from a height onto humid or damp slides. To age the slides they were first air dried then baked at 70°C for 1 hour or left at room temperature for 2 days. The slides were dehydrated trough in 70%, 90%, 100% ethanol for five minutes in each solution at room temperature, then air dried on a hot plate. Pre-warmed slides (70°C for 5 minutes in oven) were incubated in a denaturing solution (70% formamide : 2X Sodium Saline Citrate ($Na_3C_6H_5O_7$)(V:V),pH 7.0) for 2 minutes, then were immediately plunged in ice cold 70% ethanol for 5 minutes. Next they were run through another ethanol raw (90%, 100% five minute in each) at room temperature. After being air dried on a hot plate, the slides were ready for hybridisation.

Probe preparation and hybridization

In house biotin labelled probes were used (kindly provided by Dr Bridger and Mehta). First the probe DNA was precipitated into a mixture of Cot DNA and Herring or Salmon sperm; for each slide:

- 8 μl of the probe template (10 or X), 7 μl of Cot DNA, 3 μl of Herring sperm DNA were mixed.
- Then, $1/10^{th}$ of the volume (1.8 μl) of 3 M sodium acetate (pH 5.0) and 2 volumes (40 μl) of ice cold 100% ethanol were added to the mixture.

The mixture was incubated at -80°C for at least 30 minutes. Next, it was centrifuged at 300-400 (rpm) for 30 minutes at 4°C. The excess liquid was discarded and the residual white DNA pellet is then washed by adding 200μl of ice cold 70% ethanol, and then centrifuged again for another 15 min at 4°C. The supernatant was removed and the pellet was dried at about 40°C (37 to 50°C) on the hot block. When the pallet turned transparent, 12μl of

the hybridization mix (see blow) was added and the pellet was left to dissolve for at least 2 hours (with gentle tapping every 15 min) or overnight at room temperature. Next, probes are ready for denaturation by baking them at 70°C for 10 minutes and re-annealing by incubating them at 37°C for at least 30 min. The hybridization mix:

- 10% dextran sulphate (V = 2.4 μl),
- 10% 20 X Sodium Saline Citrate (SSC) (V =1.2 μl),
- 50% formamide (V = 6 μl),
- 1% Tween 20 (V = 0.12 μl),
- 29% double distilled water (V = 2.28 μl).

For hybridization, 12μl of the probe mixture was applied to each prepared slide, then covered with a coverslip and sealed with rubber cement. Finally, the slides were left to hybridise at 37°C in a moist chamber for at least 18 hours.

2 D FISH washing and signal detection

After hybridization, coverslips were removed, the slides were washed in buffers A and B as follows; first, slides were washed in the preheated to 45°C Buffer A (50% formamide: 2X SSC (v:v), pH 7) three times for five minutes and changing the buffer each time. Then the same process is repeated with the buffer B (0.1X SSC, pH 7, preheated to 60°C). Next slides were allowed to cool down in a solution of 4X SCC at room temperature. To detect the fluorescent signal, the slides were first incubated with 50 to 100 μl of a blocking solution (4% bovine serum albumin) at room temperature for 10 min. Then a similar amount of (1:200) diluted Streptavidin-Cyanine 3 (Cy3) solution was added to each slide and incubated in dark for 30 minute at 37°C, or 1 hour at room temperature. Next the slides were washed in a solution of 4X SSC with 0.05% Tween 20, at 42°C three times for five minutes, changing the buffer each time. Finally the

slides were mounted in Vectashield medium + 4, 6-diamidino-2-phenylindole (DAPI) and were ready for observation by the fluorescence microscope.

pKi-67 Staining

To distinguish proliferating cells from non proliferating ones, the 2-D FISH was combined with anti pKi-67 staining as follows.
2-D FISH slides were placed in a solution of 1X PBS to allow the coverslips to detach from the slides, then they are incubated with 40 to 100μl of the primary antibody (1:1500 rabbit anti Ki-67, diluted in 1% NCS), for one hour at room temperature. Slides were washed in 1X PBS for five minutes three times to eliminate non bound antibody, then they were incubated with the similar amount of the secondary secondary antibody conjugated to fluorescein isothiocynate (FITC) (1:30 diluted in 1% NCS, swine anti-rabbit polyclonal) for one hour at room temperature. Excess antibody was eliminated by washing the slides in 1X PBS for five minutes three times. Finally, slides were mounted in counter-stain DAPI in vectashield mounting medium (Vector Laboratories).

2.1.4 Image acquisition

The Olympus BX41 fluorescence microscope has been used to inspect the slides; the microscope is equipped with a Viewpoint digital camera (digital scientific). The cells were examined using a 100X plan oil immersion lens, 50-80 images of pKi-67 positive, randomly selected nuclei have been captured. The Smart Capture 3 software was used to visualise a merged colour picture of the three different staining (blue: DAPI, green: Cy3 and red: pKi-67). For each slide a new film strip was opened and images saved were in PICT format.

2.1.5 Small interfering RNA (siRNA)

Although, both nuclear myosin I and unconventional myosin VI have been initially chosen as possible targets for the siRNA knock down, the literature review

has shown that NMI was more likely to be involved in the chromosome repositioning as previous studies have identified a role of the NMI in chromatin movement(see Chapter 1, section 1.3.4), the siRNA experiment was only carried out for the nuclear myosin I. Despite our efforts to design a specific siRNA construct against the nuclear isoform of the *MYO1C* gene, it was technically impossible to generate functionally efficient siRNA constructs against the NMI 5' UTR region of this gene which is the only specific region for the nuclear myosin I isoform (details provided in section 2.3.3 of this chapter). For this reason, it was more sensible to opt for ready made and tested constructs. ON-TARGETplus SMARTpool siRNA (Thermo Fisher Scientific, Lafayette. CO; Dharmacon Catalog -E-015121-00) has been used to target the nuclear myosin I. The pool included four specificity-enhanced duplexes that targets different regions of the MYO1C gene, other benefits of using a SMARTpool include minimum off site effects, since the concentration of each construct is kept very low. Used sequences are as follows:

- 5'GCUCAAAGAAUCCCAUUAU3'
- 5'GCUGAAUUCUCGGUGAUAA3'
- 5'GCACUCGGCUUGGUACAGA3'
- 5'GUACAGCGUGCGGACAAUA3'

For negative control, the cells were transfected using ON-TARGETplus Non-targeting Pool.

2.2 Computer Based Methods

2.2.1 Web-based search

The aim of this search was to identify possible other nuclear myosin candidates for the role of chromosome 10 rapid repositioning. First up-to-date data about all known myosins in the nucleus were collected by searching the protein databases on the following websites:

- The National Centre for Biotechnology Information: www.ncbi.nlm.nih.gov
- The European Bioinformatics Institute: www.ebi.ac.uk
- The Universal Protein Resource :www.uniprot.org
- Expert Protein Analysis System: www.expasy.org

Different key words and searching formulae have been used, in order to establish a comprehensive and yet specific data about the nuclear myosins. After identifying all known myosins in the nucleus and respective split variants' sequences and encoding genes, the sequences alignment tool ClustralW have been used to align recognized nuclear myosins sequences with regard to determine their similarities and align the sequences of splits variant of selected nuclear myosins in order to identify possible targets for siRNA constructs.

2.2.2 Sequence alignment tool

The ClustalW2 alignment tool on the European bioinformatics institute's website, figure 2.1, has been chosen to align recognised nuclear myosins sequences with regard to determine their similarities. This program calculated the best match for the selected sequences to produce biologically meaningful multiple sequence alignments of divergent sequences, then lined them up so that the identities, similarities and differences can be seen.

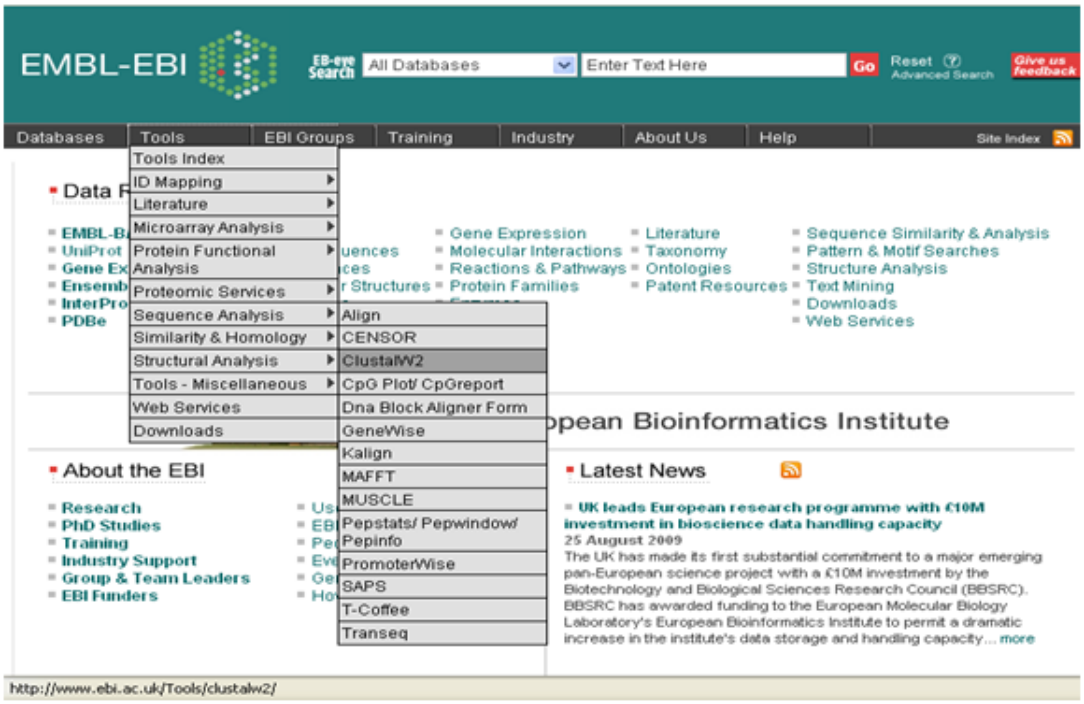

Figure 2.1: **Alignment tools on the EBI website.**
On the EBI website from the tool's window, sequence analysis, then the ClustalW2 tool, which allows the alignment of multiple sequences, was chosen.

Using ClustalW2, sequences of myosin I and myosin VI have respectively been lined up together with the other the splits variants encoded by the same respective gene. This program permits visualisation of peculiar segments of the myosin I and myosin VI which can be targeted when designing siRNA constructs.

To align the three transcripts variants of the MYO1C gene together their respective RNA sequences in a FASTA format were obtained from the NCBI website; NP-001074248.1 for isoform a, NP-001074419.1 for isoform b (NMI), NP-203693.3 for isoform c. The three sequences were entered in the designated space and the program was run using default setting as shown in figure 2.2.

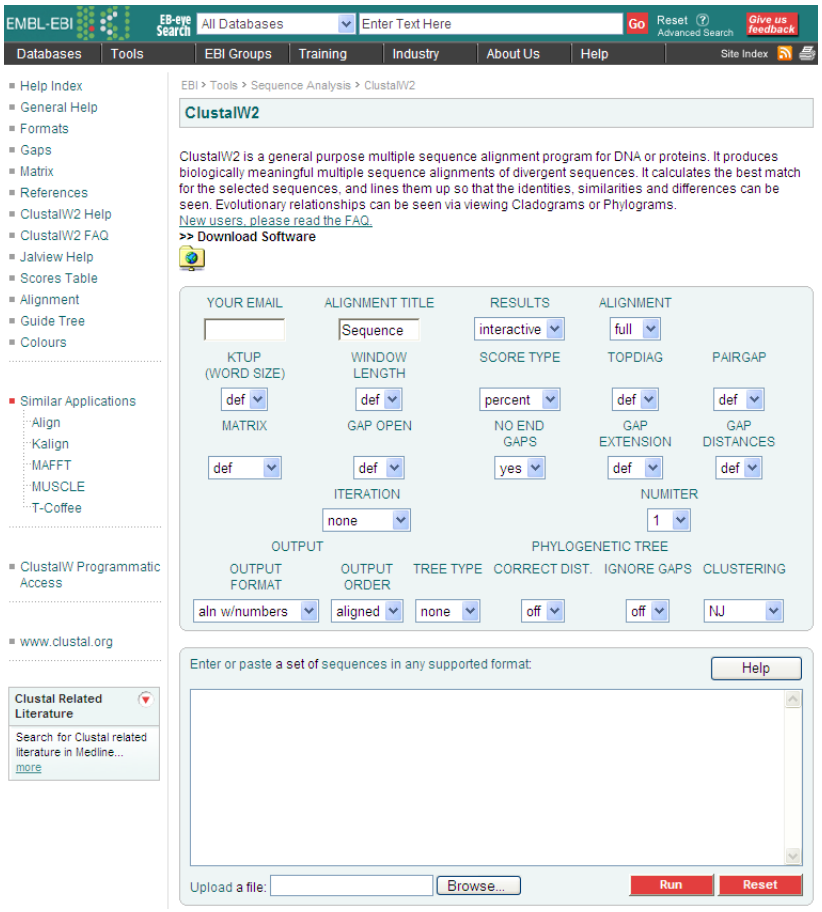

Figure 2.2: **ClustalW2 alignment tool settings.**
Sequences of the transcript variants were entered in the designated space, the default setting were selected to run the analysis.

2.2.3 Design of siRNA constructs

Nuclear myosin I and unconventional myosin VI have been chosen as initial targets to be investigated for their possible role in the Chromosome 10 low serum induced repositioning. To generate a list of candidates' sequences for siRNA targeting *MYO1C* and *MYO6* genes respectively, the siRNA design tool; The siDESIGN Center on the Dharmacon website (www.dharmacon.com/designcenter) has been used. This tool allows to choose an identifier type (Accession Number, Gene ID, Nucleotide sequence, GI Number), to select desired region(s) for siRNA design. Since, the nuclear myosin I is distinguished from other transcripts variants encoded by the *MYO1C* only by its 5'UTR region, this section has been initially selected as target region for siRNA design by using the NMI accession number as identifier. Unfortunately, no siRNA candidates could be built with these given inputs. The next step was to extend the target region to include the ORF section and specify the transcript target to be the isoform b of the *MYO1C* by entering the gene ID (4641). No siRNA candidates could be built with these given inputs also, the reason why it was decided to use commercially tried construct and ON-TARGET plus SMARTpool siRNA was chosen for the *MYO1C* knock-down.

2.2.4 Image analysis

Part of the images used in this analysis were kindly provided by Ishita Mehta, a fellow PhD student, she also gratefully, provided me with the the FISH slides from which another part of the images were taken. The image analysis was carried out using a number of software, depending on the aim of the study.

Chromosome positioning

The erosion analysis in IPLab Spectrum software was used to determine the position of chromosome 10 and X territories in cells at 0 and 15 min before and after the NMI knock down. For each analysis at 45 to 90 images are used in PICT format. The images were treated by data erosion program which divides the nuclear surface into five concentric zones or shells, zone 1 being the most peripheral and zone 5 the central. This program measures both the DAPI and the Cy3 signal in each zone of the nucleus and the final results are then displayed in a table. Which was then transferred to Microsoft spreadsheet and used to for further data analysis; for every image, the chromosome territory signal in each of the five shells was normalized to the DAPI signal of the same zone. The means of the calculated ratios were then plotted into histograms to determine the position of the chromosome territories; the t-test was used to evaluate the significance of the results.

Nucleus and chromosome territories analysis

This analysis has been carried out in three main steps, different software or data analysis tools has been used in each step depending on the aim of the study.

1. **Corel Paint Shop Pro XI:** The images obtained from the fluorescent microscope were transformed from a PICT format to a Tiff uncompressed format using a trial version of the "Corel Paint Shop Pro XI". Then each image was split to the three channel colours RBG (Red Bleu Green) and saved as Tiff to be used for the area analysis, as illustrated in figure 2.3.

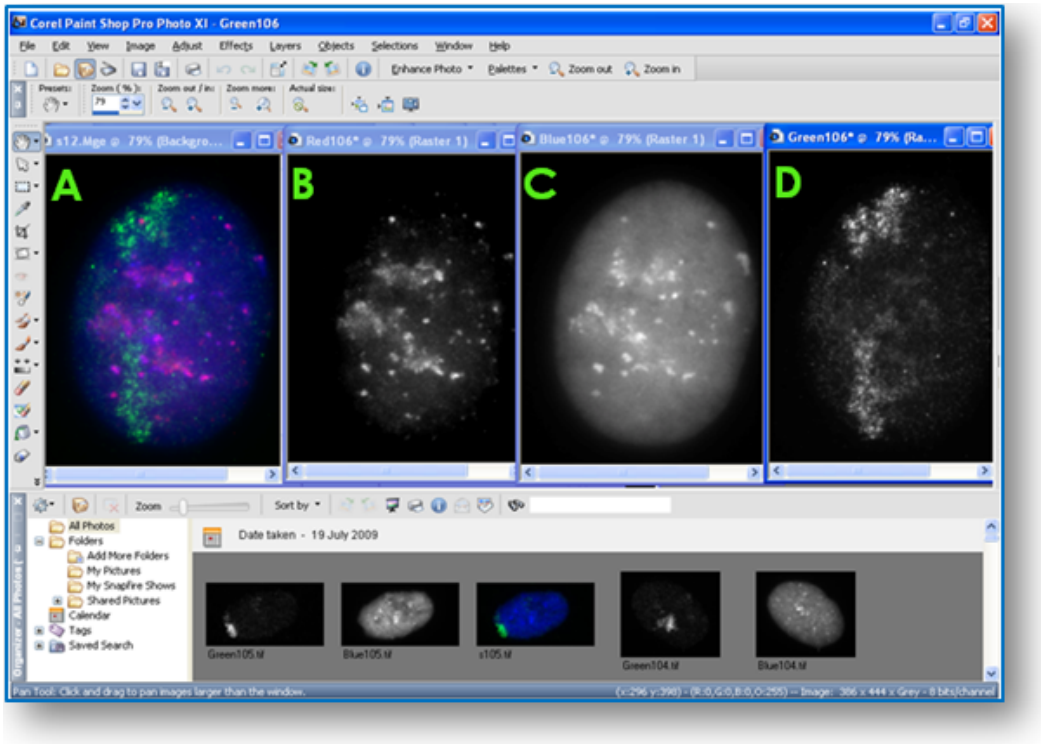

Figure 2.3: **Corel Paint Shop Pro XI (RGB Split channels)** A:immono-FISH original image before the split (nucleus in blue, chromosome 10 territories in green, nucleolus in red). B: red channel (only the red staining from the original image is highlighted, corresponding to the FICT staining or the nucleolus). C: blue channel (only the blue staining is selected corresponding to the DAPI staining or nucleus). D: Green channel (only the green staining is selected corresponding to the Cy3 staining or chromosome territories).

2. **Scion image analysis:** The Scion image software was used for nuclear and chromosome territories analysis; it carries out area measurement, as well as details about contour/ perimeter, minor and major ellipse, mean density. This tool can only open grayscale images saved in uncompressed TIFF format. When this software was opened, a bar menu, a tool and LUT box, an Info and Map window appeared on the screen as illustrated in figure 2.4.

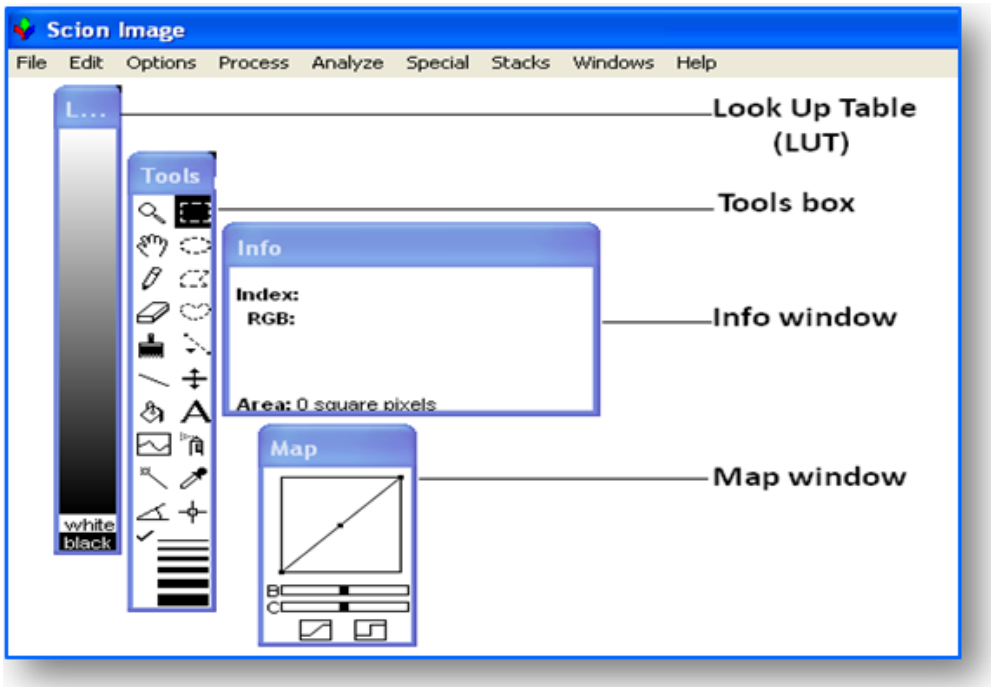

Figure 2.4: **Scion image analysis.**
LUT: permits to set and change the gray scale intensity. Tool box: include image treatment and measurement tools. Info window: displays details about the open image. Map window: shows the colour distribution

For nuclear analysis, the blue channel image of each colored nucleus image was opened using "import" command from the file menu, then the density slice option was selected which highlights the area of interest in red figure 2.5 according to a gray scale threshold, this could be manipulated using the LUT window depending on the clarity and the brightness of the picture.

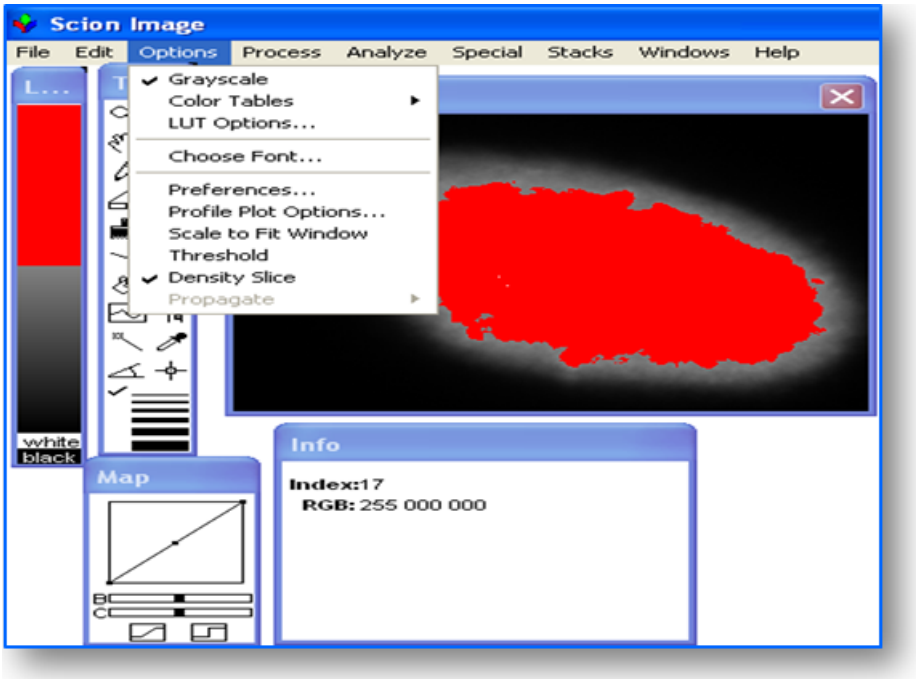

Figure 2.5: **Density slice on Scion image.**
The LUT box permits to establish a grayscale threshold for the density slice, which permits to highlight the region of interest.

Next, on the menu bar the "analyze" window was dropped and the options command was selected to set the parameter desired to be measured. Figure 2.6.

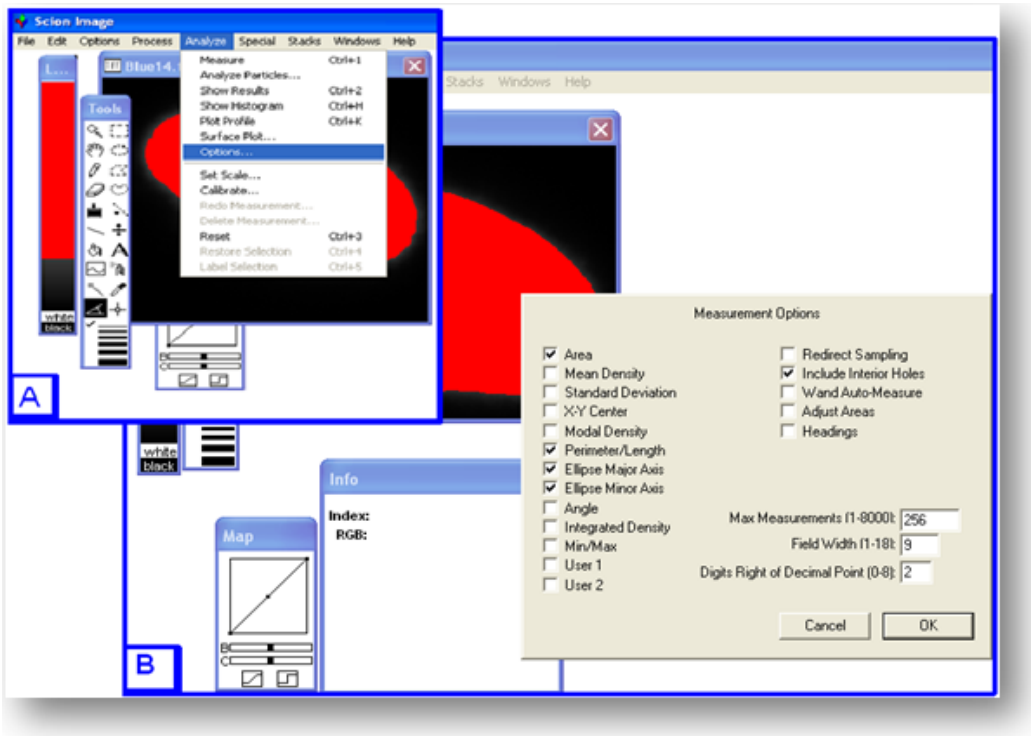

Figure 2.6: **Setting the measurements options.**
A: bar menu the analyze drop window is opened and the option command is selected. B: desired parameters to be measured are checked, including: area, perimeter, minor ellipse and major ellipse.

The following step consisted in setting the measurement scale from the analyse command box, figure 2.7, the scale was set to 10.8 pixels per μm. this value has been calculated using a graticule picture.

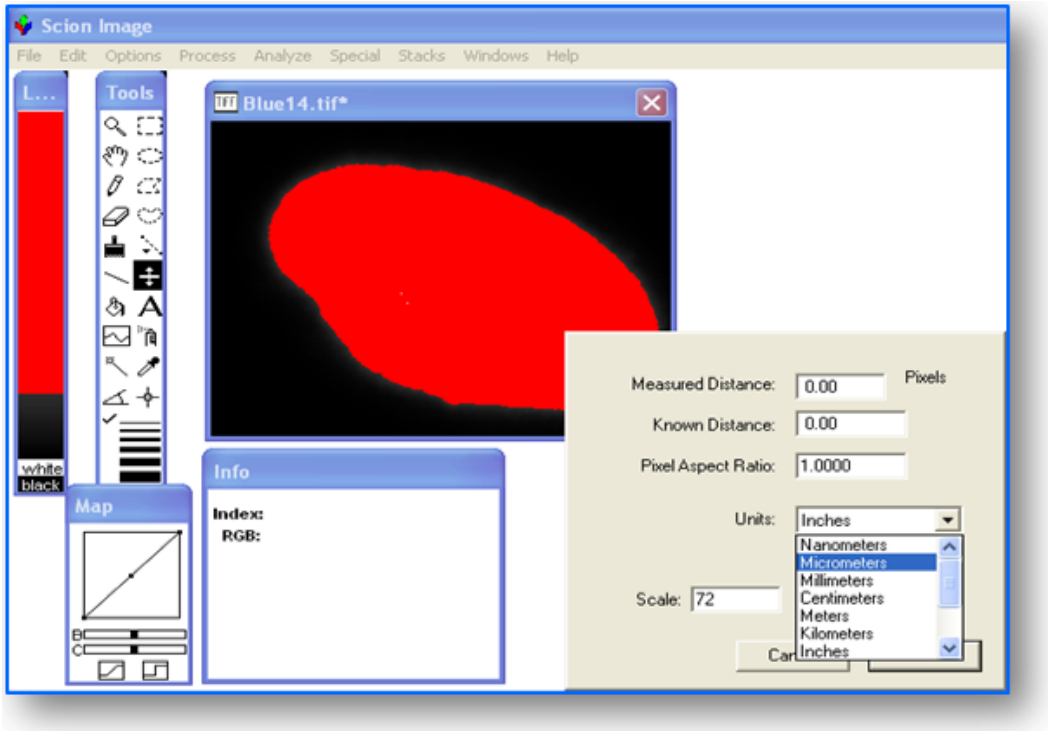

Figure 2.7: **Setting the measurement scale to micrometers.**
from the "analyze" drop window, set the scale option was selected and the scale is set to the desired value.

Microsoft Excel

The raw data obtained from the image analysis software, were transferred to a Microsoft Excel worksheet for further statistical analysis.

Chapter 3

The role of Nuclear Myosin 1 in interphase chromosomes positioning

3.1 Chromosome 10 positioning

Images obtained from FISH slides performed as described in chapter 2, were run through a simple erosion script using IP-Lab image analysis software, which divided the nucleus into 5 equal concentric shells . The DAPI and Cy3 signals were measured in each shell. The raw data was then transferred to an Excel worksheet, the chromosome territory's (Cy3) signal was normalised to the nuclear (DAPI) signal in each shell where the mean of the ratio (% of the cy3 signal / % of the DAPI signal) has been calculated for each shell, then plotted in charts. The position of the chromosomes was then defined as periphery, intermediate or interior. A chromosome territory was identified to locate at the nuclear periphery, when after normalisation; the mean Cy3 signal was the highest in shell 1 and 2; intermediate if the shells 2, 3 and 4 had higher probe signal with shell 3 having the highest signal or all the three shells showed equal amount of Cy3 signal. Finally, the chromosome position is defined as interior when the highest probe signal is localised in shells 4 and 5. To identify the role of nuclear myosin 1 in chromosome 10 repositioning , the low serum inuduced relocation of chromosome 10 from an intermediate region in the nucleus to the nuclear periphery was first confirmed by analysing chromosome 10 positions before and after the low serum assay. Next the NMI expression has been suppressed, and the low serum assay was repeated using the NMI depleted cells and chromosome 10 positioning before and after the low serum incubation has been analysed and compared to chromosome positioning in cells expressing the NMI. For each experiment 45 to 60 images were analysed .

3.1.1 Chromosome 10 repositioning before and after the low serum assay

To confirm the low serum induced Chromosome 10 relocation from an intermediate region of the nucleus to its periphery 15 minutes after the cells have been incubated in low serum media, the low serum assay using normal proliferation

HDF (as described in section 2.2.2 of chapter 2) has been repeated. FISH images (figure 3.1) of nuclei from control cells (cells at 0 minute; that have not been incubated in low serum media), and FISH images (figure 3.2) of nuclei after the low serum assay at 15 minutes), were treated by a simple erosion analysis using IPLab program as discribed in section 2.3.4 of chapter 2.

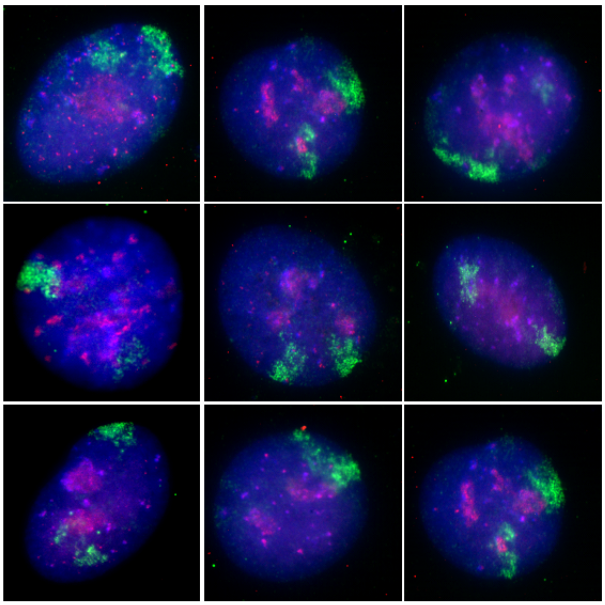

Figure 3.1: **Sample of chromosome 10 FISH images at 0 minute.** Representative images displaying nuclei prepared for fluorescence in situ hybridization (2D-FISH) before the low serum incubation. With whole-chromosome 10 painting probes (green), nuclear DNA was counterstained with DAPI (blue) and indirect immunofluorescence with anti-pKi-67 antibodies (red staining) permitted the selection of normal proliferating cells.

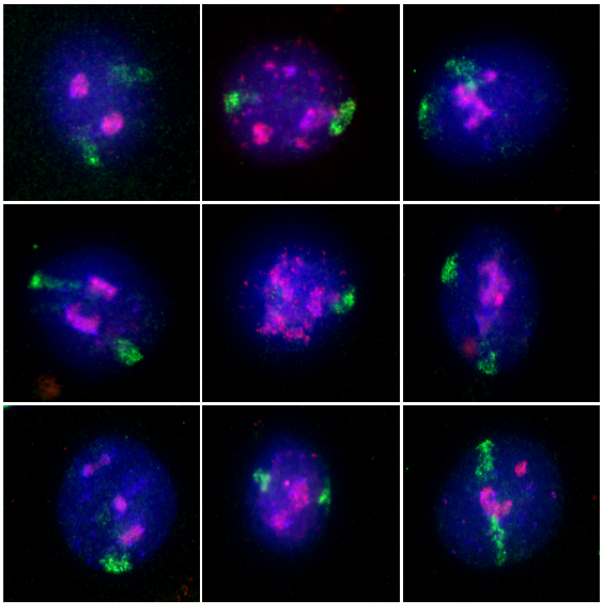

Figure 3.2: **Sample of chromosome 10 FISH images at 15 minutes.** Representative images displaying nuclei prepared for fluorescence in situ hybridization (2D-FISH) after the cells have been subjected to the low serum assay. With whole-chromosome 10 painting probes (green), nuclear DNA was counterstained with DAPI (blue) and indirect immunofluorescence with anti-pKi-67 antibodies (red staining) permitted the selection of normal proliferating cells.

Chromosome 10 position at 0 minute in $NMI^{(+)}$ nuclei

Chromosome 10 in normal proliferating cells before the low serum assay (at 0 minute) has been confirmed to locate at an intermediate region of the nucleus as the highest cy3 signals were localised in shells 2 and 3, as shown in figure 3.3. Calculated paired t test has confirmed the significant cy3 signal difference between shells 2 and 3 and the other shells.

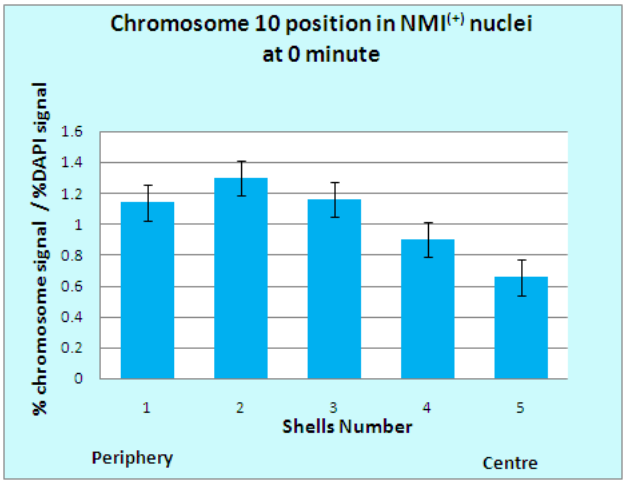

Figure 3.3: **Chromosome 10 positioning in nuclei of normal proliferating HDFs at 0 minute.**
Displays the distribution of the chromosome 10 signal for 2D FISH before the low serum incubation, as analyzed with erosion analysis. The percentage of chromosome signal measured in each shell was divided by the percentage of DAPI signal in that shell. Bars represent the mean normalised percentage of chromosome 10 signal in each shell (1-5) with shell 5 being the most intern and 1 the most peripheral.

Chromosome 10 position at 15 minutes in $NMI^{(+)}$ nuclei

After the low serum incubation, Chromosome 10 in normal proliferating HDFs nuclei is found to relocate to the periphery of the nucleus (figure 3.4), with the highest chromosome signal (cy3) in shell 1 followed by shell 2, and considerably lower signals in shells 3 and 4 and nearly null signal in shell 5. the paired t test for means has confirmed the significantly diffrence between signals in shells 1 and 2 and the rest of the shells. $p \leqslant 0.005$.

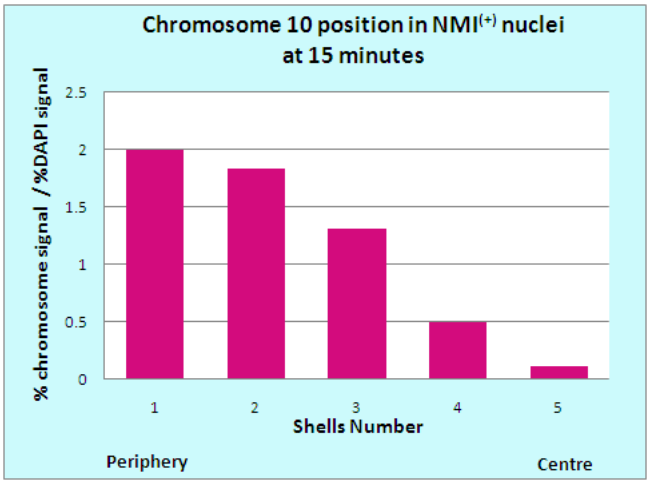

Figure 3.4: **Chromosome 10 positioning in nuclei of normal proliferating HDFs at 15 minutes.**
Displays the distribution of the chromosome 10 signal for 2D FISH after the low serum incubation, as analyzed with erosion analysis. The percentage of chromosome signal measured in each shell was divided by the percentage of DAPI signal in that shell. Bars represent the mean normalised percentage of chromosome 10 signal in each shell (1-5) with shell 5 being the most intern and 1 the most peripheral.

In order to better visualise the chromosome 10 relocation to the periphery after the low serum incubation, both charts of chromosome 10 position at 0 and 15 minutes have been aligned in figure 3.5, in blue is chromosome 10 position before the low serum assay and in pink is chromosome 10 position after the low serum assay.

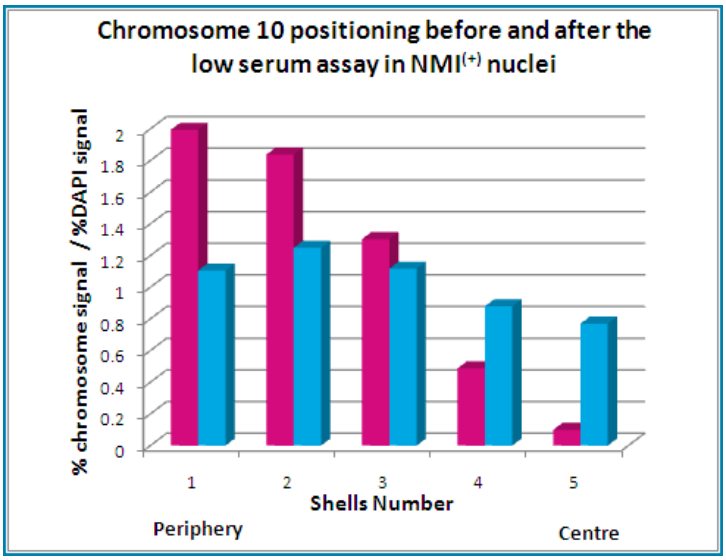

Figure 3.5: **Chromosome 10 positioning in nuclei of normal proliferating HDFs before and after the low serum incubation.**
Displays a juxtaposition of the chromosome 10 positioning graphs before and after the low serum assay in normal proliferating HDFs. Blue: chromosome 10 signals at 0 minute. Pink: chromosome 10 signal at 15 minutes.

3.1.2 Chromosome 10 positioning before and after the low serum assay in NMI depleted cells $[NMI^{(-)}]$

Low serum assay has been repeated using cells where the expression of the NMI has been suppressed using ON-TargetPlus NMI siRNA, then FISH images of Chromosome 10 territories at 0 minute ; before the low serum incubation and at 15 minutes, figure 3.6, then after 15 minutes of low serum incubation, figure3.7 have been subjected to simple erosion using IPlab.

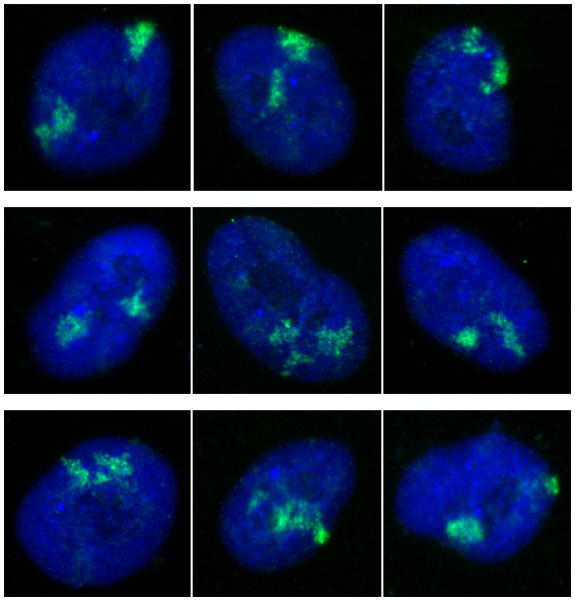

Figure 3.6: **Sample of chromosome 10 FISH images at 0 minute in NMI depleted cells.**
Representative images displaying nuclei prepared for fluorescence in situ hybridization (2D-FISH) before the low serum incubation of NMI depleted cells. With whole-chromosome 10 painting probes (green), nuclear DNA was counterstained with DAPI (blue).

Chromosome 10 position at 0 minute in $NMI^{(-)}$ nuclei

The results obtained from the erosion analysis of chromosome 10 FISH images at 0 minute (before the low serum assay), have been plotted in the chart below, Chromosome 10 signals are found to be the highest in shell 3 followed by shell 2, indicating an intermediate position of the chromosome 10 territories in nuclei where the expression of the NMI has been blocked using siRNA, figure 3.8.

Chromosome 10 position at 15 minutes in $NMI^{(-)}$ nuclei

The results obtained from the erosion analysis of chromosome 10 FISH images at 15 minutes (after the low serum assay), have been plotted in the chart below. this time also, Chromosome 10 signals are found to be the highest in shell 3 followed by shell 2, and 4 indicating an intermediate position of the chromosome 10 territories in $NMI^{(-)}$ nuclei after the low serum incubation, as shown in figure 3.9.

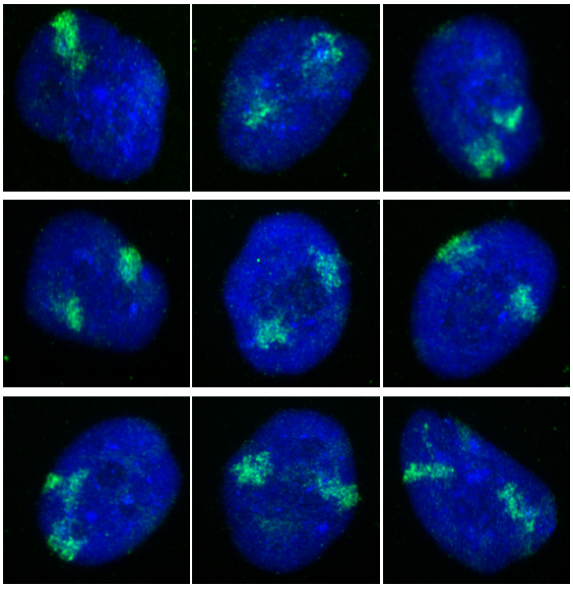

Figure 3.7: **Sample of chromosome 10 FISH images at 15 minute in NMI depleted cells.**

Representative images displaying nuclei prepared for fluorescence in situ hybridization (2D-FISH) after the low serum incubation of NMI depleted cells. With whole-chromosome 10 painting probes (green), nuclear DNA was counterstained with DAPI (blue).

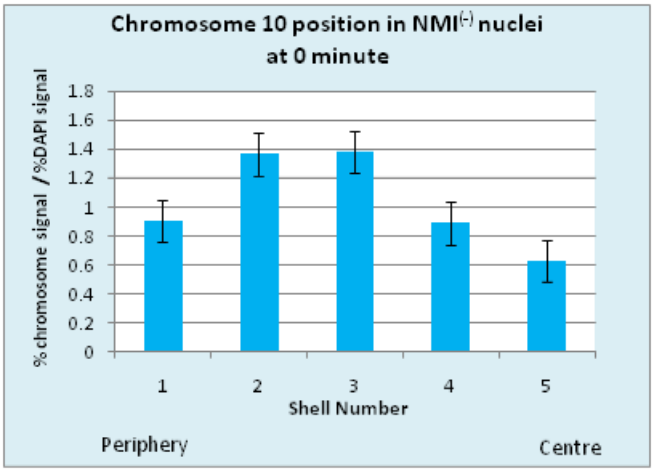

Figure 3.8: **Chromosome 10 positioning in NMI depleted nuclei before the low serum assay.**

Displays the distribution of the chromosome 10 signal for 2D FISH of $NMI^{(-)}$ nuclei before the low serum incubation of NMI depleted cells analysed with simple erosion analysis. The percentage of chromosome signal measured in each shell was divided by the percentage of DAPI signal in that shell. Bars represent the mean normalised percentage of chromosome 10 signal in each shell (1-5) with shell 5 being the most intern and 1 the most peripheral.

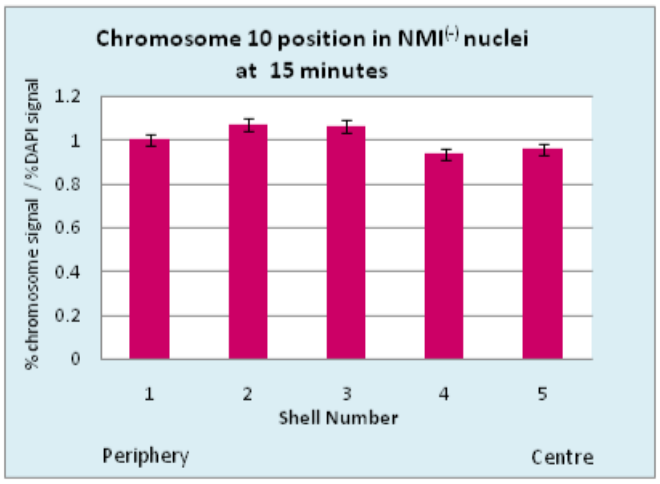

Figure 3.9: **Chromosome 10 positioning in NMI depleted nuclei after the low serum assay.**

Displays the distribution of the chromosome 10 signal for 2D FISH of $NMI^{(-)}$ nuclei after the low serum incubation of NMI depleted cells analysed with simple erosion analysis. The percentage of chromosome signal measured in each shell was divided by the percentage of DAPI signal in that shell. Bars represent the mean normalised percentage of chromosome 10 signal in each shell (1-5) with shell 5 being the most intern and 1 the most peripheral.

3.2 Chromosome X positioning

Chromosome X position in the nucleus was studied in normal proliferating HDF control, cells before the siRNA silencing of the nuclear myosin I; at 0 minute (before the low serum assay) then at 15 minute (after incubation in low serum medium for 15 minutes). The same study was repeated after the siRNA knock-down of the NMI gene. The results obtained from the IP-lab analysis of pro and post siRNA images of chromosome X before and after the low serum assay are displayed in charts as follows:

Chromosome X position at 0 minute in $NMI^{(+)}$ nuclei

Chromosome X in normal proliferating cells before the low serum assay (at 0 minute) has been confirmed to locate at the nuclear periphery as the highest cy3 signals were registered in shells 1 and 2, as shown in figure 3.10. the paired t test has confirmed the significant cy3 signal difference between shells 1 and 2 and the other shells.

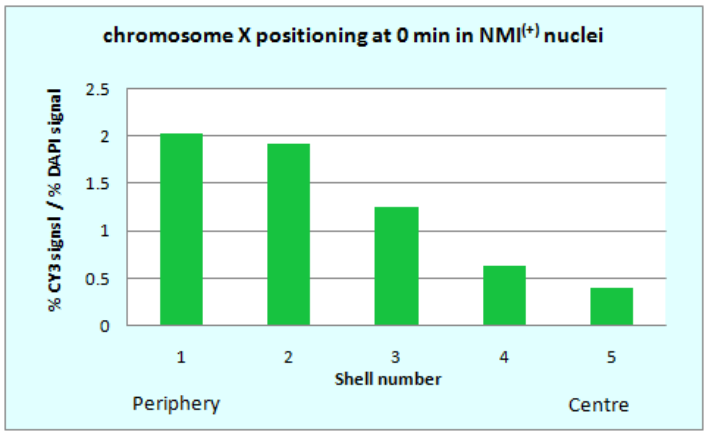

Figure 3.10: **Chromosome X positioning in NMI expressing nuclei at 0 minute.**
Displays the distribution of the chromosome X signal for 2D FISH before the low serum incubation, as analysed with erosion analysis. The percentage of chromosome X signal measured in each shell was divided by the percentage of DAPI signal in that shell. Bars represent the mean normalised percentage of chromosome signal in each shell (1-5) with shell 5 being the most intern and 1 the most peripheral.

Chromosome X position at 15 minutes in $NMI^{(+)}$ nuclei

After the low serum incubation, Chromosome X in normal proliferating HDFs nuclei is found to locate also to the periphery of the nucleus (figure 3.11), with the highest chromosome signal (cy3) in shell 1 followed by shell 2, and considerably lower signals in shells 3 and 4 and nearly null signal in shell 5. the paired t test for means has confirmed the significantly difference between signals in shells 1 and 2 and the rest of the shells.$p \leqslant 0.005$

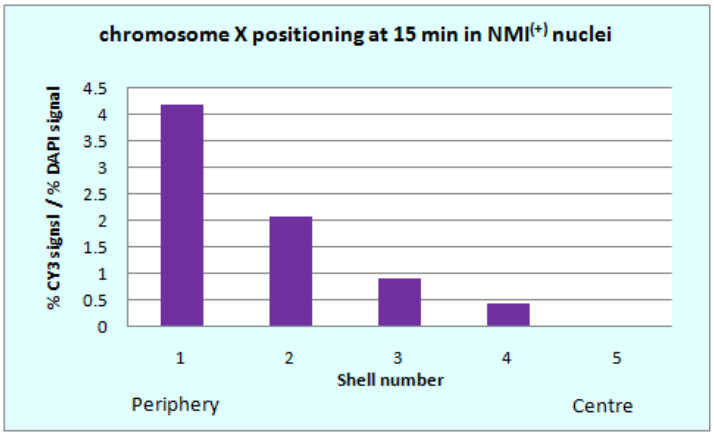

Figure 3.11: **Chromosome X positioning in NMI expressing nuclei at 15 minutes.**
Displays the distribution of the chromosome X signal for 2D FISH after the low serum incubation, as analysed with erosion analysis. The percentage of chromosome X signal measured in each shell was divided by the percentage of DAPI signal in that shell. Bars represent the mean normalised percentage of chromosome signal in each shell (1-5) with shell 5 being the most intern and 1 the most peripheral.

3.2.1 Chromosome X positioning before and after the low serum assay in NMI depleted cells $[NMI^{(-)}]$

Using NMI depleted cells, the low serum assay was repeated and FISH images of chromosome X before (at 0 minute) and after the low serum assay (at 15 minutes) have been treated through the IPLab simple erosion program. the chromosome signal (Cy3) in each shell was normalised to the DAPI signal and the mean result in each shell has been plotted in the charts below.

Chromosome X position at 0 minute in $NMI^{(-)}$ nuclei

It is evident from the distribution of the chromosome X signals, that this chromosome has a peripheral position in nuclei of NMI depleted HDFs before the low serum assay. with the highest Cy3 signal registered in shell 1 followed by shell 2, figure 3.12.

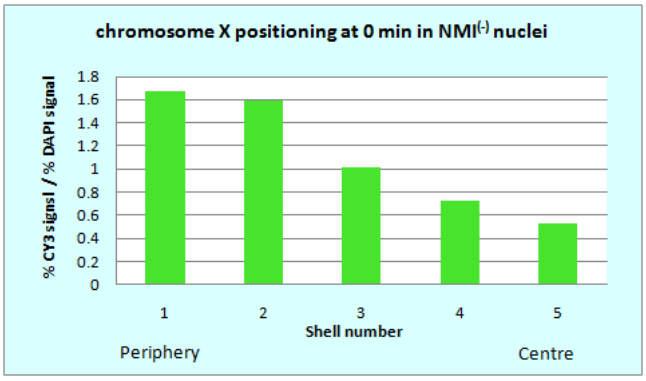

Figure 3.12: **Chromosome X positioning in NMI depleted cells at 0 minute.**
Displays the distribution of the chromosome X signal for 2D FISH of $NMI^{(-)}$ nuclei before the low serum incubation of NMI depleted cells, analysed with simple erosion analysis. The percentage of chromosome signal measured in each shell was divided by the percentage of DAPI signal in that shell. Bars represent the mean normalised percentage of chromosome X signal in each shell (1-5) with shell 5 being the most intern and 1 the most peripheral.

Chromosome X position at 15 minutes in $NMI^{(-)}$ nuclei

From the distribution of the Cy3 signals, this chromosome has also a peripheral position in the nuclei of NMI depleted HDFs after the low serum incubation. The highest Cy3 signal registered in shell 1 followed by shell 2, figure3.13.

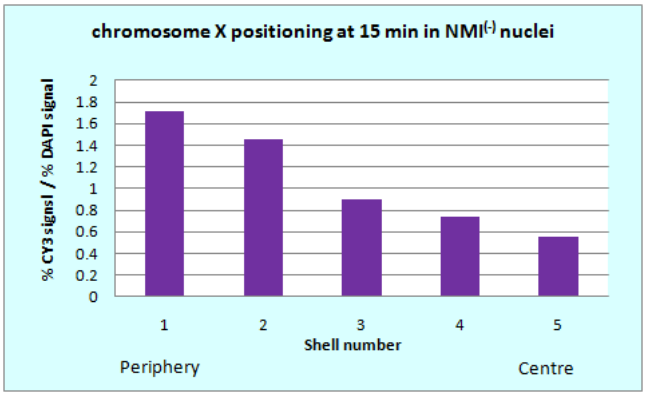

Figure 3.13: **Chromosome X positioning in NMI depleted cells at 15 minutes.**

Displays the distribution of the chromosome X signal for 2D FISH of $NMI^{(-)}$ nuclei after the low serum incubation of NMI depleted cells, analysed with simple erosion analysis. The percentage of chromosome signal measured in each shell was divided by the percentage of DAPI signal in that shell. Bars represent the mean normalised percentage of chromosome X signal in each shell (1-5) with shell 5 being the most intern and 1 the most peripheral.

conclusion

The study of chromosome 10 positions before and after the low serum assay has permitted the confirmation of the low serum induced chromosome 10 repositioning from an intermediate position to the periphery of the nucleus. In nuclei where the expression of the NMI has been suppressed using siRNA, chromosome 10 position before and after the low serum assay did not seem to have changed from the intermediate position. This indicates that the NMI is necessary for the low serum induced relocation of the chromosome 10 from the intermediate position to the peripheral location in interphase HDFs. On the other hand, chromosome X positioning analysis showed no significant changes of its position. Chromosome X was found to locate at nuclear periphery before and after the low serum assay in both, NMI depleted and expressing cells.

Chapter 4

Results: Image Analysis

4.1 Analysis of nuclear size

Introduction

The raw data obtained from Scion analysis of the nuclei and the chromosome territories were transferred to an Excel worksheet where data analysis tools have been utilized to compare the resulting means of each studied parameter. To test the statistical significance of any encountered differences, the T-test for unpaired samples assuming unequal variances has been employed; as is convention any tested difference is said to be statistically significant if the calculated t-Stat is bigger than the given t-Critical for two samples and the value of P is smaller than 0.05 at 95 % confidence intervals. Finally, results have been presented in charts to aid interpretation .

4.1.1 Investigating the effects of the low serum assay on the nuclear size

The aim of this study is to investigate any changes in nuclear size that may have occurred as a result of subjecting the cells to the low serum assay. Since we have already identified a strikingly rapid chromosome rearrangement as a result to incubating the cells in low serum for just 15 minutes. It was important

to these assay, to know whether this chromatin reorganization is accompanied by any changes in the nuclear size. To achieve this the nuclear sizes of randomly selected FISH images of normal proliferating HDF cells at 0 minute have been compared with the nuclear sizes at 15 minutes. The 0 minute refers to samples of FISH taken from cells before the low serum assay, while the 15 minutes refers to FISH samples taken from cells after the low serum assay (after the cells have been incubated in low serum for 15 minute). Only images of cells that had a positive pKi-67 staining were analysed. Three sets of 40 to 50 images have been analysed; the first set was of FISH images performed on cells at passage 12, the second and third sets of images are derived from the control cells used for the siRNA experiment, chromosome 10 and chromosome X images respectively.

First data set

The analysis of the nuclear area before and after the low serum assay in normal proliferating HDFs at passage 12 shows that the mean nuclear area of cells after the low serum assay is smaller than that of control cells (before the low serum assay), as displayed in figure 4.1. The two samples t-test assuming unequal variances shows a calculated value of t Stat = 3.03 > t critical two tails = 1.99 and $P = 0.003$ suggesting that the difference observed between the nuclear size at 0 and 15 minutes is statistically significant. Results are listed in table 4.1

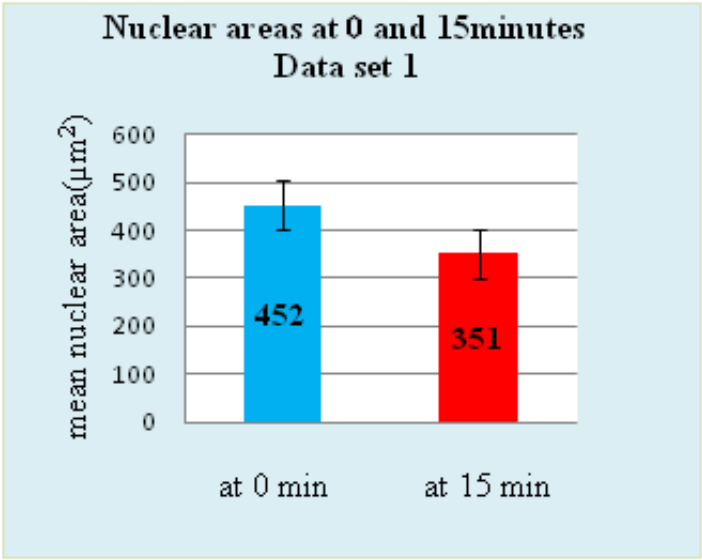

Figure 4.1: **First comparison of the means nuclear area before and after the low serum assay.**
Blue: nuclear area at 0 minute or before the low serum incubation, Red:nuclear area at 15 minute after the low serum incubation, all measurements are shown in μm^2

t-Test: Two-Sample Assuming Unequal Variances		
	Nuclear area at 0 min	**Nuclear area at 15 min**
Mean	452.46	350.31
Variance	26898.77	18275.97
Observations	40	40
Hypothesized Mean Difference	0	
df	75	
t Stat	3.03951	
p(T<=t) one-tail	0.001631	
t Critical one-tail	1.665425	
p(T<=t) two-tail	0.003262	
t Critical two-tail	1.992102	

Table 4.1: Significance test for the nuclear size difference before and after low serum assay, data set 1.

Second data set

The analysis of the nuclear area before and after the low serum assay in normal proliferating HDF was repeated using FISH images from cells at passage 10. From the results of this analysis it seems that the nuclear area is also smaller after the low serum treatments of the cells, as shown in figure 4.2.

The t-test this time shows that this difference is statistically insignificant with a t Stat<t Critical two tails and p=0.13, results are displayed in table 4.2

t-Test: Two-Sample Assuming Unequal Variances		
	Nuclear area at 0 min	**Nuclear area at 15 min**
Mean	725.334	659.69
Variance	50240.29954	44060.4481
Observations	50	50
Hypothesized Mean Difference	0	
df	98	
t Stat	1.51155	
p(T<=t) one-tail	0.066933	
t Critical one-tail	1.660551	
$\boldsymbol{p}$T<= t two-tail	0.133866	
t Critical two-tail	1.984467	

Table 4.2: Significance test for the nuclear size difference before and after low serum assay, data set 2.

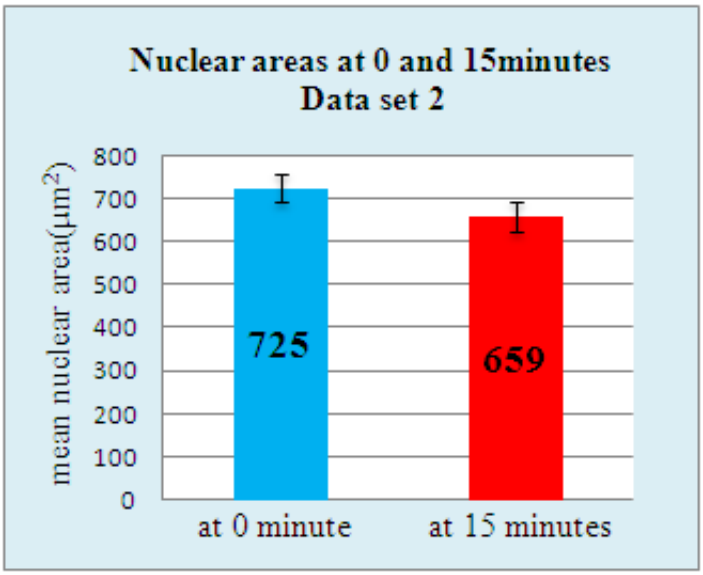

Figure 4.2: **Second comparison of the means nuclear area before and after the low serum assay.**
Blue: nuclear area at 0 minute or before the low serum incubation, Red : nuclear area at 15 minute after the low serum incubation, all measurements are shown in μm^2

Third data set

The analysis of the nuclear area before and after the low serum assay in normal proliferating HDF has been repeated using a third set of FISH images from cells from the same passage 10 as the previous one. From the results of this analysis it seems that the mean nuclear area is bigger, after the low serum treatments of the cells, figure 4.3, but the t-test this time shows that this difference is statistically insignificant (t Stat $<$ t Critical two tails and $p = 0.14$). The results are displayed below in in the table 4.3.

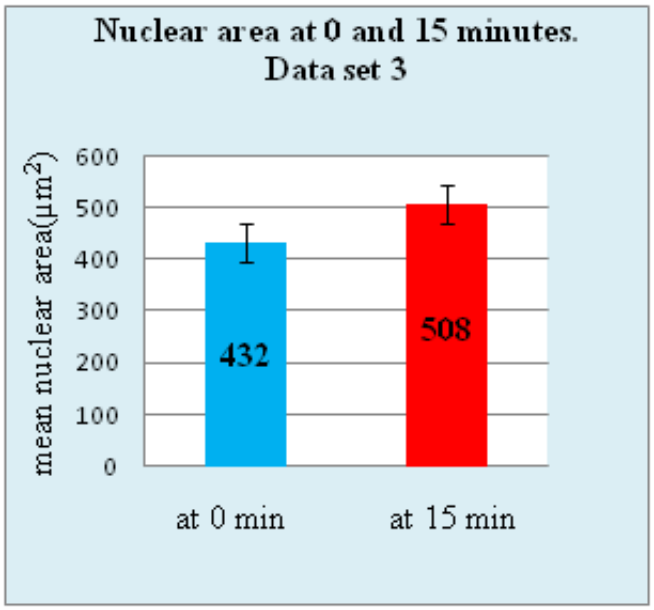

Figure 4.3: **Third comparison of the means nuclear area before and after the low serum assay.**
Blue: nuclear area at 0 minute or before the low serum incubation, Red:nuclear area at 15 minute after the low serum incubation, all measurements are shown in μm^2.

t-Test: Two-Sample Assuming Unequal Variances		
	Nuclear area at 0 min	**Nuclear area at 15 min**
Mean	433.19	508.2881
Variance	62326.4	45818.15
Observations	42	42
Hypothesized Mean Difference	0	
df	80	
t Stat	-1.47996	
p(T<=t)one-tail	0.071405	
t Critical one-tail	1.664125	
p(T<=t) two-tail	0.14281	
t Critical two-tail	1.990063	

Table 4.3: Significance test for the nuclear size difference before and after low serum assay, data set 3

Conclusion

There is no significant difference between the nuclear size of cells subjected to the low serum assay and control cells. Initially, it seemed that the nuclear size had become smaller after incubating the cells in low serum for 15 minutes when

compared to the size of nuclei of control cells (data set 1 and 2). To test the significance of this difference of mean nuclei areas between 0 and 15 minute, a two samples t-test for unequal variances have been calculated. While, the calculated t-test for the first set of data showed that the observed difference between the nuclei sizes at 0 and 15 minutes was significant (t stat = 3.03 > t critical two tails = 1.99; $p = 0.003$), the second t-test for data set 2 was found to be insignificant (t stat = 1.51< t critical two tails = 1.98; $p = 0.066$). In data set 3 a different trend was observed; it appeared that the nuclear size increased after the low serum incubation of the cells, this time again the t-test has indicated that this difference observed between the nuclei size at 0 and 15 minutes is statistically insignificant (t stat = 1.47 < t critical two tails = 1.99 ; p= 0.07). It is evident that the differences observed in the nuclei size between the cells that have been subjected to the low serum assay and those that have not been, is statistically insignificant, therefore there are no notable changes in the nuclei size when the cells have been incubated in low serum for 15 minutes. Thus, subjecting the cells to the low serum assay has not induced any significant changes in the nuclear area.

4.1.2 Investigating effects of the siRNA- mediated suppression of NMI on the nuclear size

The aim of this part of the study was to investigate whether the siRNA-mediated knock down of nuclear myosin I protein resulted in any changes in the overall nuclear size of the cells. This was achieved by conducting a series of comparisons of the mean nuclear area of cells where the siRNA transfection have been used to block the expression of the nuclear myosin I with control cells that have not been transfected. Next the comparison of the nuclear size before and after the low serum assay has been repeated in cells where the NMI gene has been silenced. Then comparing the mean nuclear area of cells incubated in low serum for 15 minutes before and after the nuclear myosin I has been silenced, as follows. Whenever, a significant difference between the $NMI^{(+)}$ nuclei and the $NMI^{(-)}$

had arisen, the results were compared to the negative control (cells transfected using the same reagents as used for the NMI transfection but with no NMI targeting constructs) to confirm that the observed difference has resulted from the depletion of the NMI and not from the transfection itself.

1. Comparison of nuclear size before and after the siRNA-mediated knock down of the NMI (comparing area of $NMI^{(+)}$ or control and area of $NMI^{(-)}$ nuclei)

2. Repeat the low serum comparison in NMI silenced nuclei (comparing area of $NMI^{(-)}$nuclei at 0 minute and $NMI^{(-)}$nuclei at 15 minute of low serum assay

3. Comparison of the nuclear area after the low serum incubation before and after blocking the expression of the NMI (control nuclei($NMI^{(+)}$) at 15 minutes and ($NMI^{(-)}$) at 15 minutes)

1. Comparison of nuclear size before and after the siRNA-mediated knock down of the NMI

To investigate whether silencing the NMI gene has affected the overall nuclear size, a comparison of nuclear size before and after the siRNA-mediated knock down of the NMI has been done, at first nuclei expressing NMI($NMI^{(+)}$) seemed to be smaller as compared to nuclei where the NMI expression has been blocked [$NMI^{(-)}$] as shown in figure 4.4 , but the the calculated two tails unpaired t test has confirmed this difference to be statistically insignificant, P(T<=t) two-tail = 0.31, as displayed in table 4.4

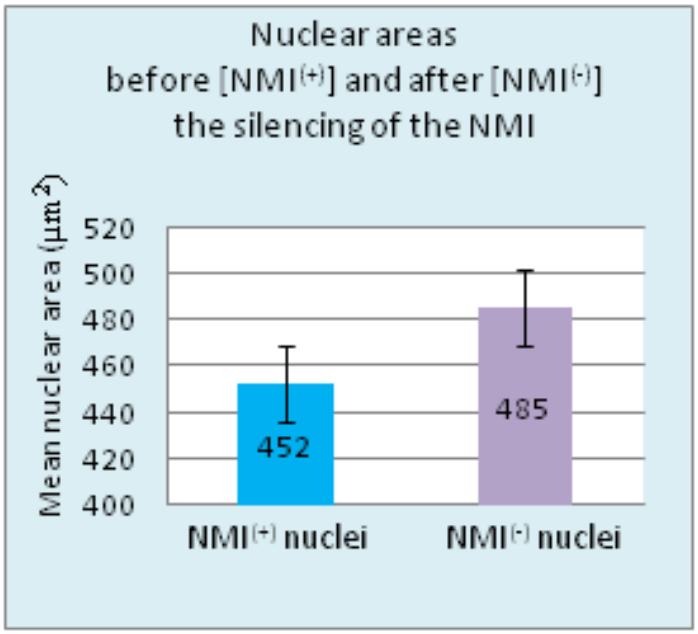

Figure 4.4: **Comparison of the means nuclear area before and after the silencing of the NMI.**

Blue: nuclear area at before the siRNA knock down of the NMI , Purple: nuclear area after the siRNA knock down of the NMI, standard error bars have been plotted, all measurements are shown in μm^2

t-Test: Two-Sample Assuming Unequal Variances		
	Mean area of $NMI^{(+)}$	Mean area of $NMI^{(-)}$ nuclei
Mean	452.3768	485.704
Variance	0.002179	0.003219
Observations	50	50
Hypothesized Mean Difference	0	
df	93	
t Stat	-1.00804	
P(T<=t) one-tail	0.157972	
t Critical one-tail	1.660715	
P(T<=t) two-tail	0.315943	
t Critical two-tail	1.984723	

Table 4.4: Significance test for the difference in nuclear area before and after the silencing of the NMI.

2. Comparison of the nuclei size before and after the low serum assay in NMI depleted nuclei($NMI^{(-)}$)

The low serum assay has been repeated using cells where the expression of the NMI has been blocked using siRNA ($NMI^{(-)}$). To investigate whether

subjecting $NMI^{(-)}$ cells to low serum assay has resulted in any significant changes in the average nuclear size. Two sets of 40 to 50 randomly selected FISH images of cells at passage 10 where the NMI gene (*MYO1C*) has been knocked down using siRNA have been analysed, as follows.

First set of data

At first instance it seemed that in nuclear myosin I depleted cells, the nuclei were getting slightly smaller after the low serum assay (at 15 minutes) compared to the initial size before the low serum incubation (at 0 minute), figure 4.5. To test the significance of this difference of nuclear size at 0 and 15 minutes a two-sample t-test assuming unequal variances has been performed which has confirmed the non significance of this difference with p value $= 0.61$, as detailed in table 4.5. This means that there is no statistically significant difference in mean nuclear area before and after the low serum assay in cells after that the expression of the NMI has been impaired.

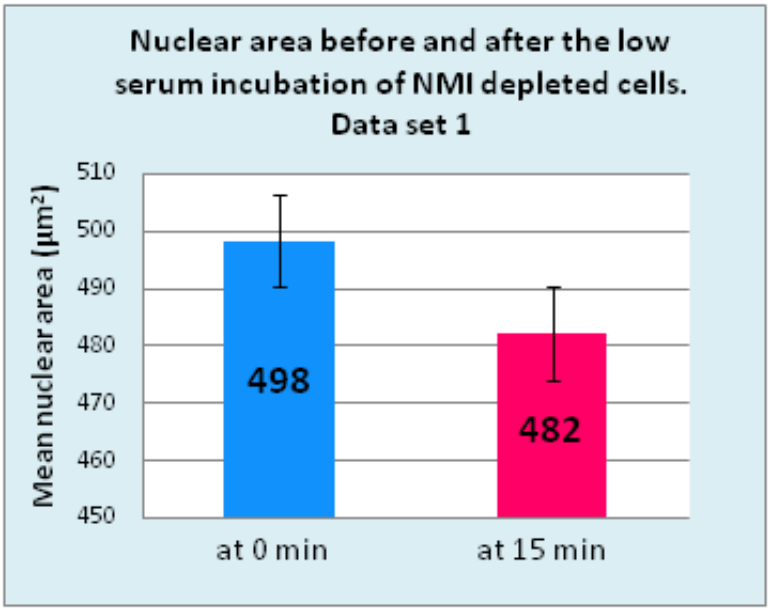

Figure 4.5: **Comparison of the means nuclear area before and after the low serum incubation in NMI depleted cells, data set 1.**
Blue: nuclear area at 0 minute (before the low serum assay) , pink : nuclear area at 15 minutes (after the low serum assay), standard error bars have been plotted, all measurements are shown in μm^2

t-Test: Two-Sample Assuming Unequal Variances		
	$NMI^{(-)}$ **nuclear area at 0 min**	$NMI^{(-)}$ **nuclear area at 15 min**
Mean	498.3443	482.0804
Variance	28316.65	24757.53
Observations	51	51
Hypothesized Mean Difference	0	
df	100	
t Stat	0.50416	
p(T<=t)one-tail	0.307629	
t Critical one-tail	1.660234	
p(T<=t) two-tail	0.615258	
t Critical two-tail	1.983971	

Table 4.5: Significance test for the nuclear size difference before and after low serum assay, in NMI depleted nuclei. data set 1

Second set of data

The analysis of this second set of images revealed that the nuclear size at 15 minutes of the low serum assay is much bigger compared to the nuclear area at 0 minute figure 4.6. The calculated t-test has confirmed this to be statistically significant, p value = 1.37×10^{-6}, result displayed in table 4.6. It seems that incubating NMI depleted cells in low serum for 15 minutes has resulted in an increase in the mean nuclear area of these cells.

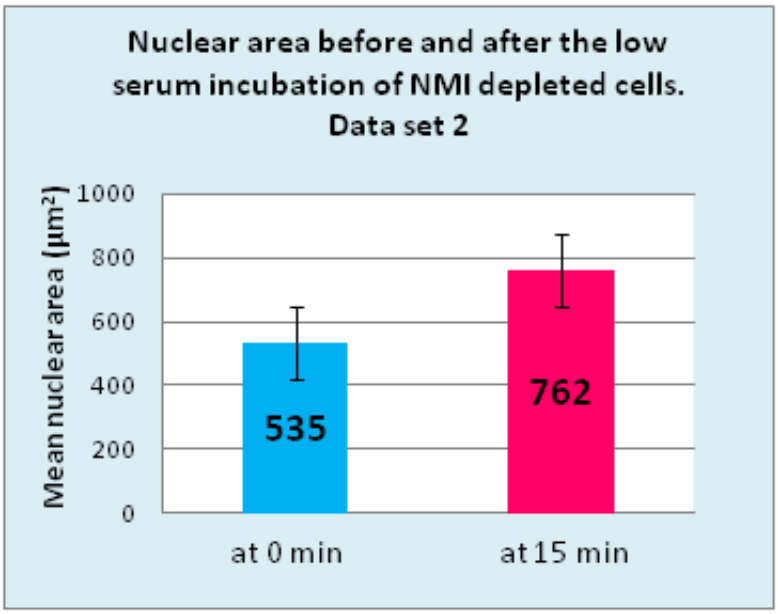

Figure 4.6: **Comparison of the means nuclear area before and after the low serum incubation of NMI depleted cells, data set 2**
Blue : nuclear area at 0 minute (before the low serum assay) , pink : nuclear area at 15 minutes (after the low serum assay), standard error bars have been plotted, all measurements are shown in μm^2

t-Test: Two-Sample Assuming Unequal Variances		
	$NMI^{(-)}$ **nuclear area at 0 min**	$NMI^{(-)}$ **nuclear area at 15 min**
Mean	535.8689	762.3461
Variance	24534.23	57182.38
Observations	44	44
Hypothesized Mean Difference	0	
df	74	
t Stat	-5.25528	
p(T<=t)one-tail	6.87×10^{-07}	
t Critical one-tail	1.665707	
p(T<=t) two-tail	1.37×10^{-06}	
t Critical two-tail	1.992543	

Table 4.6: Significance test for the nuclear size difference before and after low serum assay, in NMI depleted nuclei. data set 2

In order to check whether the increase of the nuclear size in data set 2, observed after incubating the NMI depleted cells in low serum for 15 minutes was actually due to the absence of the NMI from the nucleus or was just reflecting

a natural variation of the cells population; we repeated the same analysis in negative control (NMI^{-c}) cells (cells transfected using non targeting siRNA). The result obtained were similar to the previously observed difference in data set 2 of the NMI knocked down cells with a nuclear area after the 15 minutes low serum incubation much more bigger then the nuclear area at 0 minute (cells that have not been incubated in low serum media). As shown in figure 4.7, the t test in this case, showed that this difference is significant; p value $=6.98\times10^{-11}$ as displayed in table 4.7.

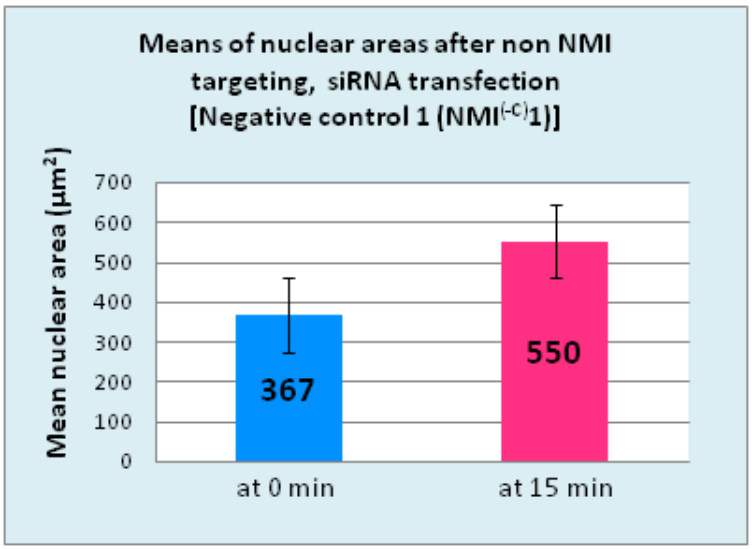

Figure 4.7: **Comparison of the means nuclear area before and after the low serum incubation of non NMI targeting siRNA transfected nuclei 1.**

Blue: nuclear area at 0 minute (before the low serum assay), Pink: nuclear at 15 minutes(after the low serum assay), standard error bars have been plotted, all measurements are shown in μm^2

t-Test: Two-Sample Assuming Unequal Variances		
	$NMI^{(-C)}$ **nuclear area at 0 min**	$NMI^{(-C)}$ **nuclear area at 15 min**
Mean	367.2568	550.99
Variance	8006.035	19832.3
Observations	47	47
Hypothesized Mean Difference	0	
df	78	
t Stat	-7.54944	
p(T<=t)one-tail	3.49×10^{-11}	
t Critical one-tail	1.664625	
p(T<=t) two-tail	6.98×10^{-11}	
t Critical two-tail	1.990847	

Table 4.7: Significance test for the nuclear size difference before and after low serum assay, in negative control($NMI^{(-C)}$)cells, 1.

Since the comparisons of nuclear size before and after the low serum assay in this first set of siRNA negative control ($NMI^{(-C)}$) cells showed a similar trend compared to the data set 2 of the NMI depleted cells (bigger nuclei after the low serum incubation) it became obvious that silencing the NMI could not justify the difference in measured nuclei sizes before and after the low serum assay. In order to test the probability that the transfection procedure is responsible for this difference, the same analysis has been carried out using a second set of siRNA negative control cells (cells transfected using non targeting siRNA oligonucleotides). This time, the mean nuclear area at 15 minutes seemed to be just above the mean nuclear area at 0 minute, figure 4.8. the t test has confirmed this difference to be insignificant with a p value = 0.76, as displayed in table 4.8.

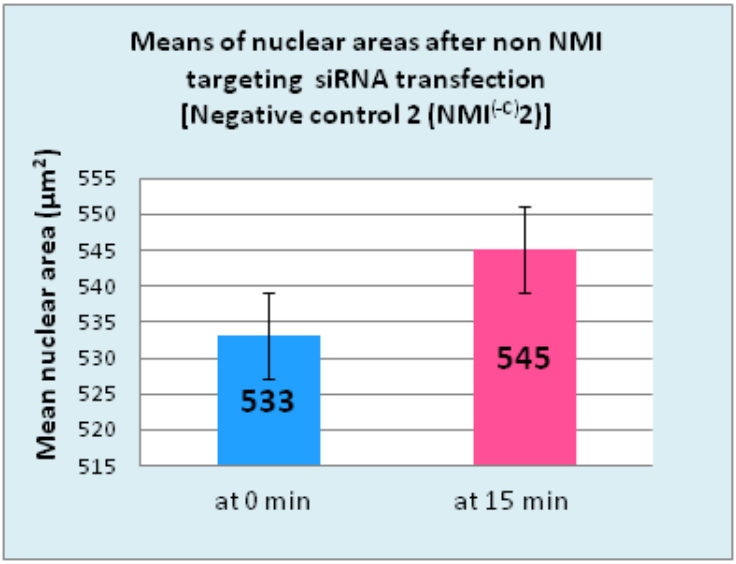

Figure 4.8: **Comparison of the means nuclear area before and after the low serum incubation in non NMI targeting siRNA transfected nuclei 2.**

Blue: nuclear area at 0 minute (before the low serum assay) , Pink: nuclear area at 15 minutes (after the low serum assay), standard error bars have been plotted, all measurements are shown in μm^2

t-Test: Two-Sample Assuming Unequal Variances		
	$NMI^{(-C)}$ nuclear area at 0 min	**$NMI^{(-C)}$ nuclear area at 15 min**
Mean	533.1143	545.14152
Variance	42010.3844	28953.94272
Observations	46	46
Hypothesized Mean Difference	0	
df	87	
t Stat	0.306212181	
p(T<=t)one-tail	0.380087344	
t Critical one-tail	1.66255735	
p(T<=t) two-tail	0.760174687	
t Critical two-tail	1.987608241	

Table 4.8: Significance test for the nuclear size difference before and after low serum assay, in siRNA NMI negative control(NMI$^{(-C)}$)nuclei, 2.

Conclusion

The comparison of the nuclear size at 0 and 15 minutes of the low serum assay after the NMI depletion, has revealed a significant increase in nuclear size after

the low serum incubation in one set of data while no significant change has been registered in the other set. A comparable pattern has been identified in negative control cells (cells that have been transfected using non targeting siRNA) obtained from cells issued from the same culture as data set 2. In this case also, a significantly larger mean nuclear area at 15 minutes compared to 0 minute was registered. Thus, we can conclude that even so there was significant difference between nuclear areas before and after the low serum incubation in NMI depleted nuclei, the observed difference could not have been caused by the silencing of the NMI, since a comparable difference was also observed in negative control cells where the NMI has not been targeted by the siRNA (negative control 1). The probability that this difference could be have been due the transfection procedure itself, has been eliminated because, a separately non targeting siRNA transfected sample (negative control 2) showed no significant difference in the nuclear size before and after the low serum assay. Thus, the apparent increase in nuclear size after the low serum incubation observed in only one cells sample could not have been induced by the siRNA transfection nor by the NMI depletion, as other samples showed no significant difference in nuclear size before and after the low serum incubation. Hence, this difference was probably secondary to sample variations; repeating similar experiments in the future should provide us with more conclusive evidence.

4.2 Analysis of the nuclear shape

The aim of this study is to investigate if there are any changes in nuclear shape that may have occurred as a result of silencing the nuclear myosin 1 gene by siRNA, or that may be caused by the low serum assay before and/or after the siRNA knockdown of the nuclear myosin I. We looked at the overall shape of nuclei by calculating the nuclear roundness or contour ratio (4Π area/perimeter^2). The contour ratio for a circle is 1 and this ratio approaches 0 as the nucleus becomes more lobulated (Erikson et al 2004). The values of the area and nuclear perimeter were obtained using the Scion image program, the rest of the calculations were performed on an excel worksheet, then the t-test was used to determine the significance of the findings.

4.2.1 Investigating the effect of the low serum assay on nuclear shape

In order to identify whether the low serum assay has had any effects on the nuclear shape, we compared the results of the calculated nuclear contour ratio (4Π area/perimeter^2) in normal proliferating cells before the low serum assay (at 0 minute) with the nuclear contour ratio after the low serum incubation (at 15 minutes). All the compared cells were from same cultures at same passage, and fixed using the same procedure described in section 2.2.3 of chapter 2. The results of the calculated contour ratio at 0 minute and 15 minutes, were quite similar at (0.38) and (0.37) respectively results. To evaluate how significant these results , a t-test for two samples assuming unequal variances has been calculated which confirmed that the difference between the contour ratio of cells at 0 minute and 15 minutes is statistically insignificant with a value of $p = 0.68$, details of the t-test are displayed in table 4.9. This suggested that there is no significant difference between the nuclear shape before and after the low serum assay, hence subjecting the cells to low serum for 15 minutes had no significant effect on the nuclear shape.

t-Test: Two-Sample Assuming Unequal Variances		
	Nuclei contour ratio at 0 min	Nuclei contour ratio at 15 min
Mean	0.380799	0.377022
Variance	0.002185	0.002169
Observations	50	50
Hypothesized Mean Difference	0	
df	98	
t Stat	0.404686	
P(T<=t) one-tail	0.343295	
t Critical one-tail	1.660551	
P(T<=t) two-tail	0.68659	
t Critical two-tail	1.984467	

Table 4.9: Significance test for the difference in nuclear contour ratio before and after the low serum assay

4.2.2 Investigating the effect of NMI silencing on nuclear shape

To investigate whether the siRNA knock down of the nuclear myosin I has resulted in any changes in the nuclear shape, a comparison of the calculated nuclear contour ratio was performed. First, this ratio was compared between cells transfected with non targeting control siRNA and cells transfected with NMI-targeting siRNA. The calculated nuclear contour ratio was then compared in cells after they were subjected to the low serum assay for 15 minutes. Next the comparison of the nuclear roundness before and after the low serum assay has been performed on cells where the NMI gene has been silenced. In addition, the nuclear shape comparison before and after the low serum assay has been repeated in siRNA negative control cells (cells that have been transfected with the same reagent used for the knockdown of the NMI but with no siRNA sequences/oligonucleotides).

Comparison of the nuclear shape of $NMI^{(+)}$ and $NMI^{(-)}$ at 0 minute

Using the blue channel (DAPI channel) images obtained from colour split of FISH images of NMI expressing nuclei (figure 4.9), and NMI depleted nuclei (figure 4.10) on the Scion image analysis software, the area and the perimeter of each nuclei have been measured.

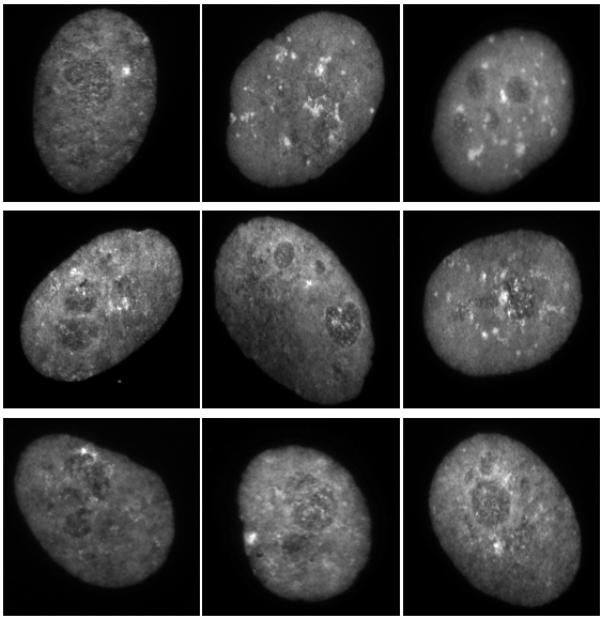

Figure 4.9: **HDFs, $NMI^{(+)}$ nuclei at 0 minute.**
displays the blue channel of the FISH images of nuclei expressing the NMI before the low serum assay, were obtained by colour channels spliting using the Corel software. the blue channel corresponds to the DAPI staining (nuclei).

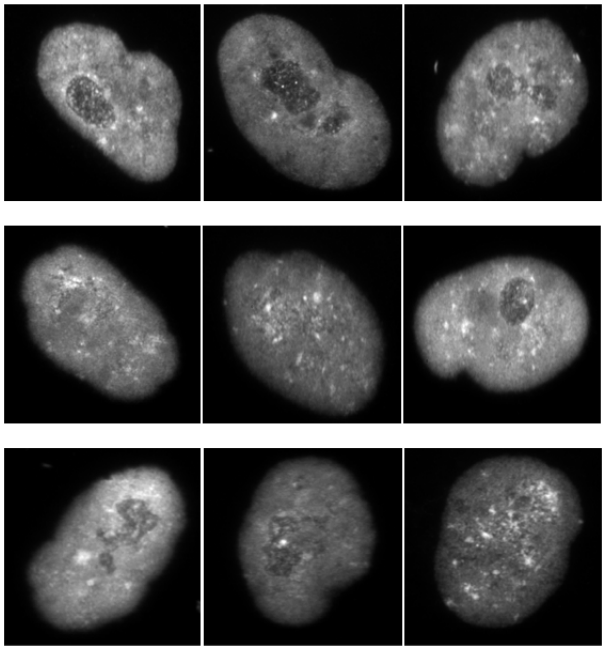

Figure 4.10: **HDFs, $NMI^{(-)}$ nuclei at 0 minute.**
displays the blue channel of the FISH images NMI depleted nuclei before the low serum assay, were obtained by colour channels spliting using the Corel software. the blue channel corresponds to the DAPI staining (nuclei).

First data set

Using area and perimeter measurements of cells at 0 minute (before the low serum assay) of the control cells, and similar measurements of cells at 0 minute of nuclear myosin I supressed cells, the contour ratio for each set of cells was calculated and compared, the results were respectively (=0.38) and (=0.32) . The t-test has confirmed that this difference between the nuclear contour at 0 minute before and after siRNA knockdown of the NMI, is statistically significant (P= 1.49×10^{-7}) as shown in table 4.10. In other words, nuclear shape of cells at 0 minute is significantly different from the nuclei shape of similar cells after that the NMI gene have been silenced with nuclei getting more lobulated after the siRNA.

t-Test: Two-Sample Assuming Unequal Variances		
	Contour ratio of $NMI^{(+)}$ nuclei at 0 min	Contour ratio of $NMI^{(-)}$ nuclei at 0 min
Mean	0.380799	0.325588
Variance	0.002185	0.002562
Observations	50	50
Hypothesized Mean Difference	0	
df	97	
t Stat	5.666532	
P(T<=t) one-tail	7.47E-08	
t Critical one-tail	1.660715	
P(T<=t) two-tail	1.49E-07	
t Critical two-tail	1.984723	

Table 4.10: Significance test for the difference in nuclear contour ratio before and after the silencing of the NMI

Second data set

To verify whether these changes in nuclear lobulation followed a general trend, a second set of images have been used to repeat the same study. It was evident this time that this second set of data showed a different trend then what was previously described in table 4.11. The nuclear contour ratio at 0 minutes before the siRNA knock down of the NMI was found this time to be bigger after the

NMI suppression. Despite fact that these findings are opposite to the results obtained from the previous analysis , the calculated t-test has also confirmed their significance, $p = 0.02$, as detailed in table 4.9.

t-Test: Two-Sample Assuming Unequal Variances		
	Contour ratio of $NMI^{(+)}$ nuclei at 0 min	Contour ratio of $NMI^{(-)}$ nuclei at 0 min
Mean	0.326362	0.360738
Variance	0.006204	0.002565
Observations	42	42
Hypothesized Mean Difference	0	
df	70	
t Stat	-2.379	
P(T<=t) one-tail	0.010045	
t Critical one-tail	1.666914	
P(T<=t) two-tail	0.020091	
t Critical two-tail	1.994437	

Table 4.11: Significance test for the difference in nuclear contour ratio before and after the silencing of the NMI

While the the calculated contour ratio for the First data seemed to become smaller for nuclei where the expression of the NMI has been blocked , the second data set showed an opposite trend with a bigger nuclear contour ratio in NMI depleted nuclei. Meanwhile, the t test has confirmed both differences to be significant.

Comparison of the nuclear shape of $NMI^{(+)}$ and $NMI^{(-)}$ at 15 minute

To asses the possible effects of the low serum incubation on the nuclear shape of NMI depleted cell ($NMI^{(-)}$) , a comparison of the nuclear contour ratio has been was established between normal proliferating cells ($NMI^{(+)}$) that have been incubated in low serum for 15 minutes (figure 4.11) and cells where the NMI expression has been suppressed by the siRNA then incubated in low serum (figure 4.12).

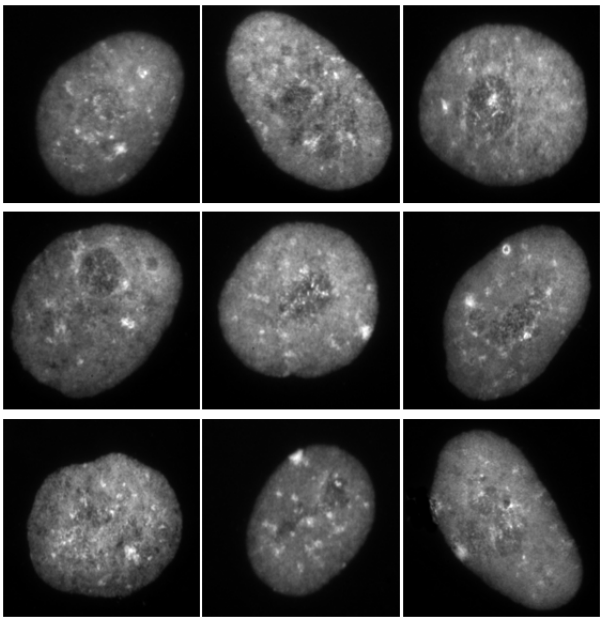

Figure 4.11: **HDFs, $NMI^{(+)}$ nuclei at 15 minutes**
displays the blue channel of the FISH images of nuclei expressing the NMI after the low serum assay, were obtained by colour channels spliting using the Corel software. the blue channel corresponds to the DAPI staining (nuclei).

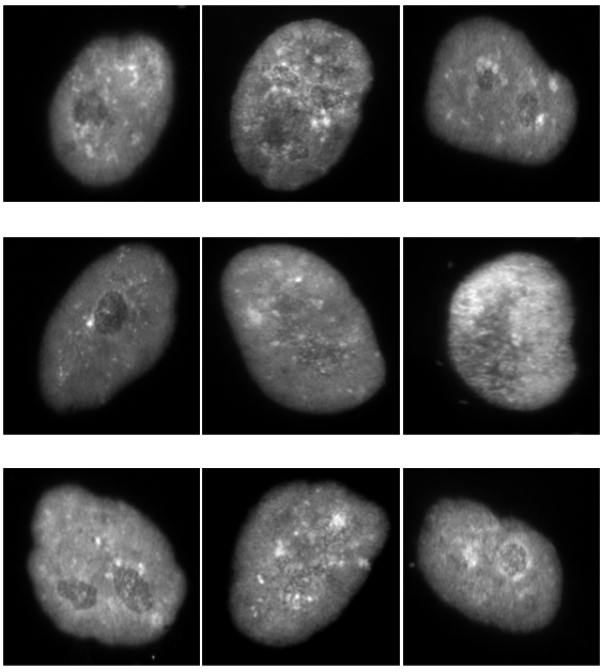

Figure 4.12: **HDFs, $NMI^{(-)}$ nuclei at 15 minutes**
displays the blue channel of the FISH images NMI depleted nuclei after the low serum assay, were obtained by colour channels spliting using the Corel software. the blue channel corresponds to the DAPI staining (nuclei).

The results showed a smaller roundness ratio at 15 minutes for nuclei non expressing the NMI suggesting that they are more lobulated than the nuclei of cells expressing the NMI after the low serum incubation. The calculated t test has confirmed this difference to be statistically significant with a p value = 0.015, as shown in table 4.12

t-Test: Two-Sample Assuming Unequal Variances		
	Contour ratio of $NMI^{(+)}$ nuclei at 15 min	Contour ratio of $NMI^{(-)}$ nuclei at 15 min
Mean	0.377861	0.352056
Variance	0.002179	0.003219
Observations	49	49
Hypothesized Mean Difference	0	
df	93	
t Stat	2.458648	
P(T<=t) one-tail	0.007898	
t Critical one-tail	1.661404	
P(T<=t) two-tail	0.015797	
t Critical two-tail	1.985802	

Table 4.12: Significance test for the difference in nuclear contour ratio before and after the silencing of the NMI at 15 minute of the low serum assay

In order to verify whether these changes in nuclear lobulation represent a general trend, a second set of images have been used to repeat the same study. This second set of data showed a similar trend, with a significantly smaller nuclear contour ratio of $NMI^{(-)}$ at 15 minutes compared to $NMI^{(+)}$ at 15 minutes. The p value = 0.05, as shown in table 4.13.

t-Test: Two-Sample Assuming Unequal Variances		
	Contour ratio of $NMI^{(+)}$ nuclei at 15 min	Contour ratio of $NMI^{(-)}$ nuclei at15 min
Mean	0.353302	0.376605
Variance	0.002744	0.003369
Observations	44	44
Hypothesized Mean Difference	0	
df	85	
t Stat	-1.97708	
P(T<=t) one-tail	0.025637	
t Critical one-tail	1.662979	
P(T<=t) two-tail	0.051274	
t Critical two-tail	1.988268	

Table 4.13: Significance test for the difference in nuclear contour ratio before and after the silencing of the NMI at 15 minute of the low serum assay, 2

Conclusion

It has emerged from the previous analysis that there is no significant change in the nuclear roundness ratio of nuclei after the the cells are subjected to the low serum assay, meaning that incubating the cells in low serum assay for 15 minutes had not affected the overall shape of the nuclei. On the other hand, the silencing of the nuclear myosin I has resulted in a statistically significant difference of the calculated nuclear contour ratio, between the NMI expressing cells and the NMI depleted cells. The roundness ratio was found to significantly increase in one of the analysed set of images, giving indication that the nuclei lacking the NMI are significantly more lobulated compared to the cells expressing the NMI, it has been also found to significantly decrease in the other set of images. In addition, the comparison of the nuclear shape after the low serum assay in cells expressing the NMI and in cells depleted of the NMI has revealed that, subjecting the cells where the NMI expression has been suppressed to the serum incubation, resulted in the nuclei to become more lobulated. Therefore more comparison analysis needs to be carried out to determine whether other factors beside the nuclear myosin I knock down determine the trend of these changes and thus the nuclear shape.

4.3 Image analysis of chromosome 10 and X territories

Chromosome 10 and X territories have been chosen for the image analysis study because of their distinct behavior towards the low serum incubation, while chromosome 10 was found to relocate from an intermediate to a peripheral position after the low serum incubation, chromosome X was found to remain at the nuclear periphery, from this point it was important to know these two chromosomes territories exhibited any changes secondary to the low serum incubation. Furthermore, the effect of the NMI suppression on these chromosome territories have been investigated. the sizes chromosome 10 and X territories have been measured using the Scion image analysis software. using the green channel of the respective FISH images.

4.3.1 Image analysis of chromosome 10 territories

Using the green channel of the FISH images of chromosome 10 territories obtained before (figure 4.13) and after (figure 4.19) the low serum assay; the size of the chromosome territory has been measured by the Scion image analysis program then the results we compared and unpaired two sample t test was calculated to asses the significance of any resulting difference.The same analysis has been repeated using images of cells where the NMI expression has been blocked using siRNA.

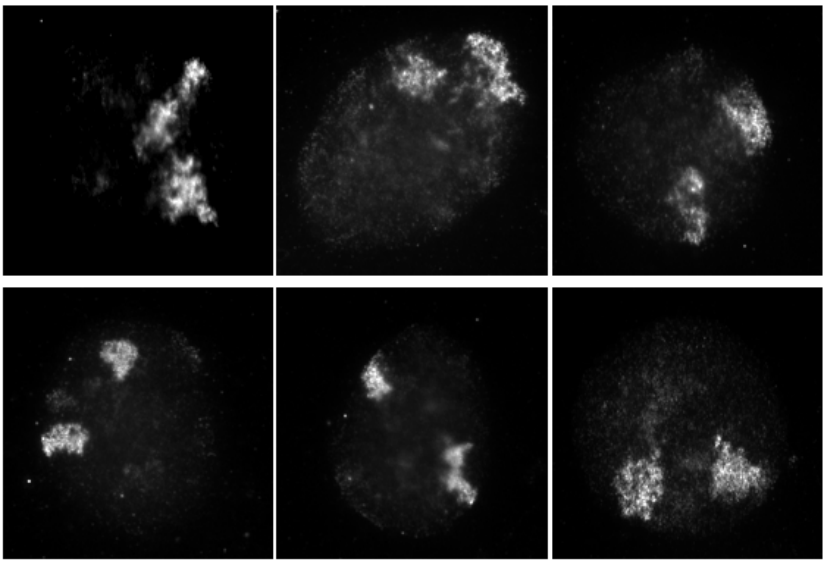

Figure 4.13: **Green channel of FISH images of chromosome 10 at 0 minute.**

displays the green channel of the FISH images of nuclei expressing the NMI before the low serum assay, were obtained by colour channels spliting using the Corel software. the green channel corresponds to the Cy3 staining (CT).

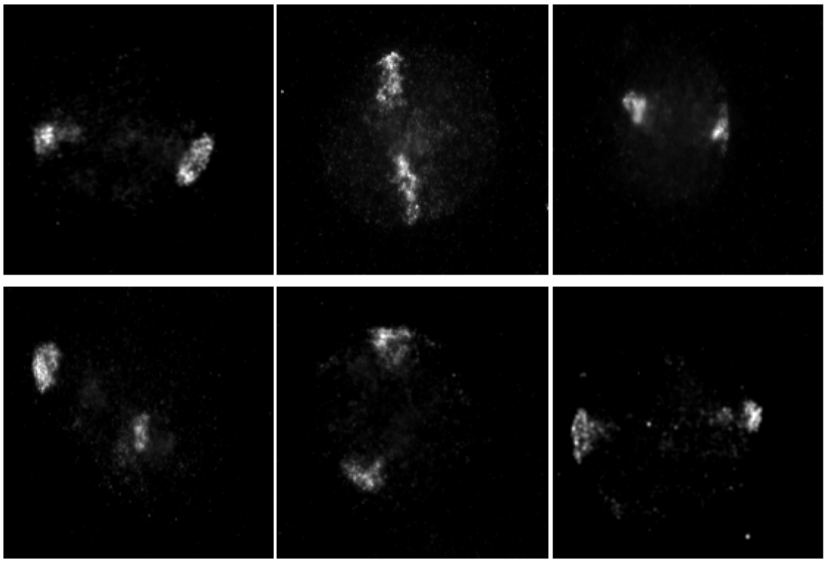

Figure 4.14: **Green channel of FISH images of chromosome 10 at 15 minutes.**

displays the green channel of the FISH images of nuclei expressing the NMI after the low serum assay, were obtained by colour channels spliting using the Corel software. the green channel corresponds to the cy3 staining (CT).

4.3.2 Comparison of chromosome chromosome 10 territories before and after the low serum assay

The size of chromosome 10 territories measured in nuclei of HDFs before the low serum assay (at 0 minute) was compared to the size of chromosome 10 territories measured after the low serum assay (at 15 minutes). It seemed that the chromosome 10 territories were getting smaller after the low serum incubation, as shown in figure 4.15, the t test has confirmed the statistical significance of this difference; $p = 3.19 \times 10^{(-13)}$.

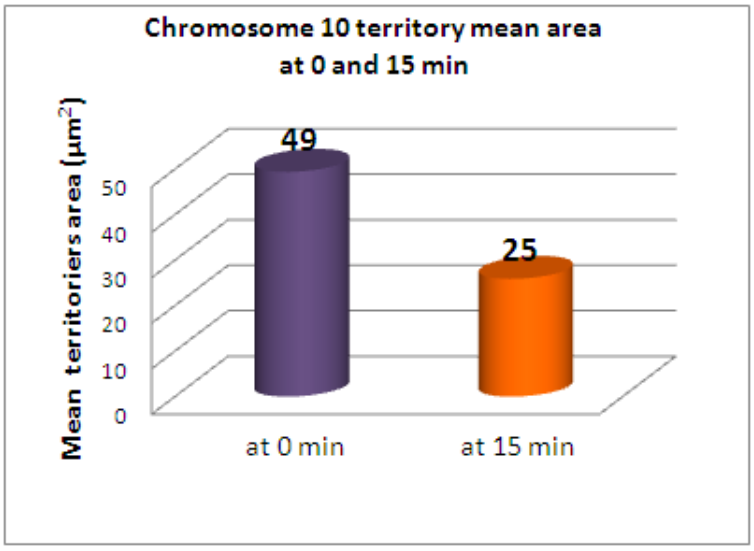

Figure 4.15: **Comparison of the size of chromosome 10 at 0 and 15 minutes.1**
Purple: the mean size of chromosome 10 territories before the low serum incubation, Orange: the mean size of chromosome 10 territories after the low serum incubation

In order to verify whether, smaller chromosome 10 territories after the low serum incubation is a general trend , a second set of images have been analysed. Similar trend have also been registered with chromosome 10 territories becoming smaller after the low serum incubation (figure 4.16), $p = 0.39$.

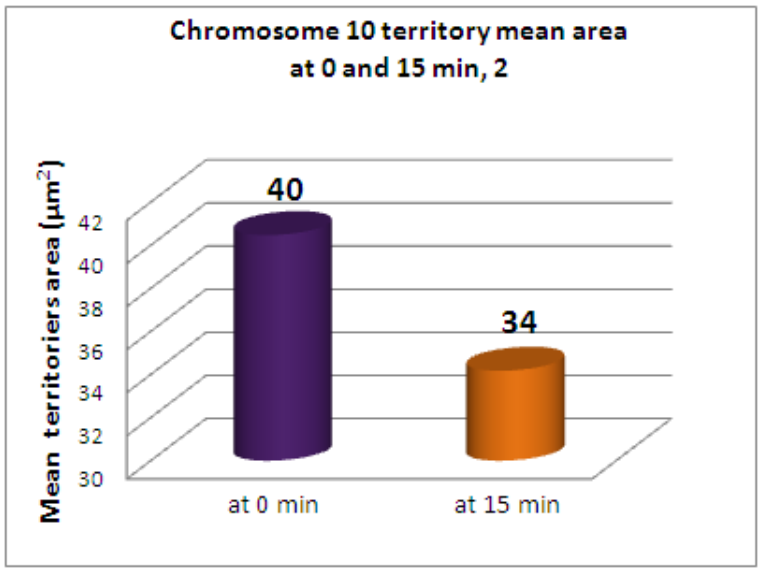

Figure 4.16: **Comparison of the size of chromosome 10 at 0 and 15 minutes.2**
Purple: the mean size of chromosome 10 territories before the low serum incubation, Orange: the mean size of chromosome 10 territories after the low serum incubation

4.3.3 Comparison of chromosome 10 territories before and after the low serum assay of NMI depleted cells

The assess the effect of the suppression of the NMI on chromosome territories sizes, the low serum assay has been repeated on cells where the NMI expression has been blocked using siRNA. Results have shown that the size of chromosome 10 territories was nearly the same before and after the low serum incubation of NMI depleted cells (figure 4.15). the t test has confirmed that there is no significant difference in chromosome 10 territories at 0 and 15 minutes in NMI depleted nuclei; $p = 0.47$.

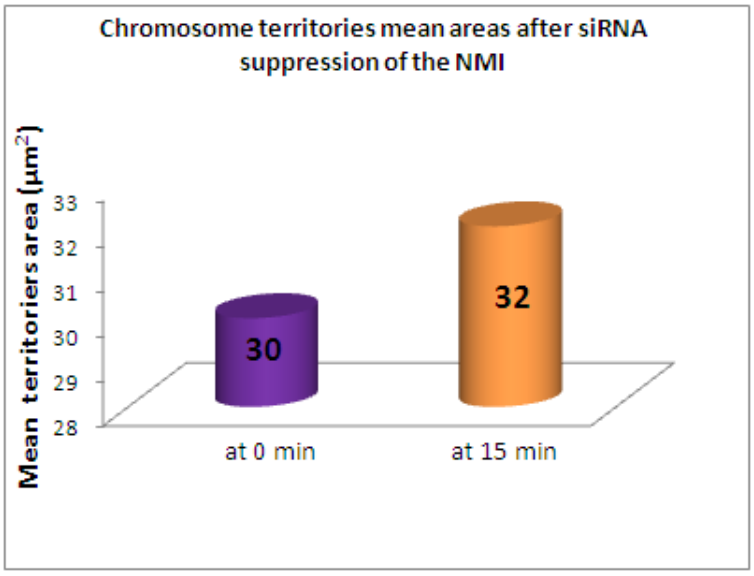

Figure 4.17: **Comparison of the size of chromosome 10 of NMI depleted nuclei before and after the low serum incubation.**
Purple: the mean size of chromosome 10 territories before the low serum incubation, Orange: the mean size of chromosome 10 territories after the low serum incubation

Conclusion

The comparison of the size of chromosome 10 territories in normal proliferating HDFs has revealed significant changes in the territory size after the cells have been incubated in low serum assay for 15 minutes. Chromosome 10 territories

seem to become smaller when the cells have been subjected to the low serum assay. The same comparison have been repeated using cells where the expression of the nuclear myosin I has been blocked by siRNA, in these cells, no significant change in the chromosome 10 territories' sizes has been identified. Chromosome 10 territories ahve similar sizes before and after incubating NMI depleted cells in low serum for 15 minutes.

4.3.4 Image analysis of chromosome X territories

Using the green channel of the FISH images of chromosome X territories obtained before (figure 4.18) and after (figure**??**) the low serum assay; the size of the chromosome territory has been measured by the Scion image analysis program then the results we compared and unpaired two sample t test was calculated to asses the significance of any resulting difference. The same analysis has been repeated using images of cells where the NMI expression has been blocked using siRNA.

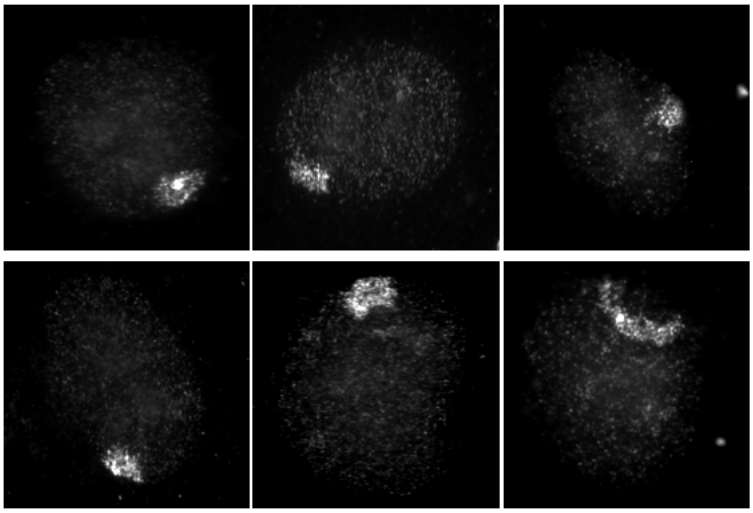

Figure 4.18: **Green channel of FISH images of chromosome X at 0 minute**

displays the green channel of the FISH images of nuclei expressing the NMI before the low serum assay, were obtained by colour channels spliting using the Corel software. the green channel corresponds to the cy3 staining (CT).

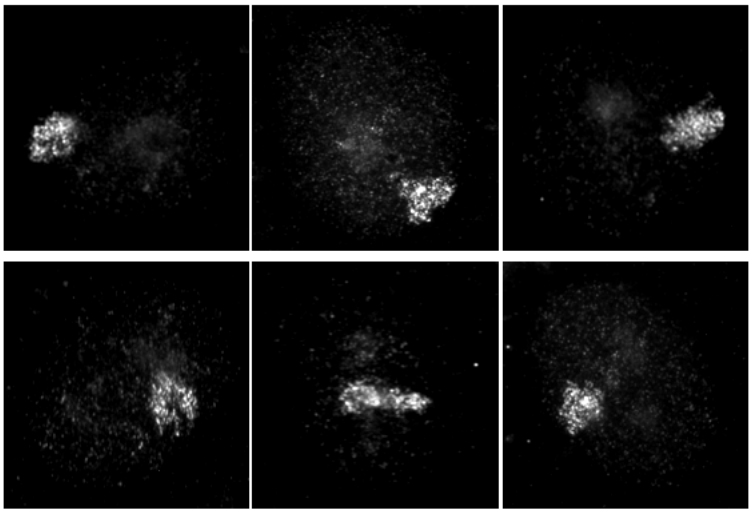

Figure 4.19: **Green channel of FISH images of chromosome X at 15 minutes**

displays the green channel of the FISH images of nuclei expressing the NMI after the low serum assay, were obtained by colour channels spliting using the Corel software. the green channel corresponds to the cy3 staining (CT).

4.3.5 Comparison of chromosome chromosome X territories before and after the low serum assay

The size of chromosome X territories measured in nuclei of normal proliferating HDFs before the low serum assay (at 0 minute) was compared to the size of chromosome X territories measured after the low serum assay (at 15 minutes). It seemed that the chromosome X territories were bigger after the low serum incubation, as shown in figure 4.20, the t test has confirmed the statistical significance of this difference; $p = 0.001$.

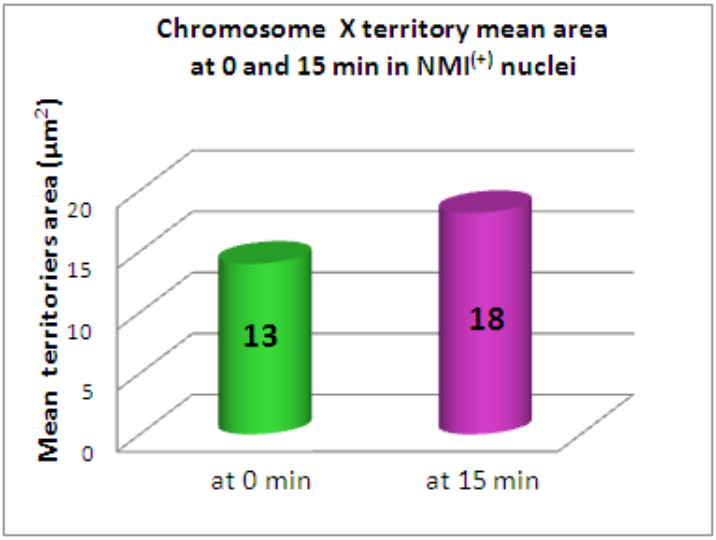

Figure 4.20: **Comparison of the size of chromosome X at 0 and 15 minutes.**
Green: the mean size of chromosome X territories before the low serum incubation, Violet: the mean size of chromosome X territories after the low serum incubation

4.3.6 Comparison of chromosome X territories before and after the low serum assay of NMI depleted cells

The assess the effect of the suppression of the NMI on chromosome territories sizes, the low serum assay has been repeated on cells where the NMI expression has been blocked using siRNA. Results have shown that the size of chromosome X territories seemed to be bigger before the low serum incubation of NMI depleted cells (at 0 minute) compared to the size of X territory at 15 minutes, as shown in figure 4.21. despite the apparent difference in chromosome X territories at 0 and 15 minutes of NMI depleted cells, the t test has confirmed that this difference was statistically insignificant, $p = 0.39$.

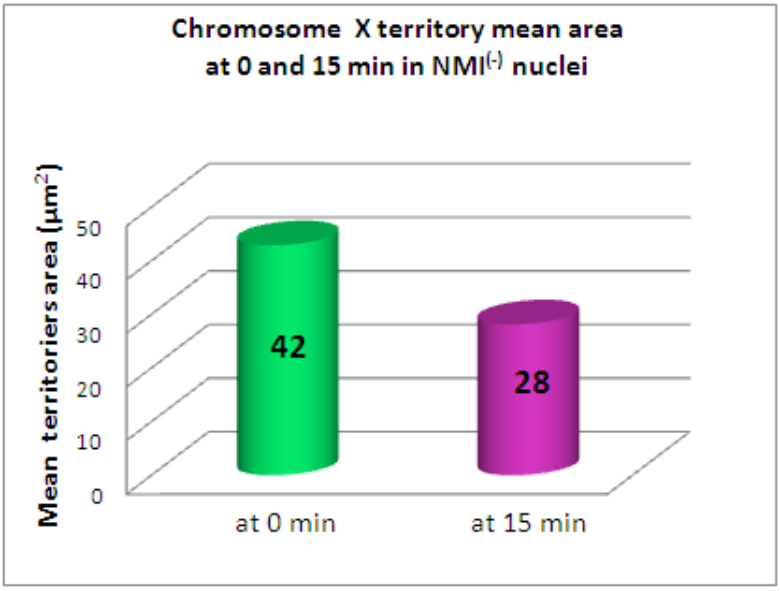

Figure 4.21: **Comparison of the size of chromosome X at 0 and 15 minutes of NMI depleted nuclei**

Green: the mean size of chromosome X territories before the low serum incubation, Violet: the mean size of chromosome X territories after the low serum incubation

Conclusion

The image analysis of the chromosome X territories before and after the low serum incubation has revealed significant changes in the size of these territories before and after the low serum assay. It has emerged that chromosome X territory becomes bigger after incubating normal proliferating cells in low serum for 15 minutes. In NMI depleted cells, subjecting the cells to low serum incubation resulted in no significant difference in the size of chromosome X territories before and after the low serum assay .

Chapter 5

Discussions

5.1 Role of the nuclear myosin I in chromosome positioning

In this study we have been able to confirm that the myosin responsible for the rapid chromosome 10 repositioning as result to low serum incubation is the nuclear myosin I. Low serum induced chromosome 10 repositioning from an intermediate position in the nucleus to the nuclear periphery has been previously identified by our to be depending on the function of both actin myosin (Mehta & Bridger unpublished), with several myosins identified in the nucleus (see section 4.2 chapter 1), it was important to know which of these nuclear myosin is actually responsible for the rapid chromosome 10 repositioning to the nuclear periphery. In this study, using RNA interference techniques to block the expression of the NMI gene performed on similar cultures and using same procedures, we provide evidence that this rapid chromosome 10 repositioning is dependent on the presence of the nuclear myosin I in the nucleus. By comparing the chromosome 10 positions at 0 and 15 minutes of the low serum assay in control cells before the siRNA transfection, with the respective chromosome positions at 0 and 15 minute of the low serum incubation repeated on cells where the NMI expression have been blocked, we have found that the relocation of chromosome 10 to the nuclear periphery after 15 minutes of the low serum incubation, pre-

viously identified in normal proliferating control cells did not manifest in NMI depleted nuclei. In nuclei where the NMI gene has been silenced using siRNA, chromosome 10 have been found to occupy an intermediate position both at 0 and 15 minutes of the low serum assay. The role of nuclear myosin I in chromatin movements have been previously reported (Chang, et al., 2006, Dundr et al., 2007, Hu, et al., 2008) but this is the first time where a whole chromosome territory relocation have been shown to be dependant on the presence of the NMI in the nucleus. While these finding confirm a model where the interphase chromatin is highly dynamic with NMI dependant active chromosome domains repositioning.

5.2 Role of the nuclear myosin I in maintaining nuclear shape

The image analysis of the nuclear shape before and after the siRNA silencing of the nuclear myosin gene, has revealed significant changes in the shape of nuclei after the low serum incubation NMI depleted nuclei compared to nuclei of cells where the expression of the NMI has not been affected, the nuclei where the NMI expression has been blocked were found to become more lobulated after the cells were subjected to the low serum assay. The low serum incubation of cells expressing the NMI did not seem to have significant effect on the shape or the size of the nuclei. A role of NMI in maintaining the nuclear shape has recently been suggested by Holaska and Wilson, (2007); NMI bound to emerin can act as a sencor and a regulator of the peripheral nuclear lamina network. In this study further evidence of the involvement of the nuclear myosin I in maintaining the nuclear shape is provided.

5.3 Effect of the nuclear myosin I on chromosome territories size

The analysis of chromosome 10 and X territories has revealed significant changes of the size of chromosome territories after the cells have been incubated in low serum for 15 minutes. while the size of chromosome 10 territories seemed to have shrunk after the low serum assay, the chromosome X territories seemed to have expanded. These changes in chromosome territories' sizes are found to be dependent on the presence of the nuclear myosin I in the nucleus, since no significant changes in both chromosome 10 and X territory size have been registered when the NMI depleted cells have been subjected to the low serum assay.

5.4 Conclusion

The newly uncovered role of the NMI in chromosome repositioning brings to mind the case of senescent cells where a study by Mehta, et al, (2010) has shown, absence of the low serum induced chromosome repositioning initially observed in normal proliferating cells. It is tempting to speculate that the abolishment of the chromosomal repositioning in this case is comparable to the one observed in this study when the NMI depleted cells were subjected to the low serum assay. Thus, the absence of the low serum induced chromosome repositioning in senescent cell, could reflect or result from impairment in the function of the NMI. In favour of this idea, is the striking difference in the distribution of the NMI in senescent cells compared to normal proliferating cells, observed by indirect-immunofluorescence (Mehta, et al ., 2010). Further studies are required to verify this hypothesis, which could result in a breakthrough in the field of progeria research where a comparable pattern has been also observed (Mehta, et al., 2010).

The study of chromosome territories has also revealed that chromosome territories (CT) are affected differently by the low serum assay (while chromosome 10 territories seem to have shrunk in size, chromosome X territories have expanded). It would be interesting to know whether these changes in CT sizes are correlating with the transcriptional status of these chromosomes and how the serum deprivation affects the CT sizes. Interestingly, the siRNA knockdown of the NMI resulted in the absence of the low serum induced changes in CT sizes. More studies are needed to investigate how the NMI is affecting the CT in serum deprived cultures.

The results of this study have provided new insights into the importance of the nuclear myosin I in nuclear organisation and architecture, this multi functional motor has been found necessary for chromosome movements, maintaining the nuclear shape, and affecting the chromosome territories sizes. The mechanism by which the NMI is maintaining these functions and whether the NMI

has been acting directly or indirectly (in a complex or as regulator), needs to be further investigated.

REFERECES

Barylko, B., Wagner, M.C., Reizes, O., Albanesi, J. P., 1992. Purification and characterization of a mammalian myosin I. *Proceedings the National Academy of Sciences USA*, 89 (2), pp. 490-494.

Berg, J.S., Powell, B.C., Cheney, R.E., 2001. A millennial myosin census. *Molecular Biology of the Cell*, 12(4), pp. 780-794.

Bernardi, R., Pandolfi, P.P., 2007. Structure, dynamics and functions of promyelocytic leukaemia nuclear bodies. *Nature Reviews Molecular Cell Biology*, 8, pp. 1006-1016.

Bettinger, B.T., Gilbert, D.M., Amberg, D.C., 2004. Actin up in the nucleus. *Nature Review Molecular Cell Biolog*, 5, pp. 410-415.

Bolzer, A., Kreth, G., Solovei, I., Koehler, D., Saracoglu, K., Fauth, C., Muller, S., Eils, R., Cremer, C., Speicher, M.R., 2005. Three-dimensional maps of all chromosomes in human male fibroblast nuclei and prometaphase rosettes. *PLoS Biology*, 3, pp. e157.

Bond, C.S., Fox, A.H., 2009. Paraspeckles: nuclear bodies built on long noncoding RNA. *The journal of cell biology*, 186(5), pp. 637-644

Cameron, R.C., Liu, C., Mixon, AS., Pihkala, J.S., Rahn, R.J., Cameron, P.L., 2007. Myosin16b: The COOH-Tail Region Directs Localization to the Nucleus and Overexpression Delays S-Phase Progression. *Cell Motility and the Cytoskeleton*, 64, pp. 19-48.

Cavellán, E., Asp, P., Percipalle, P., Farrants, A.K., 2006. The WSTF-SNF2h chromatin remodeling complex interacts with several nuclear proteins in transcription. *Journal of Biology and Chemistry*, 16; 281 (24), pp. 16264-71.

Cremer, T., Kreth, G., Koester, H., Fink, R.H., Heintzmann, R., Cremer, M., Solovei, I., Zink, D., Cremer, C., 2000. Chromosome territories, interchromatin domain compartment, and nuclear matrix: an integrated view of the functional nuclear architecture. *Critical Reviews in Eukaryotic Gene Expression*, 10 (2), pp. 179-212.

Cremer, T., Cremer, M., Dietzel, S., Müller, S., Solovei, I., Fakan, S., 2006. Chromosome territories – a functional nuclear landscape. *Current Opinion in Cell Biology*, 18(3), pp. 307-316.

Croft, J.A., Bridger, J.M., Boyle, S., Perry, P., Teague, P., Bickmore, W.A., 1999. Differences in the localization and morphology of chromosomes in the human nucleus. *Journal of Cell Biology*, 145(6), pp. 1119-31.

Dellaire, G., Bazett-Jones, D.P., 2004. PML nuclear bodies: dynamic sensors of DNA damage and cellular stress. *Bioessays*, 26, pp. 963–977.

Dundr M, Ospina JK, Sung MH, John S, Upender, M., Ried, T., Hage,r G.L., Matera, A.G., 2007. Actin-dependent intranuclear repositioning of an active gene locus in vivo. *Journal of Cell Biology*, 17;179(6), pp., 1095-103.

Finlan, L.E., Sproul, D., Thomson, I., Boyle, S., Kerr, E., Perry, P., Ylstra, B., Chubb, J.R., Bickmore, W.A., 2008. Recruitment to the nuclear periphery can alter expression of genes in human cells. *PLoS Genetics*, 4 (3), pp. e1000039.

Foster, H.A., Bridger, J.M., 2005. The genome and the nucleus: a marriage made by evolution. Genome organisation and nuclear architecture, 14 (4), pp. 212-29.

Fox, A.H., Lam, Y.W., Leung, A.K., Lyon, C.E., Andersen, J., Mann, M., Lamond, M.I., 2002. Paraspeckles: a novel nuclear domain. *Current Biology*, 12, pp. 13-25.

Fradelizi, J., Noireaux, V., Plastino, J., Menichi, B., Louvard, D., Sykes, C., Golsteyn, R.M, Friederich, E., 2001. ActA and human zyxin harbour Arp2/3-independent actin-polymerization activity. *Nature Cell Biology*. 3, pp. 699-707.

Gedge, L.J., Morrison , EE., Blair GE, Walker, JH., 2005. Nuclear actin is partially associated with Cajal bodies in human cells in culture and relocates to the nuclear periphery after infection of cells by adenovirus 5. *Experimental cell research*, 15,303(2), pp. 229-39.

Gilbert, N., Boyle, S., Fiegler, H., Woodfine, K., Carter, N.P., Bickmore, W.A., 2004. Chromatin Architecture of the Human Genome: Gene-Rich Domains Are Enriched in Open Chromatin Fibers. *Cell*, 118, pp. 555-566.

Gillespie, P.G., Cyr, J.L., 2002. Calmodulin binding to recombinant myosin-1c and myosin-1c IQ peptides. *BMC Biochemistry*, 26, pp. 3-31.

Gonsior, M.S., Platz, S., Buchmeier, S., Scheer, U., Jockusch, B.M., Hinssen, H., 1999. Conformational difference between nuclear and cytoplasmic actin as detected by a monoclonal antibody. *Journal of Cell Science*, 112, pp. 797–809.

Hofmann, W.A., Gabriela M.V., Ramchandran, R., Stojiljkovic, L., James, A.G., De Lanerolle, P., 2006. Nuclear myosin I is necessary for the formation of the first phophodiester bond during transcription initiation by RNA polymerase II. *Journal of Cell Biochemistry*, 1;99 (4), pp. 1001-9.

Hofmann, W.A., Johnson, T., Klapczynski, M., Fan, J.L., de Lanerolle. P., 2006. From transcription to transport: emerging roles for nuclear myosin I. *Biochemistry Cell Biology*, 84, pp. 418-426.

Hofmann, W.A., Stojiljkovic, L., Fuchsova, B., Vargas, G.M., Mavrommatis, E., Philimonenko, V., Kysela, K., Goodrich., J.A., Lessard, J.L., Hope, T.J., Hozak, P., De Lanerolle, P., 2004. Actin is part of pre-initiation complexes and is necessary for transcription by RNA polymerase II. *Nature Cell Biology*, 6(11), pp. 1094-101.

Hofmann, W.A., Thomas, A.R., De Lanerolle, P., 2009. Ancient animal ancestry for nuclear myosin. *Journal of Cell Science*, 1;122 (Pt 5), pp. 636-43.

Holaska, J.M., Kowalski, A.M., Wilson, K.L., 2004. Emerin caps the pointed end of actin filaments: evidence for an actin cortical network at the nuclear inner membrane. *PLoS Biology*, 2, pp. 1354-1362.

Holaska, J.M. and Wilson, K.L. 2007. An emerin "proteome": purification of distinct emerin-containing complexes from HeLa cells suggests molecular basis for diverse roles including gene regulation, mRNA splicing, signaling, mechanosensing, and nuclear architecture. *Biochemistry*. , 46(30), pp. 8897-908.

Hu, P., Wu, S., Hernandez, N., 2003. A minimal RNA polymerase III transcription system from human cells reveals positive and negative regulatory roles for CK2. *Moecular Cell*, 12, pp. 699-709.

Hu, P., Wu, S., Hernandez, N., 2004. A role for beta-actin in RNA polymerase III transcription. *Genes and Development*. 18(24), pp. 3010-5.

Hu,Q., Kwon,Y.S., Nunez, E., Cardamone, M.D., Hutt, K.R., Ohgi, K.A., Garcia-Bassets, I., Rose, D.W., Glass, C.K., Michael G. Rosenfeld, Fu, X.D., 2008. Enhancing nuclear receptor-induced transcription requires nuclear motor and LSD1-dependent gene networking in interchromatin granules. *Proceeding of the National Academy of Sciences* 9; 105(49), pp. 19199-19204.

Jockusch, B.M., Schoenenberger, C.A., Stetefeld, J., Aebi, U., 2006. Tracking down the different forms of nuclear actin. *Trends in Cell Biology,* 16, pp. 391-396.

Kahle, M., Pridalová, J., Spacek, M., Dzijak, R., Hozák, P., 2007. Nuclear myosin is ubiquitously expressed and evolutionary conserved in vertebrates. *Histochemistry and cell biology*, 127(2), pp. 139-48.

Khatau, SB., Hale, CM., Stewart-Hutchinson, PJ., Patel, MS., Stewart, CL., Searson, PC., Hodzic, D., Wirtz D., 2009. Perinuclear actin cap regulates nuclear shape. *Proceedings of the National Academy of Sciences of the United States of America,* (Electrinc publication ahead of print, www.pubmed.com)

Kiseleva, E., Drummond, S.P., Goldberg, M.W., Rutherford, S.A Allen, T, D Wilson, K. L., 2004. Actin- and protein-4.1-containing filaments link nuclear pore complexes to subnuclear organelles in Xenopus oocyte nuclei. *Journal Cell Science*, 117, pp. 2481–2490.

Kysela, K., Philimonenko, A.A., Philimonenko, V.V., Janacek,J., Kahle, M., Hozak, P., 2005. Nuclear distribution of actin and myosin I depends on transcriptional activity of the cell. *Histochemistry of the Cell Biology*, 124(5), pp. 347-58.

Laakso, J.M., Lewis, J.H., Shuman, H., Ostap, E.M., 2008. Myosin I can act as a molecular force sensor. *Science*, 4;321 (5885), pp. 133-6.

Lamond, A.I and Spector, D.L., 2003. Nuclear speckles: a model for nuclear organelles. *Nature Reviews Molecular Cell Biology*, 4, pp. 605-612

Lane, N.J., 1969. Intranuclear fibrillar bodies in actinomycin D-treated oocytes. *Journal of Cell Biology*, 40, pp. 286–29.

Laskey, R. A., 1987. Basic Molecular and Cell Biology: The cell nucleus. *The British Medical Journal*, 295.

Manuelidis, L and Borden, J., 1988. Reproducible compartmentalization of individual chromosome domains in human CNS cells revealed by in situ hybridization and three-dimensional reconstruction. *Chromosoma,* 96, pp. 397-410.

Manuelidis, L., 1984. Different central nervous system cell types display distinct and nonrandom arrangements of satellite DNA sequences. *Proceedings of the National Academy of Sciences of the United States of America,* 81, pp. 3123-3127.

Matera, A. G, 1999. Nuclear bodies: multifaceted subdomains of the interchromatin space. *Trends Cell Biol*. 9, pp. 302-309.

McDonald, D., Carrero, G., Andrin, C., De Vries, G., Hendzel, M. J., 2006. Nucleoplasmic beta-actin exists in a dynamic equilibrium between low-mobility polymeric species and rapidly diffusing populations. *Journal of Cell Biology*, 172, pp. 541-552.

Melnick, A and Licht, J. D., 1999. Deconstructing a disease: RARα, its fusion partners and their roles in the pathogenesis of acute promyelocytic leukemia. *Blood*, 93, pp. 3167-3215.

Misteli, T and Spector, D. L., 1998. The cellular organization of gene expression. *Current Opinion in Cell Biology*, 10, pp. 323-331.

Nix, D.A and Beckerle, M.C., 1997. Nuclear-cytoplasmic shuttling of the focal contact protein, zyxin: a potential mechanism for communication between sites of cell adhesion and the nucleus. *Journal of Cell Biology*, 138, pp. 1139-1147.

Obrdlik, A., Louvet, E., Kukalev, A., Naschekin, D., Kiseleva, E., Fahrenkrog, B., Percipalle, P., 2009. Nuclear myosin 1 is in complex with mature rRNA transcripts and associates with the nuclear pore basket. *The FASEB journal (official publication of the Federation of American Societies for Experimental Biology*, 24(1), pp. 146-57

Onoda, K., Yu, F.X., Yin, H.L., 1993. gCap39 is a nuclear and cytoplasmic protein. *Cell Motility Cytoskeleton*, 26(3), pp. 227-238.

Pederson, T and Aebi, U., 2002. Actin in the nucleus: What form and what for? *Journal of Structural Biology*, 140, pp. 3-9.

Pederson, T and Aebi, U., 2005. Nuclear actin extends, with no contraction in sight. *Molecular Biology of the Cell*, 16, pp. 5055-5060.

Pendleton, A., Pope, B., Weeds, A., Koffer, A., 2003. Latrunculin B or ATP depletion induces cofilin-dependent translocation of actin into nuclei of mast cells. *Journal of Biological Chemistry*, 278, pp. 14394-14400.

Pestic-Dragovich, L., Stojiljkovic, L., Philimonenko, A.A., Nowak, G., Ke, Y., Settlage, R.E., Shabanowitz, J., Hunt, D.F., Hozak, P., De Lanerolle, P., 2000. A myosin I isoform in the nucleus. *Science,* 290(5490), pp. 337-41.

Philimonenko, V.V., Zhao, J., Iben, S., Dingova, H., Kysela, K., Kahle, M., Zentgraf, H., Hofmann, W.A., De Lanerolle, P., Hozak, P., et al., 2004. Nuclear actin and myosin I are required for RNA polymerase I transcription. *Nature Cell Biology*, pp. 1165-1172.

Percipalle, P., Fomproix, N., Cavellan, E., Voit, R., Reimer, G., Kruger, T., Thyberg , J. Scheer, U., Grummt, I., Farrants, AK., 2006. The chromatin remodelling complex WSTF–SNF2h interacts with nuclear myosin 1 and has a role in RNA polymerase I transcription. *EMBO report*, 7(5), pp. 525-30

Pranchevicius, M.S., Baqui, M.A., Ishikawa-Ankerhold, H.C., Lourenc, E.V., Lea, M.L., Banzi, S.R., dos Santos, CT., Barreira, M.C., Esprea, E.M., Larson, R.E., 2008. Myosin Va Phosphorylated on Ser1650 IsFound in Nuclear Speckles and Redistributes to Nucleoli Upon Inhibition of Transcription. *Cell Motility Cytoskeleton,* 65, pp. 441-456

Rando, O.J., Zhao, K., Crabtree, G.R., 2000. Searching for a function for nuclear actin. *Trends. Cell Biology,* 10, pp. 92-97.

Salomoni, P and Pandolfi, P.P., 2002. The role of PML in tumor suppression. *Cell,* 108, pp. 165-170.

Sasseville, A.M and Langelier, Y., 1998. In vitro interaction of the carboxy-terminal domain of lamin A with actin. *FEBS Letters*, 425(3), pp. 485-9.

Shumaker, D.K., Kuczmarski, E.R., Goldman, R.D., 2003 The nucleoskeleton: lamins and actin are major players in essential nuclear functions. *Current Opinion in Cell Biologgy*. 15, pp. 358-366.

Spector, D.L., 1993. Nuclear organization of pre-mRNA processing. *Current Opinion in Cell Biology*, 5, pp. 442-447.

Spector, D. L., 2001. Nuclear domains. *Journal of Cell Science*, 114, pp. 2891-2893.

Stuven, T., Hartmann, E., Görlich, D., 2003. Exportin 6 : A novel nuclear export receptor that is specific for profiling-actin complexes. *The EMBO Journal,* 22, pp. 5928–5940.

Vandekerckhove, J and Weber, K., 1978. At least six different actins are expressed in a higher mammal: An analysis based on the amino acid sequence of the amino-terminal tryptic peptide. *Journal of Molecular Biology*, 126(4), pp. 783-802.

Vartiainen, M.K, 2008. Nuclear actin dynamics – From form to function. *FEBS Letters*, 582, pp. 2033-2040.

Vecerová, J., Koberna, K., Malínsky, J., Soutoglou, E., Sullivan, T., Stewart, C.L., Raska, I., Misteli, T., 2004. Formation of Nuclear Splicing Factor Compartments Is Independent of Lamins A/C. *Molecular Biology of the Cell*, 15(11), pp. 4904-10.

Voeltz, G.K., Rolls, M.M., Rapoport, T.A, 2002. Structural organization of the endoplasmic reticulum. *EMBO reports,* 3(10), pp. 944-50.

Vreugde, S., Ferrai, C., Miluzio, A., Hauben, E., Marchisio, P.C., Crippa, M.P., Bussi, M., Biffo, S. 2006. Nuclear Myosin VI Enhances RNA Polymerase II-Dependent Transcription . *Molecular cell*, 23(5) 1, pp. 749-755

Webster, M., Witkin, K. L., Cohen-Fix.O., 2009. Sizing up the nucleus: nuclear shape, size and nuclear-envelope assembly. *Journal of Cell Science*, 122, pp. 1477-1486.

Weins, A., Schwarz, K., Faul, C., Barisoni, L., Linke, W.A., Mundel, P., 2001. Differentiation and stress-dependent nuclear cytoplasmic redistribution of myopodin, a novel actin-bundling protein, *Journal of Cell Biology*, 155, pp. 393-404.

Wells, A.L., Lin, A.W., Chen, L.Q., Safer, D., Cain, S.M., Hasson, T., Carragher, B.O., Milligan, R.A., Sweeney, H.L., 1999. Myosin VI is an actin-based motor that moves backwards, *Nature*. 401. pp. 505-508.

Wu, X., Yoo, Y., Okuhama, N.N., Tucker, P.W., Liu, G., Guan, J. L., 2006. Regulation of RNA-polymerase-II-dependent transcription by N-WASP and its nuclear-binding partners. *Nature Cell Biology*, 8, pp. 756-763.

Yahara, I., Aizawa, H., Moriyama, K., Iida, K., Yonezawa, N., Nishida, E., Hatanaka, H., Inagaki, F., 1996. Role of cofilin/destrin in reorganization of actin cytoskeleton in response to stresses and cell stimuli, *Cell Structure and Function*, 21, pp. 421-424.

Yanaihara, N., Nishioka, M., Kohno, T., Otsuka, A., Okamoto, A., Ochiai, K., Tanaka, T., Yokota, J., 2004. Reduced expression of MYO18b, a candidate tumor-suppressor gene on chromosome arm 22q, in ovarian cancer. *International Journal of Cancer,* 112, pp. 150-154.

Ye, J., Zhao, J., Hoffmann-Rohrer, U., Grummt, I., 2008. Nuclear myosin I acts in concert with polymeric actin to drive RNA polymerase I transcription. *Gene & Development journal* 1; 22(3), pp. 322-30

Yu, C., Feng, W., Wei, Z., Miyanoiri, Y., Wen, W., Zhao, Y., Zhang, M., 2009. Myosin VI undergoes cargo-mediated dimerization. *Cell.* 138(3), pp. 537-48.

Zhen, Y.Y., Libotte, T., Munck, M., Noegel, A.A., Korenbaum, E., 2002. NUANCE, a giant protein connecting the nucleus and actin cytoskeleton. *Journal of Cell Science,* 115, pp. 3207-3222.

Zhu, X.J., Huang, B.Q., Wang, X.Z., Hao, S., Zeng, X.L., 2006. Actin and nuclear myosin I are associated with RNAP II and function in gene transcription. *Chinese Science Bulletin,* 52(6), pp. 766-770.

Zirbel, R.M., Mathieu, U.R., Kurz, A., Cremer, T., Lichter, P., 1993. Evidence for a nuclear compartment of transcription and splicing located at chromosome domain boundaries. *Chromosome Research, Journal of Cell Science*, 1(2), pp. 93-106.

Nuclear motors and nuclear structures containing A-type lamins and emerin: is there a functional link?

Ishita S. Mehta, Lauren S. Elcock, Manelle Amira, Ian R. Kill and Joanna M. Bridger[1]

Laboratory of Nuclear and Genomic Health, Centre for Cell and Chromosome Biology, Division of Biosciences, School of Health Sciences and Social Care, Brunel University, Uxbridge UB8 3PH, U.K.

Abstract

Rapid interphase chromosome territory repositioning appears to function through the action of nuclear myosin and actin, in a nuclear motor complex. We have found that chromosome repositioning when cells leave the cell cycle is not apparent in cells that have mutant lamin A or that are lacking emerin. We discuss the possibility that there is a functional intranuclear complex comprising four proteins: nuclear actin, lamin A, emerin and nuclear myosin. If any of the components are lacking or aberrant, then the nuclear motor complex involved in moving chromosomes or genes will be dysfunctional, leading to an inability to move chromosomes in response to signalling events.

Interphase chromosome positioning and repositioning

Chromosomes are positioned non-randomly in interphase nuclei. In primary proliferating fibroblasts, chromosomes are positioned according to their gene density, with gene-poor chromosomes at the nuclear periphery and gene-rich chromosomes towards the nuclear interior [1,2]. The gene-density-correlated positioning of chromosomes found in different cell types gave credence to the idea that positioning of genes and regulatory elements at specific regions of the nucleus would have an impact on the regulation of gene expression or silencing. Some interphase chromosome positions alter with differentiation, whereas others remain in the same nuclear location (reviewed in [3,4]), adding further weight to the argument that interphase positioning is relevant in genome function. On the other hand, we have found that, when cells leave the proliferative cell cycle, to become either quiescent or senescent, chromosomes are still positioned non-randomly, but now according to size, with large chromosomes at the nuclear periphery and small chromosomes in the nuclear interior (I.S. Mehta, M. Figgitt, L.S. Elcock, K.J. Meaburn, G. Bonne, I.R. Kill and J.M. Bridger, unpublished work). Whether this change in location influences changes in transcription profiles has yet to be determined.

We found that, as fibroblasts became quiescent or senescent, a number of chromosomes would change position and some would remain at the same nuclear location. Quite a few chromosomes, such as chromosomes 13 and 18, change nuclear position as fibroblasts become non-proliferating and relocate to same nuclear compartment regardless of whether cells are quiescent or senescent (Figure 1). Others relocate, but are found in different nuclear compartments in both quiescent and senescent fibroblasts (I.S. Mehta, M. Figgitt, L.S. Elcock, K.J. Meaburn, G. Bonne, I.R. Kill and J.M. Bridger, unpublished work). Chromosome 10 is the most interesting chromosome, since it is found in an intermediate nuclear position in proliferating fibroblast nuclei (Figure 1A), at the nuclear periphery in quiescent fibroblasts (Figure 1B) and within the nuclear interior in senescent fibroblasts (Figure 1C). Indeed, it is one of two chromosomes that are located at three different nuclear locations in these cell states. From these analyses, we have to conclude that chromosome territories move, changing their nuclear location as cells become senescent or quiescent (Figure 1). But whether this was immediate, over a number of hours, or whether cells are required to traverse mitosis for chromosomes to become repositioned was not clear, and not trivial to study in senescent cells. However, using serum removal, we were able to show that chromosome territories are relocated very rapidly, after 15 min. This repositioning is an active process requiring energy, since inhibitors of ATPase and GTPase block the relocation of chromosomes (I.S. Mehta, L.S. Elcock, G. Bonne, I.R. Kill and J.M. Bridger, unpublished work). Rapid repositioning has been observed for individual genetic loci [5,6]. In order to understand how this rapid movement is elicited, we are looking at nuclear motors.

Nuclear motors

Molecular motors of the cell cytoplasm have been studied for many years. Over the years, there have been on/off discussions as to whether there are molecular motors within the nuclei of cells. The discussions started in the 1970s [7,8], with a role for nuclear actin and myosin being suggested in heterochromatin formation [9]. In the 1980s, evidence was

Key words: chromosome movement, emerin, nuclear actin, nuclear lamin, nuclear motor, nuclear myosin.

Abbreviations used: EDMD, Emery–Dreifuss muscular dystrophy; HGPS, Hutchinson–Gilford progeria syndrome; NMI, nuclear myosin I.

[1]To whom correspondence should be addressed (email Joanna.Bridger@brunel.ac.uk).

Figure 1 | Chromosomes occupy differential locations in normal proliferating, quiescent and senescent primary fibroblasts

(**A**) In a young proliferating fibroblast nucleus, chromosome 10 occupies an intermediate location, whereas chromosomes 13, 18 and X localize at the nuclear periphery. (**B**) In a young quiescent fibroblast nucleus, this position of chromosomes is altered and chromosome 10 localizes at the nuclear periphery, whereas territories for chromosomes 13 and 18 are positioned in the nuclear interior. Chromosome X remains at the nuclear periphery. (**C**) In senescent cells, whereas chromosomes 13 and 18 are still localized in the nuclear interior, chromosome 10 is also observed to be positioned in the nuclear interior. Chromosome X remains at the nuclear periphery.

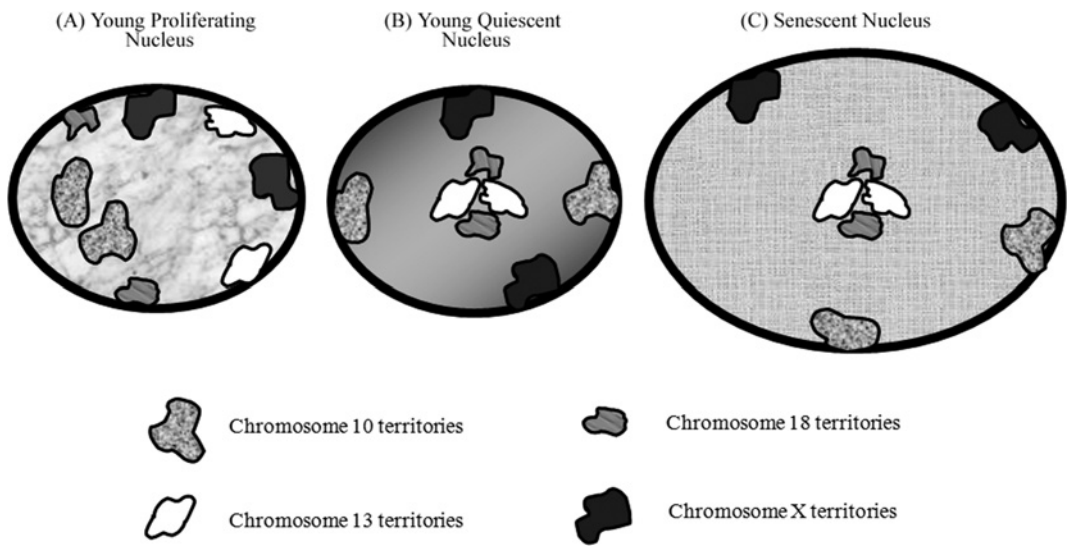

provided that nuclear actin and myosin were involved in nucleocytoplasmic transport [10], and, in the 1990s, more ultrastructural studies were performed, localizing actin and myosin in the nucleus [11,12]. Within the last 10 years, scientists have uncovered several isoforms of myosin that are found in nuclei, including NMI (nuclear myosin I) (reviewed in [13]), myosin VI [14], myosin 16b [15] and myosin Va [16]. In the 1970s, actin was also shown to be a nuclear protein [17,18]. However, it is still an unresolved question as to whether this actin in the nucleus is a polymerized or an unpolymerized form [19].

Using microinjection of antibodies, actin [20,21], and actin and myosin together [22], were shown to be involved in RNA polymerase II transcription, which has been confirmed further using drugs and mutant cell lines not only for nuclear actin and NMI [13,23], but also for myosin VI [14]. These acto–myosin motors also appear to be involved in RNA polymerase I transcription [23–25].

Both nuclear actin and NMI have also been found to associate with chromatin-remodelling complexes. Actin binds to SWI/SWF-like BAF (barrier to autointegration factor) remodelling complexes, whereas NMI associates with components of the WICH (WSTF–SNF2h complex) chromatin-remodelling complex [13].

However, the involvement of nuclear motors in transcription and chromatin remodelling appears not to be their only nuclear function. There is an increasing body of evidence that they are also involved in movement of chromatin around nuclei [5,26].

We have found that the rapid relocation of chromosomes in interphase is blocked by drugs preventing polymerization of actin and myosin (I.S. Mehta, L.S. Elcock, G. Bonne, I.R. Kill and J.M. Bridger, unpublished work).

It is interesting to note that Hozak and colleagues found that both nuclear actin and NMI are distributed quite differently in resting non-stimulated lymphocytes compared with PHA (phytohaemagglutinin)-stimulated lymphocytes [27] and Riddle et al. [28] demonstrated that nuclear actin was decreased in quiescent fibroblasts. We have stained proliferating and senescent fibroblasts with a commercial anti-NMI antibody and have seen quite different distributions of NMI in senescent cells compared with proliferating fibroblasts; it could be described as disorganized (I.S. Mehta, L.S. Elcock, M. Amira, I.R. Kill and J.M. Bridger, unpublished work).

From our studies, we know that, when quiescent cells are re-stimulated with serum, chromosomes do not relocate to a proliferating gene-density distribution until after cells have traversed mitosis with a breakdown and rebuilding of the nucleus [29]. Thus we suggest that not only do quiescent cells have a compromised nuclear motor for moving chromatin, but also the same is true for senescent cells, since we have not visualized any chromosome repositioning in senescent cells after removal of serum. This may indicate that nuclear motors containing actin and myosin do not function in the same manner in non-proliferating cells with respect to dynamic chromatin/chromosome movement.

A-type lamins and emerin

The nuclear lamina is described as a meshwork [30] or a uniparallel array [31] of interconnecting filaments underlying the inner nuclear envelope. This structure, together with the nuclear envelope and nuclear envelope proteins, is important for organizing the structure of the entire nucleus and the chromatin within it [32].

In most vertebrate cells, two major types of nuclear lamin are found: A and B. A-type lamins are encoded by *LMNA* which undergoes alternative splicing to form lamins A, delta A, C and C2, whereas B-type lamins are encoded by two separate genes *LMNB1* and *LMNB2* to form lamins B1, B2 and B3 (reviewed in [33]).

A-type lamin proteins not only are located at the nuclear periphery, but also are probably part of the nuclear matrix [34,35]. Further lamin proteins have been observed within the nuclear interior [36,37] with sites of replication [38], transcription factories [39] and splicing speckles [40]. Nuclear A-type lamins seem to be involved in many nuclear functions such as nuclear structural integrity, DNA replication, transcription, splicing, cell signalling, DNA repair, cellular proliferation, transit of mitosis, organization and stability of the genome, differentiation, normal aging, apoptosis and epigenetic control of chromatin (reviewed in [41]).

A-type lamins have a number of binding partners, and this might well explain their multifaceted roles and importance within the nucleus, but this also adds another level of complexity in assigning roles to particular complexes of proteins containing A-type lamins. One of the binding partners of nuclear A-type lamins is emerin (reviewed in [32]). The lamin–emerin interaction has been implicated to be important in maintaining the structural integrity of the nucleus, in correct localization of the complex and in efficient progression of the cell through the cell cycle [42]. The importance of this complex is emphasized by both proteins causing similar diseases when the respective genes are mutated, i.e. EDMD (Emery–Dreifuss muscular dystrophy). HGPS (Hutchinson–Gilford progeria syndrome) is a premature aging syndrome caused by a base substitution in the *LMNA* gene encoding a G608G mutation [43] resulting in the formation of a truncated lamin A protein termed progerin, which acts in a dominant-negative way [44]. Studies on patients suffering from HGPS have revealed that lamins are important in the maintenance of nuclear structure and shape as well as in heterochromatin formation, chromatin modification and gene expression [45]. Studies using emerin-null cells derived from patients suffering from X-linked EDMD have revealed that emerin may also influence gene expression, heterochromatin organization and be involved in maintaining the structural integrity of the nuclear envelope (reviewed in [32]).

A-type lamins and emerin: are they integral to the function of a nuclear motor?

If lamins A and C and emerin are involved in the function of a nuclear motor comprising nuclear actin and nuclear myosins, then there should be evidence that they bind one another in such a way as to form a complex. Indeed, *in vitro* studies have demonstrated the binding of actin to the C-terminus of lamin A [46]. In addition, the tail region of lamin A has an additional site with affinity for actin [47]. Emerin binds to both actin [F- (filamentous) and G- (globular) actin] and NMI, revealed by proteomic studies [32]. Thus we know that emerin binds lamin A that can bind to actin, which can bind to both emerin and NMI which can bind emerin. This makes an interesting hypothetical complex (Figure 2) and, although it has been discussed as being present at the nuclear envelope [48], could it also be present and functional throughout the nucleus?

Figure 2 | Model showing the interactions between the nuclear actin–myosin and the nuclear lamin–emerin complexes for efficient functioning of the nuclear motor

Nuclear lamins are known to bind to nuclear actin and nuclear emerin. Nuclear emerin binds nuclear actin, nuclear myosin and nuclear actin. Nuclear myosins are known to bind to DNA, whereas nuclear actin, emerin and lamins are known to interact with the nuclear matrix. Thus chromosome territories are bound by nuclear myosins which binds emerin which bind both nuclear actin and lamins. Thus this four-protein complex, with the support of the nuclear matrix, may function to move the chromosome territories within the nuclear space.

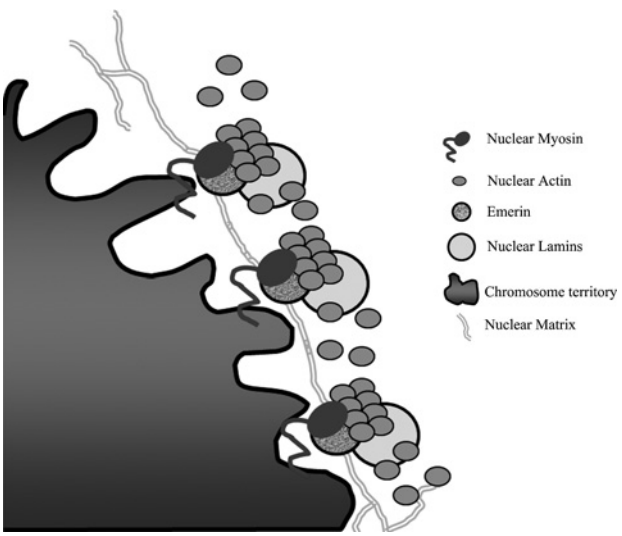

If this complex exists, does it function to move chromatin/chromosomes around the nucleus? We have started to address this question by performing chromosome positioning assays [two- and three-dimensional FISH (fluorescence *in situ* hybridization)] in proliferating fibroblasts of patients that have mutations in either *LMNA* or *EMD* genes (Figure 3B and 3D) [49] and comparing chromosome positioning when these cells have become senescent. Intriguingly, in HGPS cells that have become senescent, the chromosomes do not alter their nuclear location as they would do in normal control cells (Figure 3C). This implies that the nuclear motor function, which would have been involved in chromosome movement during transition from a proliferating to a senescent state, is not functional. Indeed, anti-NMI antibody staining reveals

Figure 3 | Chromosome 10 localizes at the nuclear periphery in proliferating HGPS and EDMD fibroblasts, and the position of chromosome 10 does not change once the cell is senescent

In senescent cells that are quiescent, the territories of chromosome 10 are in the nuclear interior (**A**). In primary proliferating fibroblasts derived from patients suffering from HGPS or EDMD, chromosome 10 territories are at the nuclear periphery (**B** and **D** respectively), and this localization of chromosome 10 does not change when these HGPS cells become senescent (**C**).

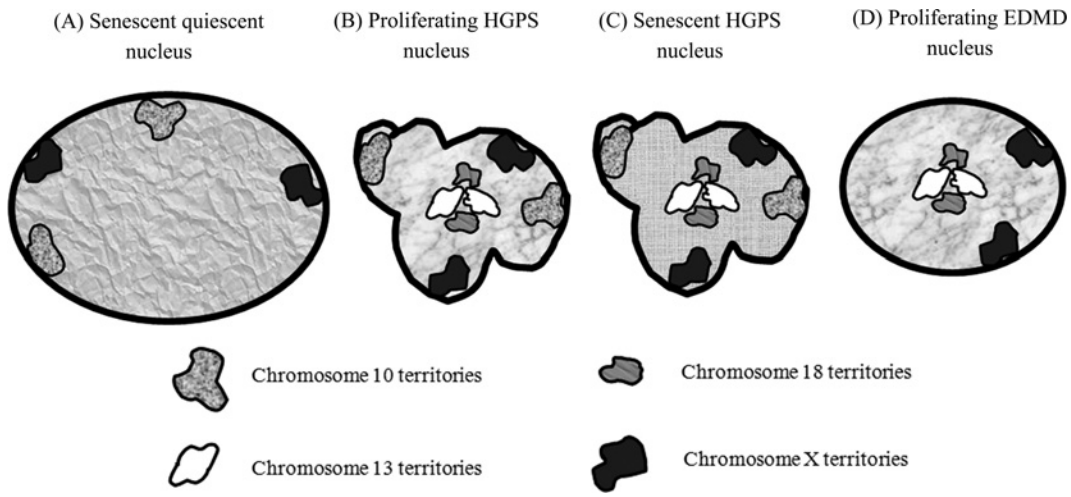

the same disorganized distribution of NMI as in senescent cells (I.S. Mehta, L.S. Elcock, M. Amira, I.R. Kill and J.M. Bridger, unpublished work).

If emerin is functionally involved in this complex, then chromosomes would also not be relocated in EDMD cells that became senescent. Unfortunately, we have only looked at chromosomes 13 and 18 (Figure 3D) so far, and they are found in the nuclear interior in both proliferating and senescent EDMD cells [49].

Thus, for efficient movement of whole chromosome territories, the formation and functionality of this protein complex including nuclear actin, myosin, lamin and emerin (Figure 2) may be vital. It has also been shown that, in normal senescent cells, there is an accumulation of the mutant form of lamin A [50,51]. This may well explain why, in senescent cells, chromosome 10 is not repositioned when senescent cells are placed in low serum (Figure 3A), indicating that the nuclear motor controlling chromosome movement in senescent cells is dysfunctional.

In order to test these hypotheses and the functionality of nuclear motors in non-proliferating and diseased cells, we need to perform a number of experiments. These would include interfering with the complex in normal cells as well as rebuilding it in cells where this complex is dysfunctional or missing; these studies are on-going in our laboratory.

References

1 Boyle, S., Gilchrist, S., Bridger, J.M., Mahy, N.L., Ellis, J.A. and Bickmore, W.A. (2001) The spatial organization of human chromosomes within the nuclei of normal and emerin-mutant cells. Hum. Mol. Genet. **10**, 211–219

2 Croft, J.A., Bridger, J.M., Boyle, S., Perry, P., Teague, P. and Bickmore, W.A. (1999) Differences in the localization and morphology of chromosomes in the human nucleus. J. Cell Biol. **145**, 1119–1131

3 Bartova, E. and Kozubek, S. (2006) Nuclear architecture in the light of gene expression and cell differentiation studies. Biol. Cell **98**, 323–336

4 Foster, H.A. and Bridger, J.M. (2005) The genome and the nucleus: a marriage made by evolution: genome organisation and nuclear architecture. Chromosoma **114**, 212–229

5 Chuang, C.H., Carpenter, A.E., Fuchsova, B., Johnson, T., de Lanerolle, P. and Belmont, A.S. (2006) Long-range directional movement of an interphase chromosome site. Curr. Biol. **16**, 825–831

6 Volpi, E.V., Chevret, E., Jones, T., Vatcheva, R., Williamson, J., Beck, S., Campbell, R.D., Goldsworthy, M., Powis, S.H., Ragoussis, J. et al. (2000) Large-scale chromatin organization of the major histocompatibility complex and other regions of human chromosome 6 and its response to interferon in interphase nuclei. J. Cell Sci. **113**, 1565–1576

7 Clark, T.G. and Rosenbaum, J.L. (1979) An actin filament matrix in hand-isolated nuclei of *X. laevis* oocytes. Cell **18**, 1101–1108

8 Lestourgeon, W.M., Forer, A., Yang, Y.Z., Bertram, J.S. and Pusch, H.P. (1975) Contractile proteins: major components of nuclear and chromosome non-histone proteins. Biochim. Biophys. Acta **379**, 529–552

9 Comings, D.E. and Okada, T.A. (1976) Nuclear proteins. III. The fibrillar nature of the nuclear matrix. Exp. Cell Res. **103**, 341–360

10 Schindler, M., Jiang, L.W., Swaisgood, M. and Wade, M.H. (1989) Analysis, selection, and sorting of anchorage-dependent cells under growth conditions. Methods Cell Biol. **32**, 423–446

11 Amankwah, K.S. and De Boni, U. (1994) Ultrastructural localization of filamentous actin within neuronal interphase nuclei *in situ*. Exp. Cell Res. **210**, 315–325

12 Milankov, K. and De Boni, U. (1993) Cytochemical localization of actin and myosin aggregates in interphase nuclei *in situ*. Exp. Cell Res. **209**, 189–199

13 Hofmann, W.A., Johnson, T., Klapczynski, M., Fan, J.L. and de Lanerolle, P. (2006) From transcription to transport: emerging roles for nuclear myosin I. Biochem. Cell Biol. **84**, 418–426

14 Vreugde, S., Ferrai, C., Miluzio, A., Hauben, E., Marchisio, P.C., Crippa, M.P., Bussi, M. and Biffo, S. (2006) Nuclear myosin VI enhances RNA polymerase II-dependent transcription. Mol. Cell **23**, 749–755

15 Cameron, R.S., Liu, C., Mixon, A.S., Pihkala, J.P., Rahn, R.J. and Cameron, P.L. (2007) Myosin 16b: the COOH-tail region directs localization to the nucleus and overexpression delays S-phase progression. Cell Motil. Cytoskeleton **64**, 19–48
16 Pranchevicius, M.C., Baqui, M.M., Ishikawa-Ankerhold, H.C., Lourenco, E.V., Leao, R.M., Banzi, S.R., dos Santos, C.T., Barreira, M.C., Espreafico, E.M. and Larson, R.E. (2008) Myosin Va phosphorylated on Ser^{1650} is found in nuclear speckles and redistributes to nucleoli upon inhibition of transcription. Cell Motil. Cytoskeleton **65**, 441–456
17 Bremer, J.W., Busch, H. and Yeoman, L.C. (1981) Evidence for a species of nuclear actin distinct from cytoplasmic and muscles actins. Biochemistry **20**, 2013–2017
18 Goldstein, L., Rubin, R. and Ko, C. (1977) The presence of actin in nuclei: a critical appraisal. Cell **12**, 601–608
19 Hofmann, W.A. and de Lanerolle, P. (2006) Nuclear actin: to polymerize or not to polymerize. J. Cell Biol. **172**, 495–496
20 Ankenbauer, T., Kleinschmidt, J.A., Walsh, M.J., Weiner, O.H. and Franke, W.W. (1989) Identification of a widespread nuclear actin binding protein. Nature **342**, 822–825
21 Zhu, X., Zeng, X., Huang, B. and Hao, S. (2004) Actin is closely associated with RNA polymerase II and involved in activation of gene transcription. Biochem. Biophys. Res. Commun. **321**, 623–630
22 Scheer, U., Hinssen, H., Franke, W.W. and Jockusch, B.M. (1984) Microinjection of actin-binding proteins and actin antibodies demonstrates involvement of nuclear actin in transcription of lampbrush chromosomes. Cell **39**, 111–122
23 Percipalle, P. (2007) Genetic connections of the actin cytoskeleton and beyond. BioEssays **29**, 407–411
24 Philimonenko, V.V., Zhao, J., Iben, S., Dingova, H., Kysela, K., Kahle, M., Zentgraf, H., Hofmann, W.A., de Lanerolle, P., Hozak, P. et al. (2004) Nuclear actin and myosin I are required for RNA polymerase I transcription. Nat. Cell Biol. **6**, 1165–1172
25 Ye, J., Zhao, J., Hoffmann-Rohrer, U. and Grummt, I. (2008) Nuclear myosin I acts in concert with polymeric actin to drive RNA polymerase I transcription. Genes Dev. **22**, 322–330
26 Dundr, M., Ospina, J.K., Sung, M.H., John, S., Upender, M., Ried, T., Hager, G.L. and Matera, A.G. (2007) Actin-dependent intranuclear repositioning of an active gene locus *in vivo*. J. Cell Biol. **179**, 1095–1103
27 Kysela, K., Philimonenko, A.A., Philimonenko, V.V., Janacek, J., Kahle, M. and Hozak, P. (2005) Nuclear distribution of actin and myosin I depends on transcriptional activity of the cell. Histochem. Cell Biol. **124**, 347–358
28 Riddle, V.G., Dubrow, R. and Pardee, A.B. (1979) Changes in the synthesis of actin and other cell proteins after stimulation of serum-arrested cells. Proc. Natl. Acad. Sci. U.S.A. **76**, 1298–1302
29 Bridger, J.M., Boyle, S., Kill, I.R. and Bickmore, W.A. (2000) Re-modelling of nuclear architecture in quiescent and senescent human fibroblasts. Curr. Biol. **10**, 149–152
30 Aebi, U., Cohn, J., Buhle, L. and Gerace, L. (1986) The nuclear lamina is a meshwork of intermediate-type filaments. Nature **323**, 560–564
31 Goldberg, M.W., Huttenlauch, I., Hutchison, C.J. and Stick, R. (2008) Filaments made from A- and B-type lamins differ in structure and organization. J. Cell Sci. **121**, 215–225
32 Holaska, J.M. and Wilson, K.L. (2006) Multiple roles for emerin: implications for Emery–Dreifuss muscular dystrophy. Anat. Rec. A Discov. Mol. Cell. Evol. Biol. **288**, 676–680
33 Goldman, R.D., Gruenbaum, Y., Moir, R.D., Shumaker, D.K. and Spann, T.P. (2002) Nuclear lamins: building blocks of nuclear architecture. Genes Dev. **16**, 533–547
34 Barboro, P., D'Arrigo, C., Diaspro, A., Mormino, M., Alberti, I., Parodi, S., Patrone, E. and Balbi, C. (2002) Unraveling the organization of the internal nuclear matrix: RNA-dependent anchoring of NuMA to a lamin scaffold. Exp. Cell Res. **279**, 202–218
35 Hozak, P., Sasseville, A.M., Raymond, Y. and Cook, P.R. (1995) Lamin proteins form an internal nucleoskeleton as well as a peripheral lamina in human cells. J. Cell Sci. **108**, 635–644
36 Bridger, J.M., Kill, I.R., O'Farrell, M. and Hutchison, C.J. (1993) Internal lamin structures within G_1 nuclei of human dermal fibroblasts. J. Cell Sci. **104**, 297–306
37 Goldman, A.E., Moir, R.D., Montag-Lowy, M., Stewart, M. and Goldman, R.D. (1992) Pathway of incorporation of microinjected lamin A into the nuclear envelope. J. Cell Biol. **119**, 725–735
38 Kennedy, B.K., Barbie, D.A., Classon, M., Dyson, N. and Harlow, E. (2000) Nuclear organization of DNA replication in primary mammalian cells. Genes Dev. **14**, 2855–2868
39 Moir, R.D., Montag-Lowy, M. and Goldman, R.D. (1994) Dynamic properties of nuclear lamins: lamin B is associated with sites of DNA replication. J. Cell Biol. **125**, 1201–1212
40 Jagatheesan, G., Thanumalayan, S., Muralikrishna, B., Rangaraj, N., Karande, A.A. and Parnaik, V.K. (1999) Colocalization of intranuclear lamin foci with RNA splicing factors. J. Cell Sci. **112**, 4651–4661
41 Vlcek, S. and Foisner, R. (2007) Lamins and lamin-associated proteins in aging and disease. Curr. Opin. Cell Biol. **19**, 298–304
42 Fairley, E.A., Riddell, A., Ellis, J.A. and Kendrick-Jones, J. (2002) The cell cycle dependent mislocalisation of emerin may contribute to the Emery–Dreifuss muscular dystrophy phenotype. J. Cell Sci. **115**, 341–354
43 Eriksson, M., Brown, W.T., Gordon, L.B., Glynn, M.W., Singer, J., Scott, L., Erdos, M.R., Robbins, C.M., Moses, T.Y., Berglund, P. et al. (2003) Recurrent *de novo* point mutations in lamin A cause Hutchinson–Gilford progeria syndrome. Nature **423**, 293–298
44 De Sandre-Giovannoli, A., Bernard, R., Cau, P., Navarro, C., Amiel, J., Boccaccio, I., Lyonnet, S., Stewart, C.L., Munnich, A. Le Merrer, M. and Lévy, N. (2003) Lamin A truncation in Hutchinson–Gilford progeria. Science **300**, 2055
45 Verstraeten, V.L., Broers, J.L., Ramaekers, F.C. and van Steensel, M.A. (2007) The nuclear envelope, a key structure in cellular integrity and gene expression. Curr. Med. Chem. **14**, 1231–1248
46 Sasseville, A.M. and Langelier, Y. (1998) *In vitro* interaction of the carboxy-terminal domain of lamin A with actin. FEBS Lett. **425**, 485–489
47 Zastrow, M.S., Vlcek, S. and Wilson, K.L. (2004) Proteins that bind A-type lamins: integrating isolated clues. J. Cell Sci. **117**, 979–987
48 Lattanzi, G., Cenni, V., Marmiroli, S., Capanni, C., Mattioli, E., Merlini, L., Squarzoni, S. and Maraldi, N.M. (2003) Association of emerin with nuclear and cytoplasmic actin is regulated in differentiating myoblasts. Biochem. Biophys. Res. Commun. **303**, 764–770
49 Meaburn, K.J., Cabuy, E., Bonne, G., Levy, N., Morris, G.E., Novelli, G., Kill, I.R. and Bridger, J.M. (2007) Primary laminopathy fibroblasts display altered genome organization and apoptosis. Aging Cell **6**, 139–153
50 McClintock, D., Ratner, D., Lokuge, M., Owens, D.M., Gordon, L.B., Collins, F.S. and Djabali, K. (2007) The mutant form of lamin A that causes Hutchinson–Gilford progeria is a biomarker of cellular aging in human skin. PLoS ONE **2**, e1269
51 Scaffidi, P. and Misteli, T. (2006) Lamin A-dependent nuclear defects in human aging. Science **312**, 1059–1063

Received 8 July 2008
doi:10.1042/BST0361384

Mehta *et al. Genome Biology* 2010, **11**:R5
http://genomebiology.com/2010/11/1/R5

Genome Biology

RESEARCH Open Access

Rapid chromosome territory relocation by nuclear motor activity in response to serum removal in primary human fibroblasts

Ishita S Mehta1, Manelle Amira[1,2], Amanda J Harvey[2] and Joanna M Bridger*[1]

Abstract

Background: Radial chromosome positioning in interphase nuclei is nonrandom and can alter according to developmental, differentiation, proliferation, or disease status. However, it is not yet clear when and how chromosome repositioning is elicited.

Results: By investigating the positioning of all human chromosomes in primary fibroblasts that have left the proliferative cell cycle, we have demonstrated that in cells made quiescent by reversible growth arrest, chromosome positioning is altered considerably. We found that with the removal of serum from the culture medium, chromosome repositioning took less than 15 minutes, required energy and was inhibited by drugs affecting the polymerization of myosin and actin. We also observed that when cells became quiescent, the nuclear distribution of nuclear myosin 1β was dramatically different from that in proliferating cells. If we suppressed the expression of nuclear myosin 1β by using RNA-interference procedures, the movement of chromosomes after 15 minutes in low serum was inhibited. When high serum was restored to the serum-starved cultures, chromosome repositioning was evident only after 24 to 36 hours, and this coincided with a return to a proliferating distribution of nuclear myosin 1β.

Conclusions: These findings demonstrate that genome organization in interphase nuclei is altered considerably when cells leave the proliferative cell cycle and that repositioning of chromosomes relies on efficient functioning of an active nuclear motor complex that contains nuclear myosin 1β.

Background

Within interphase nuclei, individual chromosomes are organized within their own nuclear space, known as chromosome territories [1,2]. These interphase chromosome territories are organized in a nonrandom manner in the nuclei of human cells and cells from other species [3]. Chromosomes in different species are positioned radially, according to either their gene density [4-9] or their size [10-12] or both [11,13-16]. The nuclear microenvironment within which a chromosome is located could affect its gene regulation, and it has been proposed that whole chromosomes or regions of chromosomes are shifted around the nucleus to control gene expression [17,18]. Active genes appear to come together in a common nuclear space, possibly to be co-transcribed [19-21]. This fits with the increasing number of observations made of chromosome loops, containing active areas of the genome, coming away from the main body of the chromosome territory, such as regions containing *FLNA* on the X chromosome [22]; major histocompatibility complex (*MHC*) genes [23], specific genes on chromosome 11 [24]; β- globin-like genes [25], epidermal differentiation complex genes [26], specific genes within the *Hox B* cluster [27,28], and genes inducing porcine stem cell differentiation into adipocytes [29]. Chromatin looping is apparently associated with gene expression, because inhibition of RNA polymerase II transcription affects the outward movement of these chromosome loops [30].

Repositioning of whole chromosome territories has been observed in erythroid differentiation [25], adipogenesis [31], T-cell differentiation [32], porcine spermatogenesis [33], and after hormonal stimulus [34]. Even more studies revealed genomic loci being repositioned during differentiation (see [35], for comprehensive

* Correspondence: joanna.bridger@brunel.ac.uk
[1] Centre for Cell and Chromosome Biology, Division of Biosciences, School of Health Sciences and Social Care, Brunel University, Kingston Lane, Uxbridge, UB8 3PH, UK

review). We demonstrated previously that interphase chromosomes occupy alternative nuclear positions when proliferating cells become quiescent or senescent [5,7,9]. For example, chromosomes 13 and 18 move from a peripheral nuclear location to an internal nuclear location in serum-starved or senescent fibroblast cells [5,9]. From these early studies, it was not clear how other chromosomes behaved after induction of growth arrest, and so we have now positioned all human chromosomes in cells made quiescent by serum starvation. We found that just less than half of the chromosomes alter their nuclear location. The ability to control, temporally, the entry of cells to quiescence through serum starvation allows the determination of a response time of nuclear architecture to the change in environment. In this study, we demonstrate that chromosome repositioning in interphase nuclei occurs within 15 minutes.

The presence of actin [36] and myosin [37-41] have been reported in nuclei, and an increasing body of evidence suggests that they cooperate to form a nuclear myosin-actin motor [42]. Actin and myosin have been shown to be involved in the intranuclear movement of chromosomal regions [43,44] and whole chromosomes [34]. Further, nuclear actin and myosin are involved in RNA polymerase I transcription [37,40], RNA polymerase II transcription [37-41], and RNA polymerase III transcription [45]. In a model put forward by Hoffman and colleagues [42], myosin I could bind through its tail to the nuclear entity that requires movement, with actin binding to the globular head of the nuclear myosin I molecule. This nuclear motor would then translocate the nuclear entity along highly dynamic tracks of nuclear actin [42]. In this study, we demonstrated that the rapid movement of chromosome territories in response to serum deprivation is dependent on the function of both actin and myosin, probably nuclear myosin 1β.

Results

Interphase chromosome positioning in proliferating and nonproliferating cells

To determine the nuclear location of specific chromosomes, human dermal fibroblasts (HDFs) were harvested and fixed for standard 2D-fluorescence *in situ* hybridization (FISH). Representative images of chromosome territories in proliferating cells are displayed in Figure 1a-d. Digital images were subjected to erosion analysis [4-6,8,9], whereby the images of 4',6-diamidino-2-phenylindole (DAPI)-stained flattened nuclei are divided into five concentric shells of equal area, and the intensity of the DAPI signal and probe signal is measured in each shell. The chromosome signal is then normalized by dividing it by the percentage of DAPI signal. The data for each chromosome are then plotted as a histogram with error bars, with the x-axis displaying the nuclear shells from 1 to 5, representing the nuclear periphery to the nuclear interior, respectively (Figure 1e-h).

In young proliferating fibroblasts, interphase chromosomes are positioned nonrandomly in a radial pattern within nuclei [3]. In our 2D studies, we consistently found gene-poor chromosomes, such as chromosomes X, 13, and 18, located at the nuclear periphery [5,9], which fits with their having more lamina-associated domains than gene-poor chromosomes (see [46]). In this study, we recapitulated the interphase chromosome positioning with our present cultures and demonstrated that these chromosomes are located at the nuclear periphery in young proliferating cells (Figure 1b-d, f-h). Proliferating cells within the primary cultures were identified by using the proliferative marker, anti-pKi-67, which is distributed in a number of different patterns within proliferating human fibroblasts [47]. Its distribution is mainly nucleolar and is shown in red (Figure 1a-d). Figure 1a and e demonstrate the nuclear location of chromosome 10, unlike chromosomes 13, 18, and X it is found in an intermediate position in proliferating fibroblasts. The relative interphase positions of chromosomes 10 and X have been confirmed in 3D-FISH analyses (Figure 1i-k), whereby HDFs were fixed to preserve their three-dimensionality with 4% paraformaldehyde and subjected to 3D-FISH [48]. Measurements in micrometers from the geometric center the chromosome territories to the nearest nuclear periphery, as determined by the DAPI staining, were taken in at least 20 nuclei. The data were not normalized for size measurements, so that actual measurements in micrometers can be seen. However, all data were normalized by a size measurement, and this not does alter the relative positioning of the chromosomes.

We have evidence from prior studies that chromosomes such as chromosomes 13 [9] and 18 [5,9] alter their nuclear position when primary fibroblasts exit the proliferative cell cycle and that chromosome X remains at the nuclear periphery [9]. However, this is only two chromosomes of 24, and so to determine which other chromosomes reposition after cell-cycle exit into quiescence (G_0), elicited through serum removal, we positioned all human chromosomes in G_0 cells (Figures 2 and 3).

To make cells quiescent, young, HDFs were grown in 10% NCS for 48 hours, and then the cells were washed twice with serum-free medium and placed in 0.5% NCS medium for 168 hours (7 days). However, when the positioning analysis was performed on the quiescent nuclei, we found that certain chromosomes were in very different positions from those in which they were found in proliferating nuclei, that is, chromosomes 1, 6, 8, 10, 11, 12, 13, 15, 18, and 20 (Table 1).

The data demonstrated in Figure 3 and Table 1 reveal that a number of chromosomes alter their nuclear positions when cells become quiescent; as shown before, both

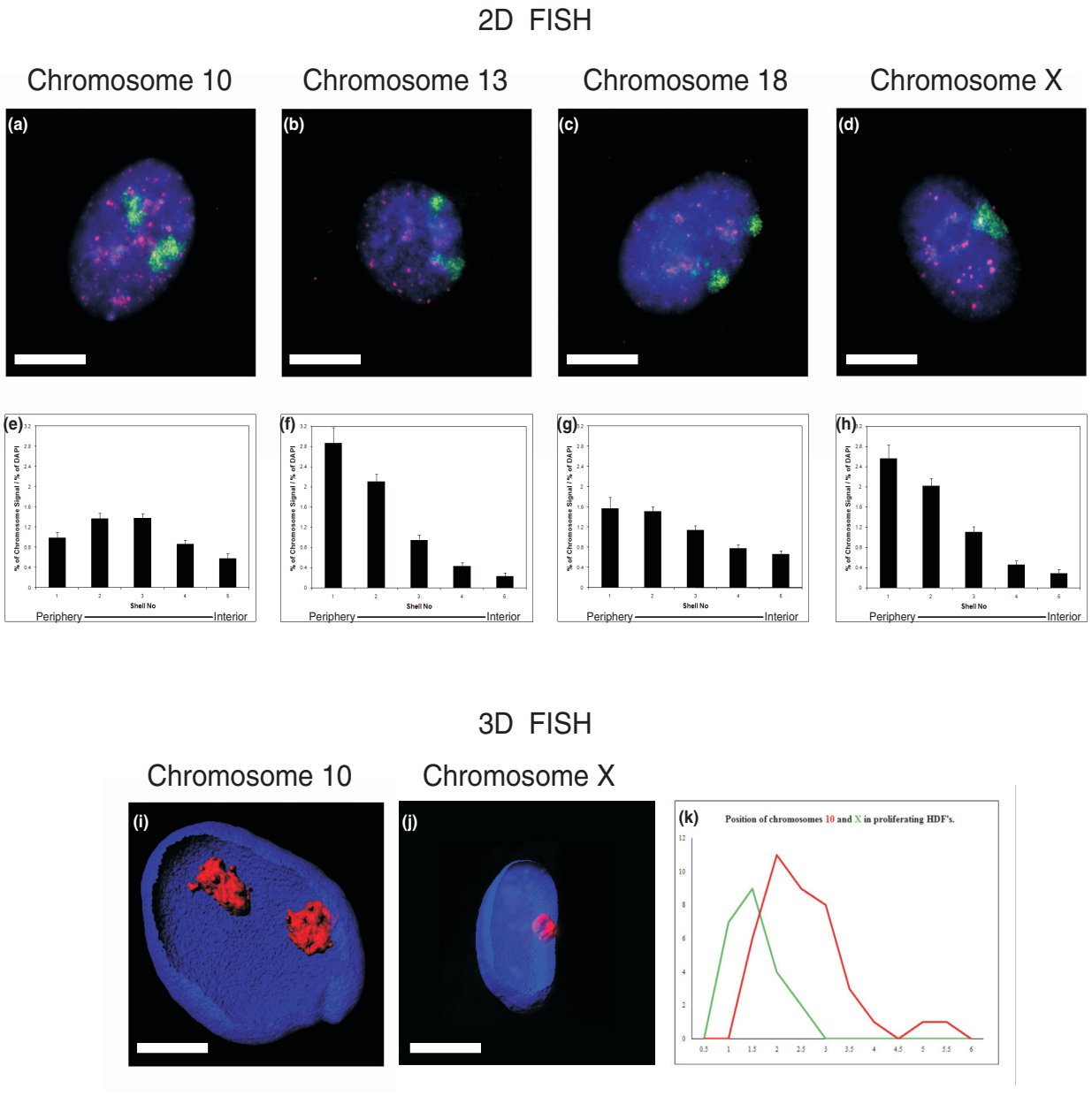

Figure 1 Chromosome positioning in proliferating interphase nuclei. Proliferating human dermal fibroblasts (HDFs) cultures were subjected to 2D- or 3D-fluorescence *in situ* hybridization (FISH) to delineate and analyze the nuclear location of chromosomes 10, 13, 18, and X. In panels **(a-d)**, the chromosome territories are revealed in green with a single chromosome territory for chromosome X, because the HDFs are male in origin. The red antibody staining is the nuclear distribution of the proliferative marker anti-pKi-67, the presence of which denotes a cell in the proliferative cell cycle. DAPI (4',6-diamidino-2-phenylindole) in blue is a DNA intercalator dye and reveals the nuclear DNA. Scale bar = 10 μm. The histograms in panels **(e-h)** display the distribution of the chromosome signal in 50 to 70 nuclei for each chromosome for 2D FISH, as analyzed with erosion analysis. This analysis divides each nucleus into five concentric shells of equal area, with shell 1 being the most peripheral shell, and shell 5 being the most interior shell [4-6,9]. The percentage of chromosome signal measured in each shell was divided by the percentage of DAPI signal in that shell. Bars represent the mean normalized proportion (percentage) of chromosome signal for each human chromosome. Error bars represent the standard error of the mean (SEM). Panels **i** and **j** display 3D projections of 0.2-μm optical sections through 3D preserved nuclei subjected to 3D-FISH and imaged with confocal laser scanning microscopy. The chromosome territories are displayed in red, and proliferating cells also were selected with positive anti-pKi-67 staining (not shown in reconstruction). Scale bar = 10 μm. The line graph in panel **(k)** displays a frequency distribution of micrometers from the geometric center of the chromosome territories to the nearest nuclear periphery, as defined by DAPI staining. Images for 20 nuclei were analyzed.

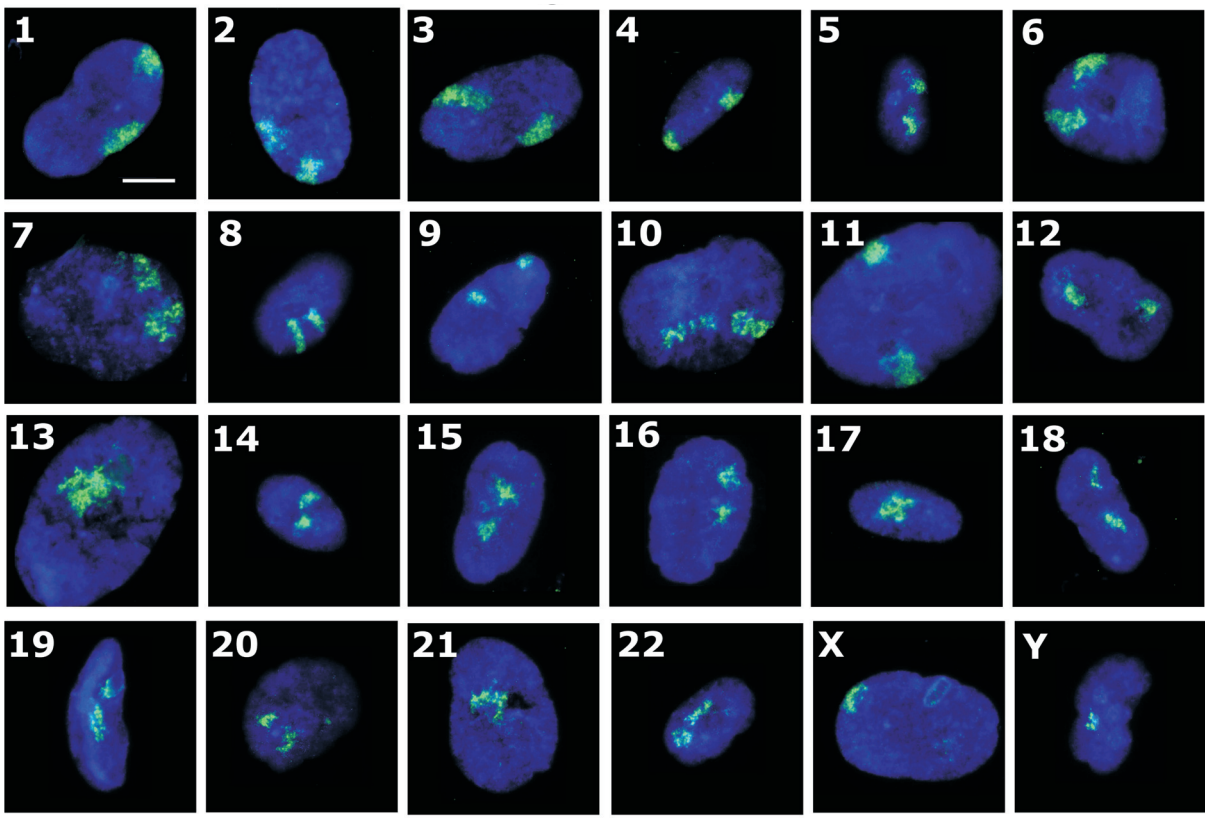

Figure 2 Chromosome positioning in quiescent interphase nuclei. Representative images displaying nuclei prepared for fluorescence *in situ* hybridization (2D-FISH), with whole-chromosome painting probes (green), and nuclear DNA is counterstained with 4',6-diamidino-2-phenylindole (DAPI) (blue). The cells were subjected to indirect immunofluorescence with anti-pKi-67 antibodies, and negative cells were selected. Cells were placed in low serum (0.5%) for 7 days, before fixation with methanol:acetic acid (3:1). The numbers (or letters) on the left side of each panel indicate the chromosome that has been hybridized. Scale bar = 10 μm.

chromosomes 13 and 18 move from a peripheral nuclear location to an interior location (Figure 3m and r). Chromosome 10 is one of a number of chromosomes that move from an intermediate nuclear location to the nuclear periphery (Figure 3j, Table 1), whereas chromosome X does not change its location at the nuclear periphery (Figure 3w), and chromosomes such as 17 and 19 do not change their interior location (Figure 3q and s, respectively).

It certainly appears that the chromosome positioning in quiescent G_0 cells is correlated with size. However, it is not clear why a repositioning of chromosomes occurs after serum removal and when and how it is elicited.

The movement of chromosomes when normal fibroblasts exit the cell cycle is rapid, active, and requires myosin and actin

To determine when the genome is reorganized on exit from the cell cycle and the speed of the response to the removal of growth factors, we took actively proliferating young cultures of primary HDFs and replaced 10% NCS medium with 0.5% NCS medium. Samples were taken at 0, 5, 10, 15, and 30 minutes after serum starvation for fixation, and chromosome position in interphase was determined with 2D-FISH and erosion analysis (Figure 4 and Additional file 1). Chromosomes 13 and 18 relocated from the nuclear periphery to the nuclear interior within 15 minutes (Figure 4h and l), with an intermediate-type nuclear positioning visible in the intervening time points (5 and 10 minutes; Figure 4f, g, j, and k). In addition, chromosome 10 moved from an intermediate location to a peripheral location in the same time window (15 minutes; Figure 4d). Chromosome X did not relocalize at all, as was reported previously [9] (Figure 4m-o), apart from some slight difference at 15 minutes (Figure 4p).

In a previous study, we demonstrated that relocation of chromosome 18 from the nuclear interior in G_0 cells to the nuclear periphery in serum-restimulated cells took 30+ hours and appeared to require cells to rebuild their nuclear architecture after a mitotic division [5]. We

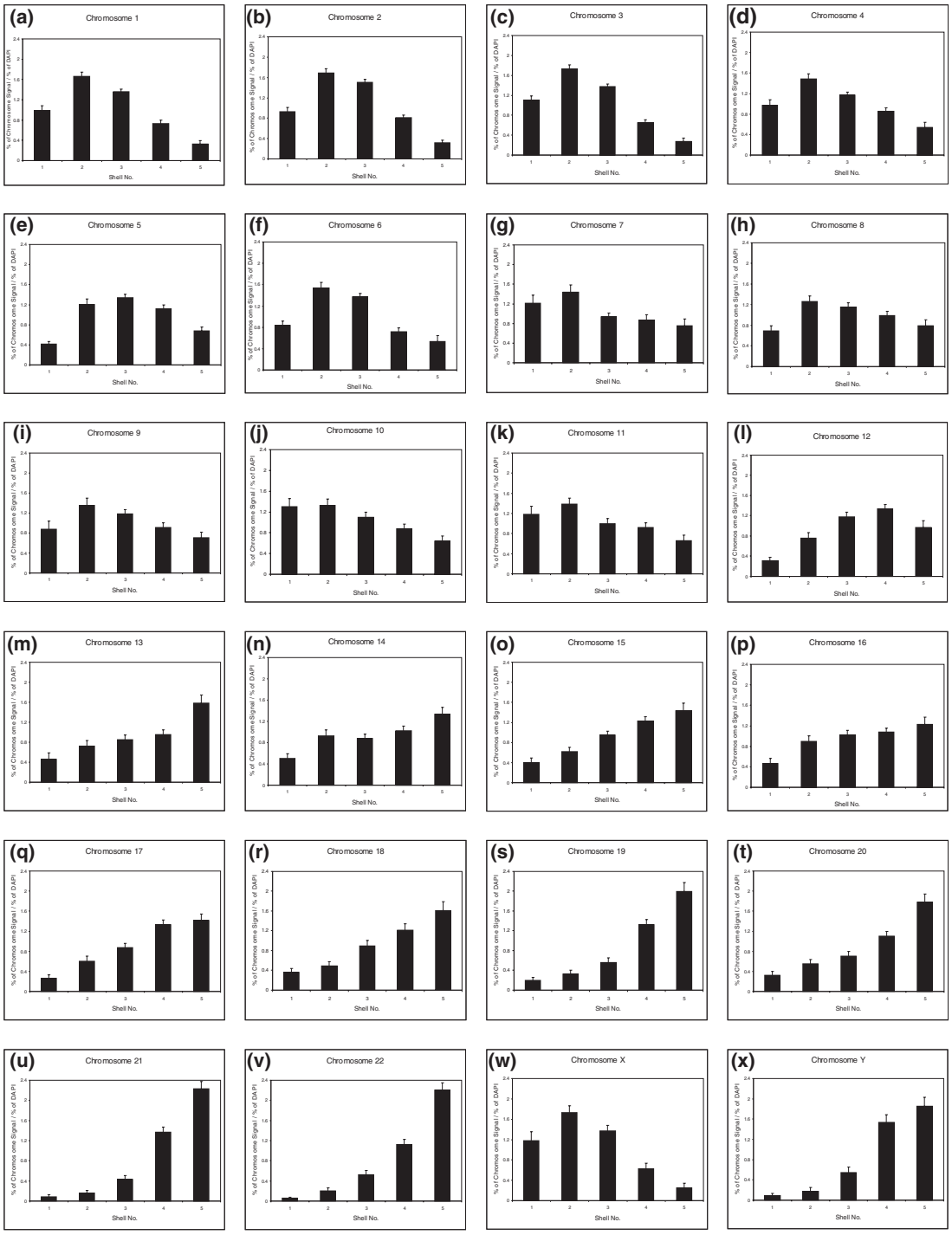

Figure 3 Analysis of radial chromosome positioning in quiescent cell nuclei. Histograms displaying chromosome positions in primary human quiescent fibroblast nuclei. The 50 to 70 nuclei per chromosome were subjected to erosion analysis, which divides each nucleus into five concentric shells of equal area, with shell 1 being the most peripheral shell, and shell 5 being the most interior shell [4-6,9]. The percentage of chromosome signal measured in each shell was divided by the percentage of 4',6-diamidino-2-phenylindole (DAPI) signal in that shell. Bars represent the mean normalized proportion (percentage) of chromosome signal for each human chromosome. Error bars represent the standard error of mean (SEM).

Table 1: The position of all chromosome territories in primary human dermal fibroblasts as determined by 2D FISH, image acquisition, and erosion analysis

Chromosome by size	Proliferating HDFs	Quiescent HDFs
1	IM[b]	P
2	P[b]	P
3	P[d]	P
4	P[cd]	P[c]
5	IM[d]	IM
6	IM[b]	P
7	P^	P
X	P[ab]	P[c]
8	IM[b]	P
9	P[d]	P
10	IM[d]	P
11	IM[d]	P
12	P[b]	I
13	P[a]	I[c]
14	I[b]	I
15	P[b]	I
16	I[b]	I
17	I[b]	I
18	P[ac]	I[ac]
19	I[a]	I[a]
20	I[d]	IM
22	I[b]	I
21	I[b]	I
Y	I^	I

This table summarizes the locations of all the chromosomes in quiescent and proliferating nuclei of human dermal fibroblasts (HDFs). The positions of chromosomes shown without a symbol have been determined for this study. [a]Data derived from [5]. [b]Data derived from [4]. [c]Data derived from [9]. [d]Data derived from [7].

showed here that the same is true for chromosome 10, with a return to an intermediate nuclear location 24 to 36 hours after restimulation of G_0 cells with 10% NCS (Figure 5d-f). We again showed that chromosome 18 requires similar times to return to the nuclear periphery (that is, 36 hours; Figure 5l). Although chromosome X remains at the nuclear periphery, a slight change in the distribution of chromosome X occurs at 32 to 36 hours (Figure 5q-r). From these data, it seems that a rapid response to the removal of growth factors reorganizes the whole genome within the interphase nucleus, and this reorganization is corrected in proliferating cells only after 24+ hours in high serum, presumably after the cells have passed through mitosis, as indicated by the peak of mitotic cells at 24 to 36 hours after serum restimulation (0 hours, none; 8 hours, none; 24 hours, 0.3%; 32 hours, 2.6%; and 36 hours, 1.2%).

Such rapid movement of large regions of the genome in response to low serum implies an active process, perhaps requiring ATP/GTP. When inhibitors of ATPase and/or GTPase, ouabain, and AG10, were incubated with proliferating cell cultures in combination with low serum, chromosome 10 did not change nuclear location (Figure 6a-d, and see Additional file 3). The relocation to the nuclear interior of chromosome 18 territories after incubation of cells in low serum also was perturbed by these

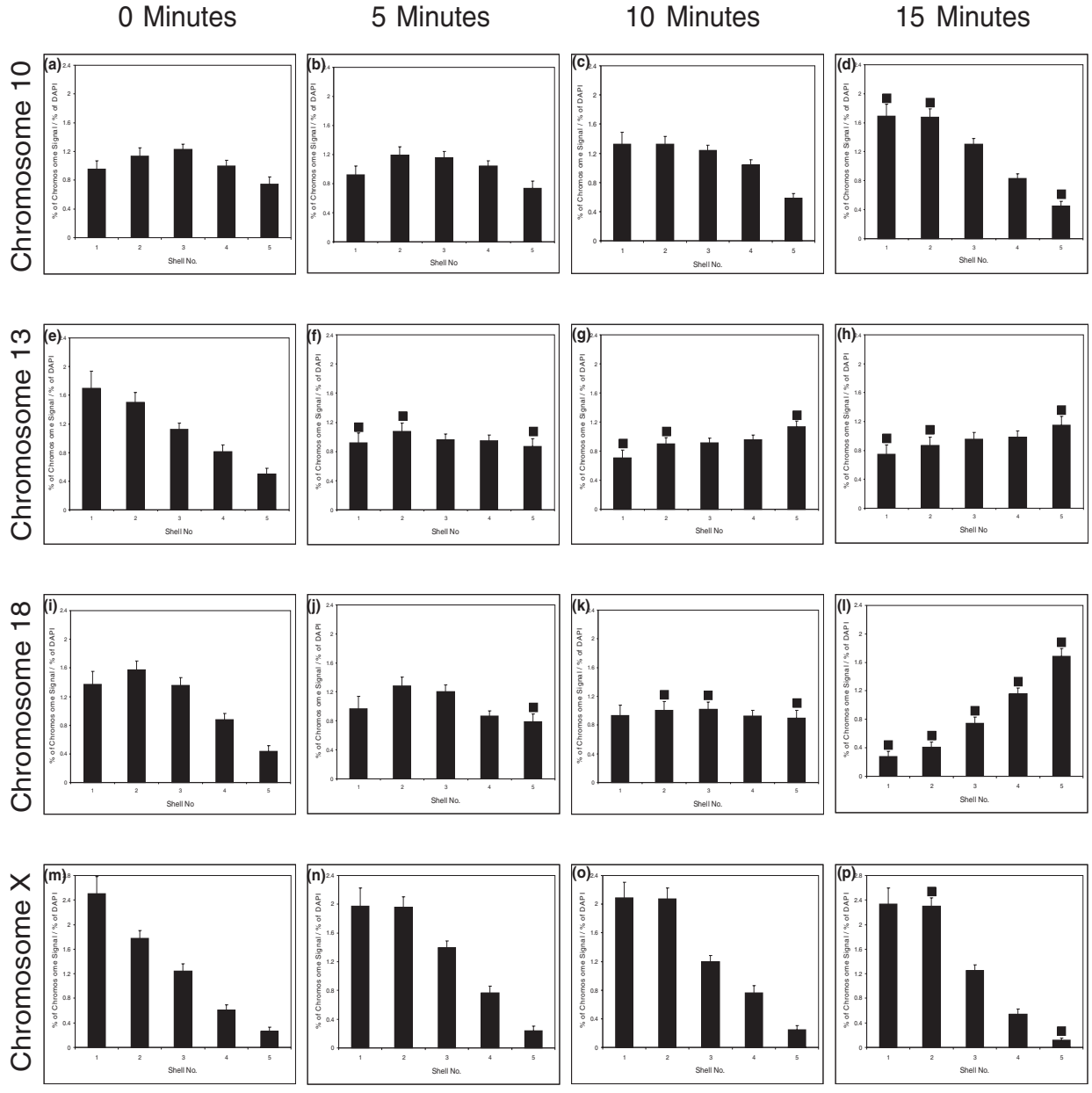

Figure 4 Rapid repositioning of chromosomes after removal of serum. Chromosomes move rapidly in proliferating cells placed in low serum. The nuclear locations of human chromosomes 10 **(a-d)**, 13 **(e-h)**, 18 **(i-l)**, and X **(m-p)** were analyzed in normal fibroblast cell nuclei fixed for 2D-FISH (fluorescence *in situ* hybridization) after incubation in medium containing low serum (0.5%) for 0, 5, 10, and 15 minutes. The filled-in squares indicate significance difference ($P < 0.05$) when compared with control proliferating fibroblast cell nuclei.

inhibitors (Figure 6a-d). The control chromosome, chromosome X, remained at the nuclear periphery (Figure 6 and Additional file 3). Because other studies suggest that nuclear motors move genomic regions around the nucleus by actin and/or myosin [42,44] we decided to use inhibitors of actin and myosin polymerization to attempt to block any chromosome movement elicited by these nuclear motors when serum was removed. Latrunculin A, an inhibitor of actin polymerization, inhibited the movement of both chromosomes 10 and 18 when cells were placed in low serum (Figure 7a and Additional file 3). In contrast, phalloidin oleate, another inhibitor of actin polymerization did not prevent relocalization of either chromosome 10 or 18, when cells were placed in low serum (Figure 7b and Additional file 3). However, two inhibitors of myosin polymerization (BDM) and function

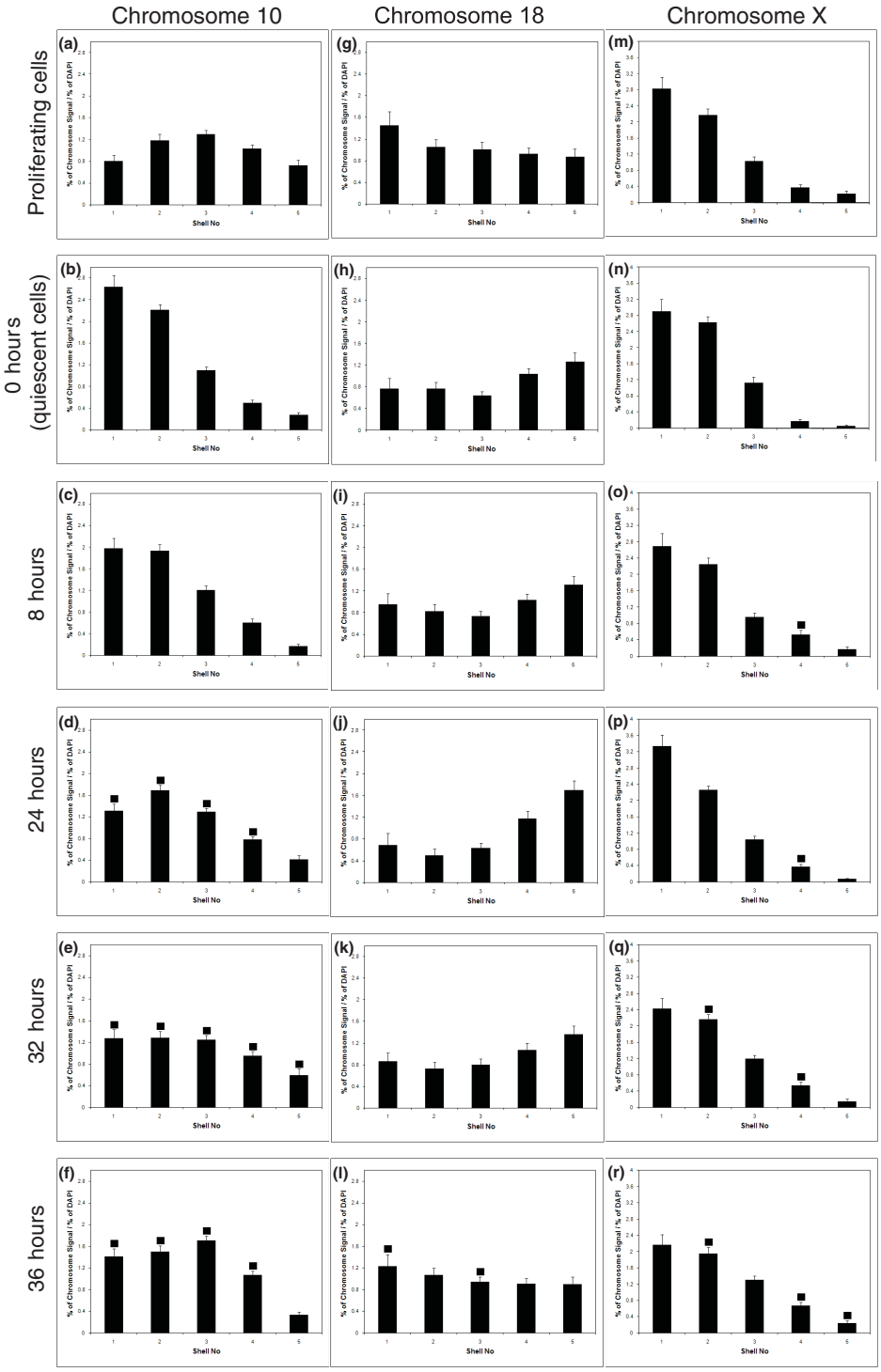

Figure 5 Restoration of proliferative chromosome position after restimulation of G_0 cells. The relocation of chromosomes to their proliferative nuclear location takes 24+ hours for chromosome 10 and 36 hours for chromosome 18. Proliferating cells (**a, g, m**) were placed in low serum (0.5%) for 7 days (**b, h, n**) and then restimulated to enter the proliferative cell cycle with the readdition of high serum. Samples were taken at 8 hours (**c, i, o**), 24 hours (**d, j, p**), 32 hours (**e, k, q**), and 36 hours (**f, l, r**) after restimulation. The graphs display the normalized distribution of chromosome signal in each of the five shells. Shell 1 is the nuclear periphery, and shell 5 is the innermost region of the nucleus. The solid squares represent a significant difference ($P < 0.05$) for that shell when compared with the equivalent shell for the time 0 data (G_0 data) for the erosion analysis.

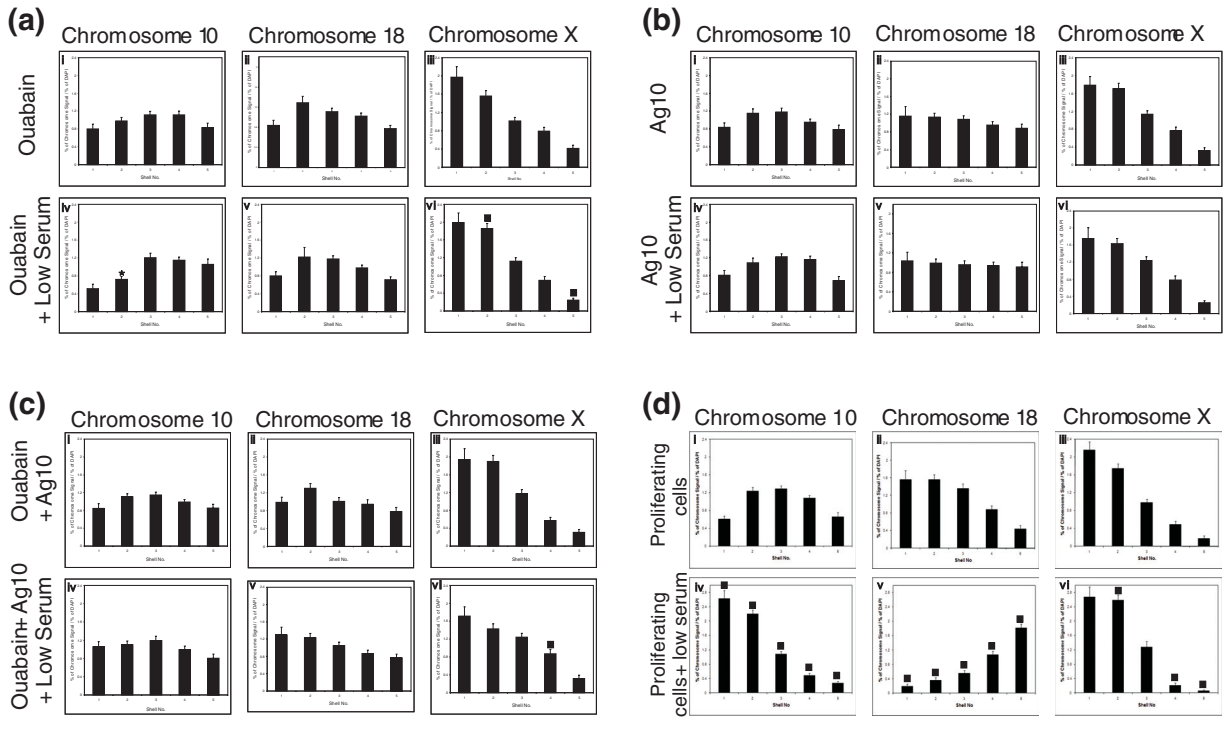

Figure 6 Chromosome repositioning requires energy. The relocation of human chromosomes 10 and 18 after incubation in low serum is energy dependent. The nuclear location of human chromosomes 10, 18, and X in were determined in normal human proliferating cell nuclei treated with ouabain (ATPase inhibitor) **(a)**, AG10 (GTPase inhibitor) **(b)**, or a combination of both **(c)** before and during incubation in low serum for 15 minutes. Normal control analysis data without any treatment is displayed in **(d)**. The error bars show the standard error of the mean. The stars indicate a significant difference ($P < 0.05$) from cells treated only with the inhibitor.

(Jasplakinolide; also affects actin polymerization) did inhibit movements of both these chromosomes upon serum removal (Figure 7c, d, and Additional file 3). Figure 7e provides a comparison for the rapid change in chromosome position when no inhibitors are used. These data imply that rapid chromosome movement observed in cells as they respond to removal of growth factors is due to an energy-driven process involving a nuclear actin:myosin motor function.

Nuclear myosin 1β is required for chromosome territory repositioning in HDFs placed in low serum

In an effort to elucidate which myosin isoform was involved in chromosome movement after serum removal in culture, we used suppression by RNA interference with small interfering RNAs (siRNAs). An siRNA pool for the gene *MYO1C* was selected because it encodes for a cytoplasmic myosin 1C and the nuclear isoform nuclear myosin 1β, a major candidate myosin for chromatin relocation [39,49]. mRNA analysis had revealed insufficient differences in sequence for suppression of myosin 1β alone (data not shown). With a double transfection of the siRNA, we observed 93% of cells displaying no nuclear myosin staining at all (Figure 8k, q, and s) but still with some cytoplasmic staining, whereas in the control cells and the cells transfected with the control construct, >95% of cells displayed a nuclear distribution of anti-nuclear myosin 1β, which was distributed in proliferating cells as accumulations at the inner nuclear envelope, the nucleoli, and throughout the cytoplasm (Figure 8g-j, m-p). These numbers did not change significantly after serum removal for 15 minutes, as per the chromosome-movement assay (data not shown).

After siRNA suppression of nuclear myosin, the chromosome-movement assay was repeated by placing the double-transfected cells into low serum for 15 minutes. The graphs in Figure 9 show that chromosomes 10, 18, and X behave as expected after removal of serum in the control cells (Figure 9a-f) and in the cells transfected with the control construct (Figure 9g-l), with chromosome 10 becoming more peripheral, chromosome 18 becoming more interior, and chromosome X remaining at the nuclear periphery. However, in the cells that had been transfected with *MYO1C*-targeting siRNA, chromosome movement was much less dramatic, with the chromo-

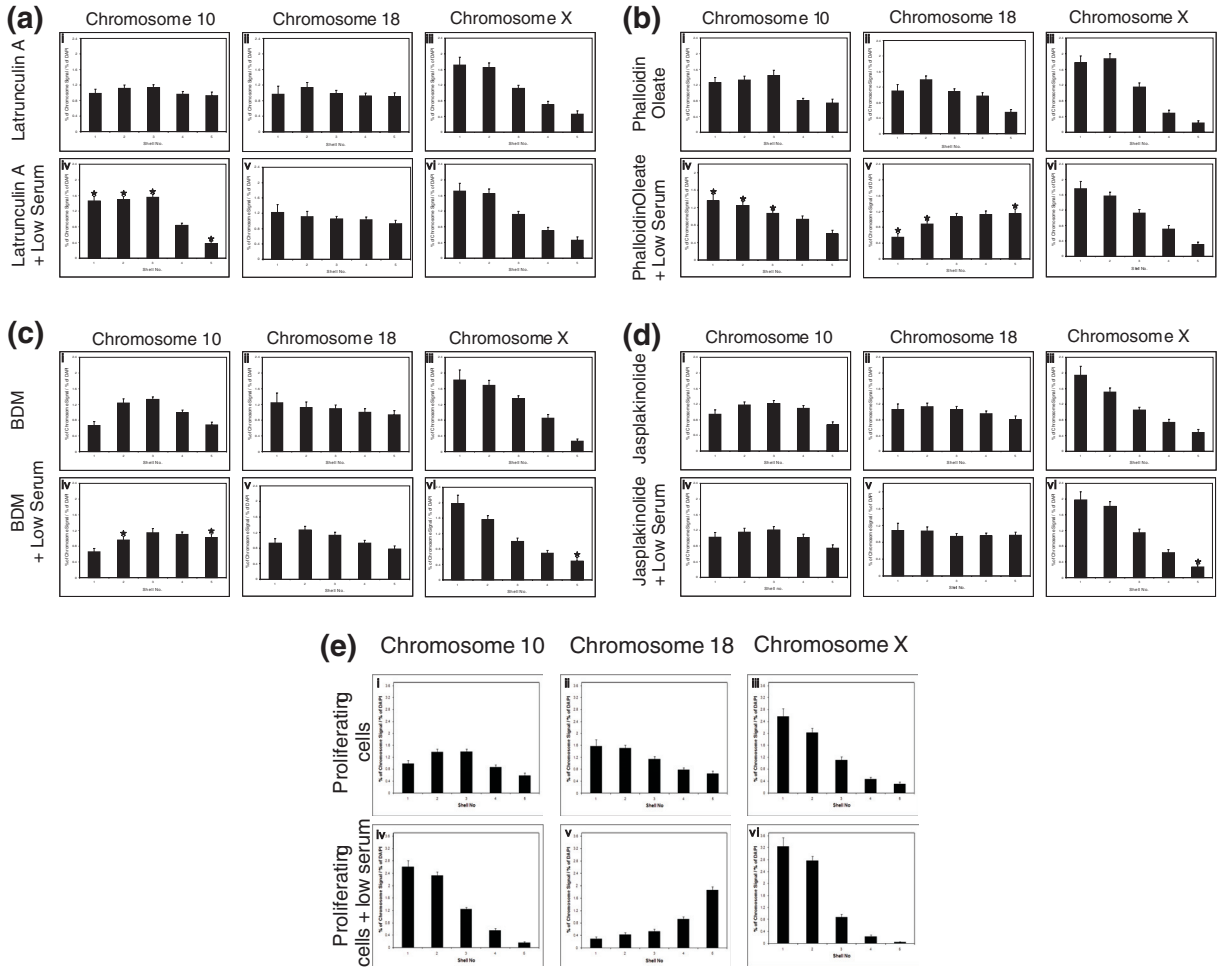

Figure 7 Chromosome repositioning requires nuclear myosin and actin. The relocation of human chromosomes 10 and 18 after incubation in low serum is myosin and actin dependent. The nuclear locations of chromosomes 10, 18, and X were determined in normal human proliferating cell nuclei treated with latrunculin A and phalloidin oleate (inhibitors of actin polymerisation) **(a, b)** and BDM and jasplakinolide (inhibitors of myosin polymerization) **(c, d)** before and during incubation in low serum for 15 minutes. The error bars show the standard error of the mean. The stars indicate a significant difference ($P < 0.05$) from cells treated only with the inhibitor. Normal control analysis data without any treatment is displayed in **(e)**.

somes still residing in similar nuclear compartments before and after the serum removal (Figure 9m-r).

The distribution of the nuclear myosin 1β is very interesting in these cells, because it gives a nuclear envelope distribution, a nucleolar distribution, and a nucleoplasmic distribution (Figure 10a-c). These distributions, although revealing, are not so surprising, because nuclear myosin has a binding affinity for the integral nuclear membrane protein emerin [50] and is involved in RNA polymerase I transcription [37,40,51]. The distribution in quiescent cells is quite different, with large aggregates of NM1β within the nucleoplasm and is missing from the nuclear envelope and nucleoli. This distribution is similar to that observed in senescent human dermal fibroblasts (Mehta, Kill, and Bridger, unpublished data). With respect to chromosome movement back to a proliferating position after incubation in low serum, we showed that it does not occur until 24 to 36 hours after repeated addition of serum to a quiescent culture (Figure 5) [5]. Correlating with this is the rebuilding of daughter nuclei after mitosis and the return of a proliferating distribution of NM1β to the nuclear envelope, nucleoli, and nucleoplasm (Figure 10g, j, p).

Discussion

This study completes the nuclear positioning of all 24 chromosomes in quiescent (serum-starved) normal primary HDFs, as assessed with 2D-FISH and erosion analysis, with a number of chromosomal positions confirmed in 3D-preserved nuclei. This study, which was performed

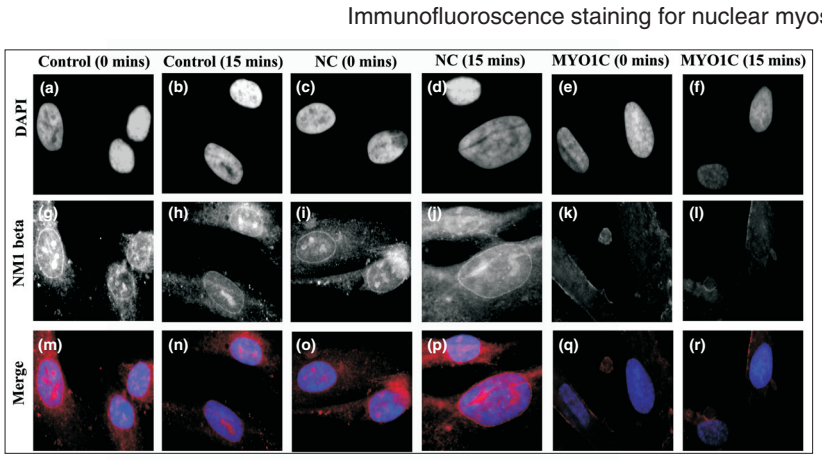

s

	% of NMIβ positive nuclei
Control 0 mins	99.3
Control 15 mins	99.6
NC 0 mins	99.1
NC 15 mins	99.6
Myo1C 0 mins	6.9
Myo1C 15 mins	5.4

Figure 8 Suppression of nuclear myosin expression by short interference RNAs (siRNAs). Normal human dermal fibroblasts (HDFs) were transfected with negative control or MYO1C targeting siRNA (double transfection) and samples for immunofluorescence staining and 2D-FISH (fluorescence *in situ* hybridization) were fixed 48 hours after the final transfection. Representative images of nuclei stained for anti-NMIβ (red) in control **(g, h, m, n)** cells transfected with negative control siRNA **(i, j, o, p)** and in cells transfected with *MYO1C* siRNA **(k, l, q, r)** after 0 and 15 minutes of serum starvation are displayed. The percentage of nuclei that are positive for NM1β in controls, in cells transfected with negative control siRNA, and in cells transfected with *MYO1C* siRNA are displayed in the adjacent table **(s)**.

on similar cell cultures and in the same way as previous studies, highlighted that some considerable difference exists in chromosomal nuclear locations between proliferating and quiescent cells. This difference cannot be due to change in nuclear size or shape, because some chromosomes move toward the nuclear interior, some, to the nuclear periphery, and some do not alter their location at all; no significant difference is found between nuclear shape and size before and after 15 minutes in low serum (data not shown). Some suggestion exists of a size-correlated distribution in quiescent cells (Table 1), with large chromosomes toward the nuclear periphery, and small chromosomes toward the nuclear interior. These results also confirm the data previously presented, whereby small chromosomes 13 and 18 had differential nuclear locations with respect to proliferating and nonproliferating cells [5,9].

How and when the alterations to chromosome positioning occur are two fundamental questions in understanding the role of genome organization in cell cycle-related events. The genome is probably anchored and influenced through a number of interactions with nuclear architecture [52,53], and so any signalled alterations/modifications to these structures could enable a reorganization of the position of chromosome territories. We know that when cells are made quiescent (for 7 days) and are restimulated to enter the cell cycle by the repeated addition of serum, chromosome 18 is not relocated back to the nuclear periphery until the cells have been through mitosis [5].

The question remained open as to when chromosomes were repositioned after serum removal. We found that repositioning of chromosomes was very rapid and complete by 15 minutes. The types of repositioning (a) requiring a rebuilding of the nucleus after mitosis, and (b) the rapid response without a nuclear envelope breakdown, imply that these processes follow different pathways and mechanisms, and the latter is consistent with an energy-dependent mechanism. This rapid movement of chromosomes after growth factor removal may be elicited through a nuclear motor such as the actin/myosin motor-complex, containing nuclear actin and nuclear myosin I, previously shown to be involved in intranuclear movements of chromatin [42-44]. This hypothesis was supported by experiments using inhibitors of ATPase and GTPase, as well as inhibitors of actin and myosin polymerization. The actin polymerization inhibitor phalloidin oleate did not inhibit chromosome movement on removal of high serum. This is important because phalloidin has been shown not to bind to nuclear actin unless the cells are treated with DMSO [54], which we had not done.

These data support other literature describing nuclear motors being involved in chromatin behavior [44]. These drugs have an effect on a broad range of myosins, and so we wanted to assess whether specific myosins were involved; thus we used an siRNA sequence that successfully suppressed the levels of nuclear myosin 1β, as shown by indirect immunofluorescence. This is the only nuclear myosin that would have been affected, but we cannot rule

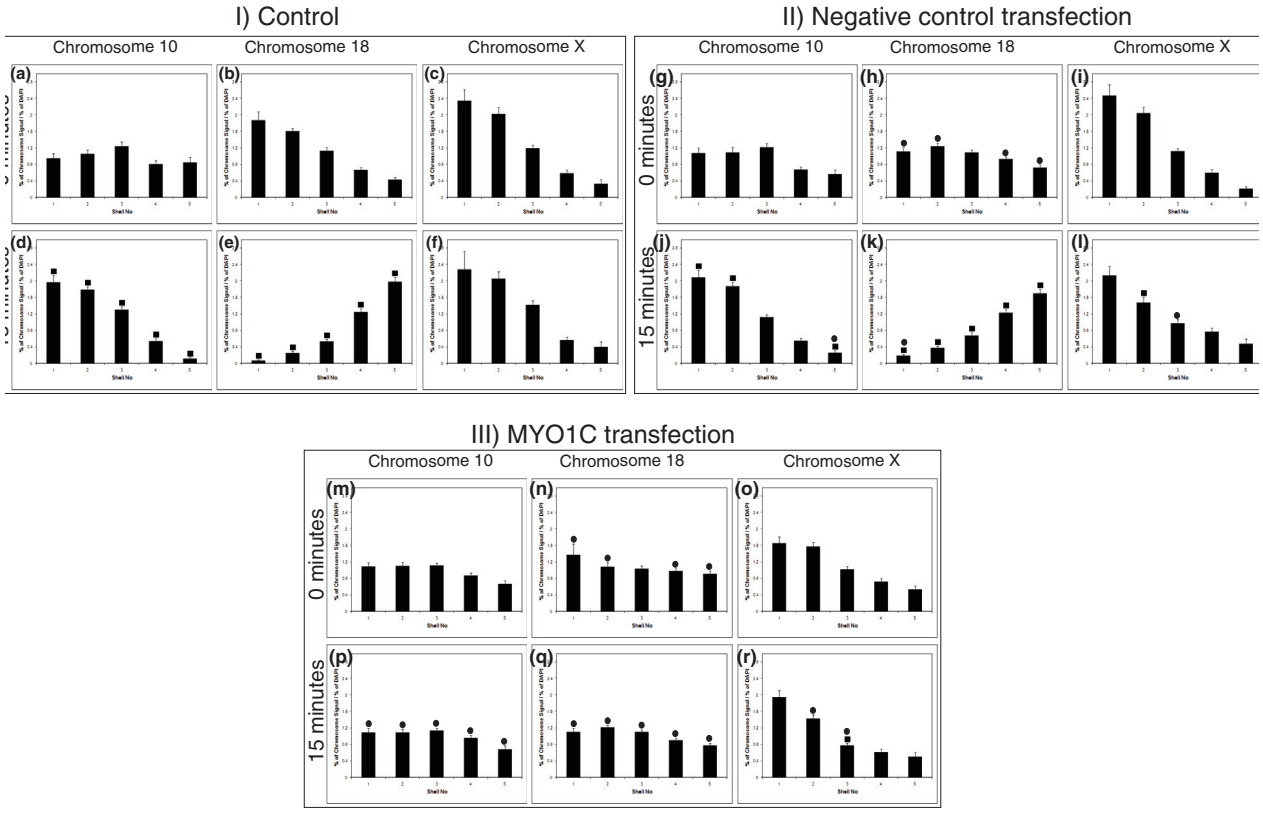

Figure 9 Chromosome repositioning is inhibited by short interference RNA (siRNA) that suppresses nuclear myosin1β. Chromosome positioning was determined with 2D-FISH (fluorescence *in situ* hybridi**z**ation) and erosion analysis, and the normalized position data plotted as histograms in control cells, in cells transfected with the negative control, and in cells transfected with the *MYO1C* siRNA construct. In control human dermal fibroblasts (HDFs) and in HDFs transfected with negative control, siRNA chromosome 10 is repositioned from an intermediate nuclear location **(a** and **g, respectively)** to the nuclear periphery **(d, j)** after 15 minutes of incubation in low serum. Chromosome 18 territories, conversely, are repositioned from the nuclear periphery **(b, h)** to the nuclear interior **(e, k)** after 15 minutes of incubation in low serum in control HDFs and in HDFs transfected with negative control siRNA. In HDFs transfected with the *MYO1C* siRNA construct, chromosomes 10 **(m, p)** and 18 **(n, q)** do not show repositioning after 15 minutes of incubation in low serum. Chromosome X remains at the nuclear periphery at all times **(c, f, i, l, o, r)**. Unpaired, unequal variances two-tailed Students *t* tests were performed to assess statistical differences. The solid squares indicate a significant difference ($P < 0.05$) from cells not incubated in, and the solid circles indicate a significant difference ($P < 0.05$) from control HDFs.

out that other myosins located within the cytoplasm (such as myosin 1A and 1C), which may be suppressed as well, could have a long-range interaction with chromatin, through the nuclear envelope, possibly through nesprins and SUN domain proteins [55,56].

However, the distribution of nuclear myosin 1β that we observe in proliferating cells correlates with its properties and functions, as described in the literature, and implicates the nuclear envelope in chromosome/chromatin movement. In previous studies, we analyzed chromosome position in cells that have defects of the nuclear lamina, through mutations in nuclear lamin A or emerin, both nuclear envelope proteins. These cells displayed a nonproliferating distribution of chromosomes even though they were proliferating [9,57]. The behavior of nuclear motor proteins in these cells must be addressed. Further, the distribution of NM1β from aggregates in quiescent cells to the nuclear envelope, nucleoli, and nucleoplasm is not observed until more than 24 hours after serum readdition, which correlated with when specific chromosomes become relocated from their quiescent position to their proliferating location.

Conclusions

We demonstrated that some chromosomes occupy different nuclear compartments in proliferating and serum-starved quiescent cells. Most interestingly, this repositioning of chromosomes is very rapid, taking less than 15 minutes, and requires energy and active actin and myosin function. The myosin involved could be nuclear myosin 1β, which has dramatically different distribution in quiescent nuclei as compared with proliferating cell nuclei.

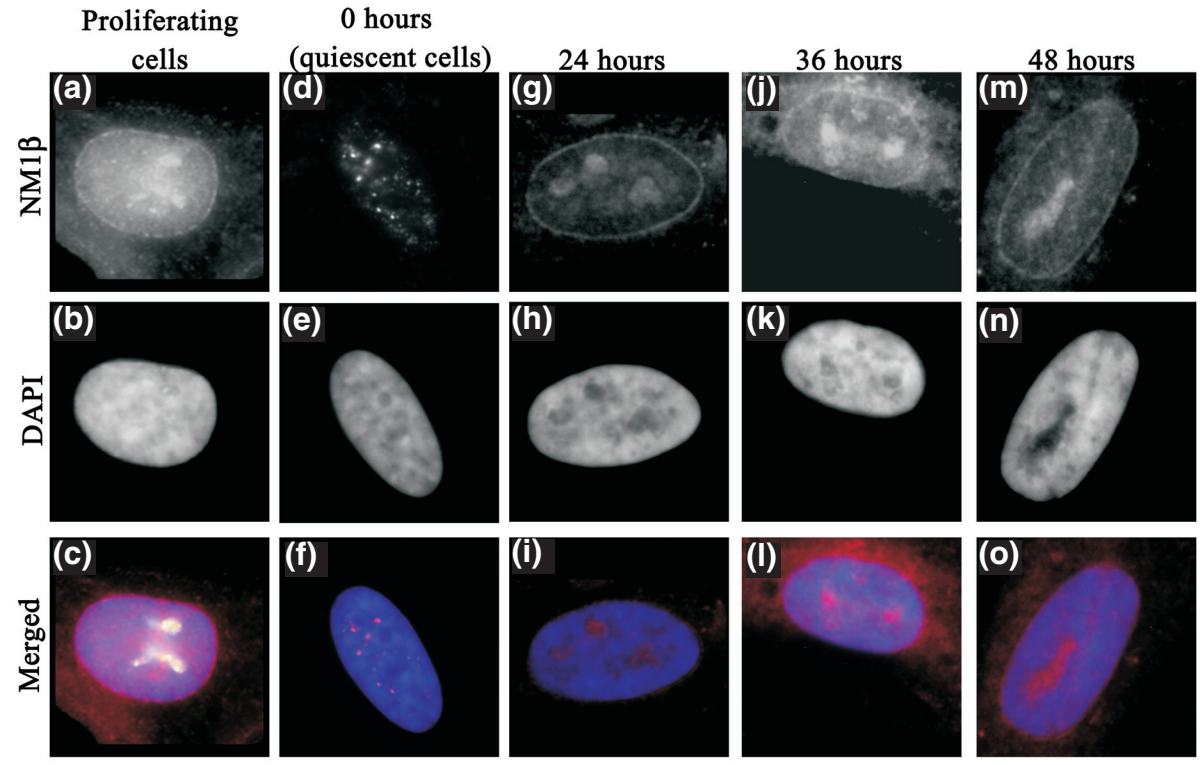

(p)

	Proliferating cells	0 hours (quiescent cells)	24 hours	36 hours	48 hours
Nucleolar + rim + nucleoplasmic	87.2 ± 10.01	0.3 ± 1.154	73.0 ± 7.234	91.9 ± 6.0	91.9 ± 3.055
Nucleolar only	0 ± 0	25.4 ± 9.0	20.0 ± 6.506	4.4 ± 2.08	2.3 ± 3.05
Aggregates	5.8 ± 4.35	72.1 ± 13.57	6.9 ± 8.144	0.6 ± 1.51	1.1 ± 1.527
Rim + nucleoplasmic	6.3 ± 4.041	0 ± 0	0 ± 0	0.3 ± 1.154	1.5 ± 4.725
Nucleoplasmic	0.7 ± 1.527	1.6 ± 4.163	0.1 ± 0.577	2.3 ± 4.0	2.4 ± 2.645
Dull	0 ± 0	0.6 ± 1.527	0 ± 0	0.6 ± 2.309	0.8 ± 2.0

Figure 10 Anti-nuclear myosin 1b (NM1β) staining patterns in proliferating cells, quiescent cells, and after restimulation. Normal 2DD human dermal fibroblasts (HDFs) were serum starved for 7 days to induce quiescence. The cells were then restimulated with fresh serum, and samples were collected at 0, 24, 36 and 48 hours after serum restoration. Samples were also collected before serum withdrawal (proliferating cells). The samples were then fixed with methanol/acetone (1:1), and the distribution of NMIβ was assessed by performing an indirect immunofluorescence assay for NMIβ. Images in **(a, c)** display the distribution of NMIβ in proliferating cells, whereas those in **(d** and **f)** show the distribution of NMIβ after 0, 24, 36 and 48 hours after restimulation of quiescent fibroblasts. The table **(p)** displays the percentage of cells displaying various patterns of NMIβ staining after restimulation. Error is indicated by standard deviation. Scale bar = 10 μm.

Materials and methods

Cell culture

Human dermal fibroblasts (HDFs), 2DD [58] were grown in Dulbecco's Modified Eagles Medium (DMEM) containing 10% newborn calf serum (vol/vol NCS), glutamine, and antibiotics, at 37°C. Cells were passaged twice a week and seeded at a density of $3 \times 10^3/cm^2$. Cells were made quiescent by incubation in 10% NCS DMEM for 2 days, washing in serum-free medium, followed by incubation in DMEM containing 0.5% NCS (vol/vol) for 7 days.

Inhibitors of ATPase, GTPase, myosin, and actin polymerization

To inhibit the activity of ATPase or GTPase, cells were treated with 100 μmol/L ouabain (Calbiochem-Novabiochem, Beeston, Nottingham, UK) for 30 minutes [59] or with 100 μmol/L AG10 (Calbiochem) for 20 or 30 minutes before serum withdrawal [60,61], respectively. To inhibit the polymerization of actin, cells were treated with 1 μmol/L either Latrunculin A (Calbiochem) [62,63] or phalloidin oleate (Calbiochem) [64] for 30 minutes. Myosin polymerization was inhibited by treating cells

either with 10 mmol/L 2,3-butanedione 2-monoxime (Calbiochem) for 15 minutes [65-67] or 1 μmol/L Jasplakinolide (Calbiochem) for 60 minutes [68]. See Additional file 5.

Fluorescence in situ hybridization

For the two-dimensional FISH assay, fibroblasts were harvested and placed in hypotonic buffer (0.075 mol/L KCl, wt/vol) for 15 minutes at room temperature. After centrifugation at 400 g, cells were fixed in 3:1 (vol/vol) methanol/acetic acid (vol/vol) for 1 hour on ice. The fixation step was repeated between 5 and 7 times before cells were dropped onto humidified glass microscope slides. The slides were aged at room temperature for 2 days or for an hour at 70°C before being subjected to dehydration through an ethanol series of 70%, 90%, and 100%, for 5 minutes each. The cells were denatured in 70% formamide, 2 × sodium saline citrate buffer (SSC), pH 7, at 70°C for 2 minutes. After denaturation, the slides were immediately plunged into ice-cold 70% ethanol for 5 minutes and then taken through the ethanol series and air-dried.

For three-dimensional FISH assay, fibroblasts were washed in 1 × PBS and then fixed in 4% paraformaldehyde (wt/vol) in 1 × PBS for 10 minutes. The cells were then permeabilized with 0.5% Triton-X100 (vol/vol) and 0.5% saponin (wt/vol) in 1 × PBS solution for 20 minutes. The cells were then incubated in 20% glycerol, 1 × PBS solution for at least 30 minutes before being snap-frozen in liquid nitrogen. The cells were repeatedly frozen and thawed for up to 5 times. After the freeze/thaw cycles, the cells were then washed in 1 × PBS for at least 30 minutes and then incubated in 0.1 N HCl for 10 minutes for depurination. The cells were then washed in 2 × SSC for 15 minutes, with three changes of the buffer, and incubated in 50% formamide, 2 × SSC, at pH 7.0, overnight. For denaturation, cells were incubated at 73°C to 76°C in 70% formamide, 2 × SSC, pH 7 solution for 3 minutes and then were immediately transferred to 50% formamide, 2 × SSC, pH 7 solution for 1 minute at the same temperature. Chromosome paints for HSA 10, 13, 18, and X were amplified from flow-sorted whole-chromosome templates and labelled with biotin-dUTP by DOP-PCR [69]. The 200- to 400-μg chromosome paints, 7 μg of C_0t-1 DNA, and 3 μg of herring sperm were used per slide. All other chromosome territories were delineated with directly labelled whole human chromosome paints (Qbiogene, Cambridge, UK). Probes were denatured at 70°C for 10 minutes with reannealing of repetitive sequences at 37°C for 30 to 120 minutes. Hybridization was performed in a humified chamber for 18 to 24 hours at 37°C. The slides were washed in three changes of 50% formamide, 2 × SSC, pH 7, at 45°C over a 15-minute period, followed by three changes of 0.1 × SSC prewarmed to 60°C over a 15-minute period at 45°C.

The slides were then transferred to 4 × SSC at room temperature. Slides hybridized with the in-house biotin-labelled probes were then incubated with a blocking solution of 4% bovine serum albumin (BSA; Sigma Aldrich) of 4 × SSC followed by detection with streptavidin-cyanine 3 (Amersham Life Science Ltd; 1:200 dilution in 0.1% BSA/4 × SSC). The slides were washed in three changes of 4 × SSC/0.05% Tween 20 (vol/vol) for 5 minutes each.

Suppressing the expression of nuclear myosin 1β by interference RNA

To suppress nuclear myosin 1β expression, young proliferating HDFs were seeded at 1×10^4 cells per well in a 12-well plate. Transfection efficiency was previously determined with siGLO-labelled siRNA to be more than 95%. The siRNA transfection was carried out with 2 μl Dharmafect 1 and 50 μl of either negative control (2 μmol/L ON-TARGETplus Non-targeting Pool; Thermo Scientific) or myosin-targeting siRNA (2 μmol/L ON-TARGETplus SMART pool, human MYO1C; Thermo Scientific Cat number L-015121-00) in 200 μl serum-free medium. Complete medium was added to the transfection mix to ensure that transfections were carried out in serum-containing medium with a final siRNA concentration of 100 nmol/L per well/dish. Six hours after transfection, the medium in the well was replaced with normal growth medium. At 24 hours after the first transfection, a second identical transfection was performed to increase the amount of suppression. Samples were collected at 48 hours after final transfection and fixed for 2D FISH and indirect immunofluorescence.

Indirect immunofluorescence

Diluted rabbit anti-Ki-67 antibody (Dako; 1:1,500 dilution in PBS/1% NCS), 40 μl, was placed on the slides after FISH for 1 hour at 37°C. Slides were washed in PBS for 15 minutes, with three changes. The slides were incubated with 40 μl of swine anti-rabbit secondary antibody conjugated either to fluorescein isothiocynate (FITC, Dako) or to tetrarhodamine isothiocynate (TRITC, Dako) (1:30 dilution in 1% NCS/PBS) for 1 hour at 37°C.

For anti-nuclear myosin 1β staining, cells were grown on glass coverslips and fixed in 1:1 (vol/vol) methanol/acetone for 10 minutes on ice. Rabbit anti-NM1β (Sigma-Aldrich) was diluted in PBS/1% NCS (1:200) and incubated with the fixed cells at room temperature for 1 hour after washing thrice in PBS swine anti-rabbit conjugated to tetrarhodamine isothiocyanate was incubated for 1 hour at room temperature.

Thereafter the slides were washed in PBS with three changes over a 15-minute period and mounted in self-sealing Vectashield mounting medium (Vector Laboratories) containing the counterstain 4, 6-diamidino-2-phe-

nylindole (DAPI).

Image capture and analysis

Two-dimensional FISH

Digital grey-scale images of random nuclei were captured by using a Photometrics cooled charged-coupled device (CCD) camera, pseudocolored, and merged by using Digital Scientific software, the Quips Pathvysion, Smart Capture VP V1.4, a Leica fluorescence microscope (Leitz DMRB) with Plan Fluotar 100 × oil-immersion lens. The images were run through a simple erosion script in IPLab spectrum software, as described in [4]. The DAPI image of the nucleus is outlined and divided into five concentric shells of equal area, the first shell being most peripheral, and the innermost denoting the interior of the nucleus. The script measures the pixel intensity of DAPI and the chromosome probe in these five shells. The probe signal was normalized by dividing the percentage of the probe by the percentage of DAPI signal in each shell. Histograms were plotted with standard error bars representing the standard error of the mean (± SEM). Simple statistical analyses were performed by using the unpaired two-tailed Student's *t* test with Microsoft Excel.

Three-dimensional FISH

The images of nuclei prepared by three-dimensional FISH were captured by using a Nikon confocal laser scanning microscope (TE2000-S) equipped with a 60 ×/1.49 Nikon Apo oil-immersion objective. The microscope was controlled by Nikon confocal microscope C1 (EZ-C1) software, version 3.00. Stacks of optical sections with an axial distance of 0.2 μm were collected from 20 random nuclei. Stacks of eight-bit grey-scale 2D images were obtained with a pixel dwell of 4.56, and eight averages were taken for each optical image. The positioning of chromosomes in relation to the nuclear periphery was assessed by performing measurements with Imaris Software (Bitplane Scientific Solutions), whereby the distance in micrometers between the geometric center of each chromosome territory and the nearest nuclear periphery, as determined with DAPI staining, in three dimensions. These data were not normalized for size, but when the data were normalized by dividing by the length of the major axis + the length of the minor axis divided by 2, or the length of the major axis alone, the relative positions of the individual chromosomes in frequency distributions did not change.

Frequency distribution curves were plotted with the distance between the geometric center of chromosome territory and the nearest nuclear periphery on the x-axis in actual micrometers, and the frequency, on the y-axis.

Additional material

Additional data file 1

The chromosome position of chromosomes 10, 13, 18, and X 30 minutes after serum removal from a proliferating culture of human dermal fibroblasts in a 2D study (1A-D), and the 3D analysis of the nuclear position of chromosomes 10 and X after 15 minutes after serum removal from a proliferating culture (1E).

Additional data file 2

Treating cells with 0.1% DMSO, in which the drugs are dissolved, does not interfere with the chromosome-repositioning response.

Additional data file 3

3D analyses of chromosome position for chromosomes 10 and X after treatment with GTPase inhibitor AG10 and serum removal (3A), after treatment with phalloidin oleate and serum removal (3B) and after treatment with BDM and serum removal (3C).

Additional data file 4

The DAPI distribution with each shell of the 2D erosion analysis script for each experiment performed, revealing that the DNA content did not alter after any of the treatments (4).

Additional data file 5

A table describing the inhibitors and drugs used in this study.

Abbreviations

BDM: 2,3-butanedione 2-monoxime; FITC: fluorescein isothiocyanate; G_0: quiescence; HDF: human dermal fibroblast; I: interior; IM: intermediate; NCS: newborn calf serum; NMIβ: nuclear myosin Iβ; P: peripheral; TRITC: tetrarhodamine isothiocyanate.

Authors' contributions

ISM provided material, experimentation, data collection and analysis, writing manuscript, and intellectual input. MA provided some data for nuclear shape and size and some intellectual input for siRNA. AH provided intellectual input for siRNA experimentation and writing of the manuscript. JMB participated in data analysis, writing the manuscript, and intellectual input.

Acknowledgments

We are grateful to Prof. Wendy Bickmore and Dr. Paul Perry for the simple erosion script for analysis of 2D-FISH data. We also thank Dr. Julio Masabanda for providing whole-chromosome flow-sorted templates. The authors also thank Drs. Ian Kill and Karen Meaburn for helpful suggestions concerning the manuscript.

Author Details

[1]Centre for Cell and Chromosome Biology, Division of Biosciences, School of Health Sciences and Social Care, Brunel University, Kingston Lane, Uxbridge, UB8 3PH, UK and
[2]Brunel Institute for Cancer Genetics and Pharmacogenomics, Division of Biosciences, School of Health Sciences and Social Care, Brunel University, Kingston Lane, Uxbridge, UB8 3PH, UK

Received: 25 September 2009 Revised: 23 November 2009
Accepted: 13 January 2010 Published: 13 January 2010

References

1. Cremer T, Cremer C: **Rise, fall and resurrection of chromosome territories: a historical perspective; part II: fall and resurrection of chromosome territories during the 1950s to 1980s; part III: chromosome territories and the functional nuclear architecture: experiments and models from the 1990s to the present.** *Eur J Histochem* 2006, **50:**223-272.
2. Meaburn KJ, Misteli T: **Cell biology: chromosome territories.** *Nature* 2007, **445:**379-781.
3. Foster HA, Bridger JM: **The genome and the nucleus: a marriage made by evolution: genome organisation and nuclear architecture.** *Chromosoma* 2005, **114:**212-229.
4. Boyle S, Gilchrist S, Bridger JM, Mahy NL, Ellis JA, Bickmore WA: **The spatial organization of human chromosomes within the nuclei of normal and emerin-mutant cells.** *Hum Mol Genet* 2001, **10:**211-219.
5. Bridger JM, Boyle S, Kill IR, Bickmore WA: **Re-modelling of nuclear architecture in quiescent and senescent human fibroblasts.** *Curr Biol* 2000, **10:**149-152.
6. Croft JA, Bridger JM, Boyle S, Perry P, Teague P, Bickmore WA: **Differences in the localization and morphology of chromosomes in the human nucleus.** *J Cell Biol* 1999, **145:**1119-1131.
7. Meaburn KJ, Newbold RF, Bridger JM: **Positioning of human chromosomes in murine cell hybrids according to synteny.** *Chromosoma* 2008, **117:**579-591.
8. Meaburn KJ, Levy N, Toniolo D, Bridger JM: **Chromosome positioning is largely unaffected in lymphoblastoid cell lines containing emerin or A-type lamin mutations.** *Biochem Soc Trans* 2005, **33:**1438-1440.
9. Meaburn KJ, Cabuy E, Bonne G, Levy N, Morris GE, Novelli G, Kill IR, Bridger JM: **Primary laminopathy fibroblasts display altered genome organization and apoptosis.** *Aging Cell* 2007, **6:**139-153.
10. Bolzer A, Kreth G, Solovei I, Koehler D, Saracoglu K, Fauth C, Muller S, Eils R, Cremer C, Speicher MR, Cremer T: Three-dimensional maps of all chromosomes in human male fibroblast nuclei and prometaphase rosettes. PLoS Biol 2005, 3:e157.
11. Mora L, Sanchez I, Garcia M, Ponsa M: **Chromosome territory positioning of conserved homologous chromosomes in different primate species.** *Chromosoma* 2006, **115:**367-375.
12. Sun HB, Shen J, Yokota H: **Size-dependent positioning of human chromosomes in interphase nuclei.** *Biophys J* 2000, **79:**184-190.
13. Habermann FA, Cremer M, Walter J, Kreth G, von Hase J, Bauer K, Wienberg J, Cremer C, Cremer T, Solovei I: **Arrangements of macro- and microchromosomes in chicken cells.** *Chromosome Res* 2001, **9:**569-584.
14. Mayer R, Brero A, von Hase J, Schroeder T, Cremer T, Dietzel S: **Common themes and cell type specific variations of higher order chromatin arrangements in the mouse.** *BMC Cell Biol* 2005, **6:**44.
15. Neusser M, Schubel V, Koch A, Cremer T, Muller S: **Evolutionarily conserved, cell type and species-specific higher order chromatin arrangements in interphase nuclei of primates.** *Chromosoma* 2007, **116:**307-320.
16. Tanabe H, Habermann FA, Solovei I, Cremer M, Cremer T: **Non-random radial arrangements of interphase chromosome territories: evolutionary considerations and functional implications.** *Mutat Res* 2002, **504:**37-45.
17. Fraser P, Bickmore W: **Nuclear organization of the genome and the potential for gene regulation.** *Nature* 2007, **447:**413-417.
18. Parada L, Misteli T: **Chromosome positioning in the interphase nucleus.** *Trends Cell Biol* 2002, **12:**425-432.
19. Osborne CS, Chakalova L, Brown KE, Carter D, Horton A, Debrand E, Goyenechea B, Mitchell JA, Lopes S, Reik W, Fraser P: **Active genes dynamically colocalize to shared sites of ongoing transcription.** *Nat Genet* 2004, **36:**1065-1071.
20. Osborne CS, Chakalova L, Mitchell JA, Horton A, Wood AL, Bolland DJ, Corcoran AE, Fraser P: **Myc dynamically and preferentially relocates to a transcription factory occupied by IgH.** *PLoS Biol* 2007, **5:**e192.
21. Spilianakis CG, Lalioti MD, Town T, Lee GR, Flavell RA: **Interchromosomal associations between alternatively expressed loci.** *Nature* 2005, **435:**637-645.
22. Scheuermann MO, Tajbakhsh J, Kurz A, Saracoglu K, Eils R, Lichter P: **Topology of genes and nontranscribed sequences in human interphase nuclei.** *Exp Cell Res* 2004, **301:**266-279.
23. Volpi EV, Chevret E, Jones T, Vatcheva R, Williamson J, Beck S, Campbell RD, Goldsworthy M, Powis SH, Ragoussis J, Trowsdale J, Sheer D: **Large-scale chromatin organization of the major histocompatibility complex and other regions of human chromosome 6 and its response to interferon in interphase nuclei.** *J Cell Sci* 2000, **113:**1565-1576.
24. Mahy NL, Perry PE, Gilchrist S, Baldock RA, Bickmore WA: **Spatial organization of active and inactive genes and noncoding DNA within chromosome territories.** *J Cell Biol* 2002, **157:**579-589.
25. Galiova G, Bartova E, Kozubek S: **Nuclear topography of beta-like globin gene cluster in IL-3-stimulated human leukemic K-562 cells.** *Blood Cells Mol Dis* 2004, **33:**4-14.
26. Williams RR, Broad S, Sheer D, Ragoussis J: **Subchromosomal positioning of the epidermal differentiation complex (EDC) in keratinocyte and lymphoblast interphase nuclei.** *Exp Cell Res* 2002, **272:**163-175.
27. Chambeyron S, Da Silva NR, Lawson KA, Bickmore WA: **Nuclear re-organisation of the Hoxb complex during mouse embryonic development.** *Development* 2005, **132:**2215-2223.
28. Chambeyron S, Bickmore WA: **Chromatin decondensation and nuclear reorganization of the HoxB locus upon induction of transcription.** *Genes Dev* 2004, **18:**1119-1130.
29. Szczerbal I, Foster HA, Bridger JM: **The spatial repositioning of adipogenesis genes is correlated with their expression status in a porcine mesenchymal stem cell adipogenesis model system.** *Chromosoma* 2009, **118:**647-663.
30. Heard E, Bickmore W: **The ins and outs of gene regulation and chromosome territory organisation.** *Curr Opin Cell Biol* 2007, **19:**311-316.
31. Kuroda M, Tanabe H, Yoshida K, Oikawa K, Saito A, Kiyuna T, Mizusawa H, Mukai K: **Alteration of chromosome positioning during adipocyte differentiation.** *J Cell Sci* 2004, **117:**5897-5903.
32. Kim SH, McQueen PG, Lichtman MK, Shevach EM, Parada LA, Misteli T: **Spatial genome organization during T-cell differentiation.** *Cytogenet Genome Res* 2004, **105:**292-301.
33. Foster HA, Abeydeera LR, Griffin DK, Bridger JM: **Non-random chromosome positioning in mammalian sperm nuclei, with migration of the sex chromosomes during late spermatogenesis.** *J Cell Sci* 2005, **118:**1811-1820.
34. Hu Q, Kwon YS, Nunez E, Cardamone MD, Hutt KR, Ohgi KA, Garcia-Bassets I, Rose DW, Glass CK, Rosenfeld MG, Fu XD: **Enhancing nuclear receptor-induced transcription requires nuclear motor and LSD1-dependent gene networking in interchromatin granules.** *Proc Natl Acad Sci USA* 2008, **105:**19199-19204.
35. Bartova E, Kozubek S: **Nuclear architecture in the light of gene expression and cell differentiation studies.** *Biol Cell* 2006, **98:**323-336.
36. Bettinger BT, Gilbert DM, Amberg DC: **Actin up in the nucleus.** *Nat Rev Mol Cell Biol* 2004, **5:**410-415.
37. Fomproix N, Percipalle P: **An actin-myosin complex on actively transcribing genes.** *Exp Cell Res* 2004, **294:**140-148.
38. Grummt I: **Life on a planet of its own: regulation of RNA polymerase I transcription in the nucleolus.** *Genes Dev* 2003, **17:**1691-1702.
39. Pestic-Dragovich L, Stojiljkovic L, Philimonenko AA, Nowak G, Ke Y, Settlage RE, Shabanowitz J, Hunt DF, Hozak P, de Lanerolle P: **A myosin I isoform in the nucleus.** *Science* 2000, **290:**337-341.
40. Philimonenko VV, Zhao J, Iben S, Dingova H, Kysela K, Kahle M, Zentgraf H, Hofmann WA, de Lanerolle P, Hozak P, Grummt I: **Nuclear actin and myosin I are required for RNA polymerase I transcription.** *Nat Cell Biol* 2004, **6:**1165-1172.
41. Vreugde S, Ferrai C, Miluzio A, Hauben E, Marchisio PC, Crippa MP, Bussi M, Biffo S: **Nuclear myosin VI enhances RNA polymerase II-dependent transcription.** *Mol Cell* 2006, **23:**749-755.
42. Hofmann WA, Johnson T, Klapczynski M, Fan JL, de Lanerolle P: **From transcription to transport: emerging roles for nuclear myosin I.** *Biochem Cell Biol* 2006, **84:**418-426.
43. Dundr M, Ospina JK, Sung MH, John S, Upender M, Ried T, Hager GL, Matera AG: **Actin-dependent intranuclear repositioning of an active gene locus in vivo.** *J Cell Biol* 2007, **179:**1095-1103.
44. Chuang CH, Carpenter AE, Fuchsova B, Johnson T, de Lanerolle P, Belmont AS: **Long-range directional movement of an interphase chromosome site.** *Curr Biol* 2006, **16:**825-831.
45. Cavellan E, Asp P, Percipalle P, Farrants AK: **The WSTF-SNF2h chromatin remodeling complex interacts with several nuclear proteins in transcription.** *J Biol Chem* 2006, **281:**16264-16271.

46. Guelen L, Pagie L, Brasset E, Meuleman W, Faza MB, Talhout W, Eussen BH, de Klein A, Wessels L, de Laat W, van Steensel B: **Domain organization of human chromosomes revealed by mapping of nuclear lamina interactions.** *Nature* 2008, **453:**948-951.
47. Bridger JM, Kill IR, Lichter P: **Association of pKi-67 with satellite DNA of the human genome in early G_1 cells.** *Chromosome Res* 1998, **6:**13-24.
48. Bridger JM, Herrmann H, Munkel C, Lichter P: **Identification of an interchromosomal compartment by polymerization of nuclear-targeted vimentin.** *J Cell Sci* 1998, **111:**1241-1253.
49. Gillespie PG, Albanesi JP, Bahler M, Bement WM, Berg JS, Burgess DR, Burnside B, Cheney RE, Corey DP, Coudrier E, de Lanerolle P, Hammer JA, Hasson T, Holt JR, Hudspeth AJ, Ikebe M, Kendrick-Jones J, Korn ED, Li R, Mercer JA, Milligan RA, Mooseker MS, Ostap EM, Petit C, Pollard TD, Sellers JR, Soldati T, Titus MA: **Myosin-I nomenclature.** *J Cell Biol* 2001, **155:**703-704.
50. Holaska JM, Wilson KL: **Multiple roles for emerin: implications for Emery-Dreifuss muscular dystrophy.** *Anat Rec A Discov Mol Cell Evol Biol* 2006, **288:**676-680.
51. Percipalle P, Fomproix N, Cavellan E, Voit R, Reimer G, Kruger T, Thyberg J, Scheer U, Grummt I, Farrants AK: **The chromatin remodelling complex WSTF-SNF2h interacts with nuclear myosin 1 and has a role in RNA polymerase I transcription.** *EMBO Rep* 2006, **7:**525-530.
52. Bridger JM, Foeger N, Kill IR, Herrmann H: **The nuclear lamina: both a structural framework and a platform for genome organization.** *FEBS J* 2007, **274:**1354-1361.
53. Mehta IS, Figgitt M, Clements CS, Kill IR, Bridger JM: **Alterations to nuclear architecture and genome behavior in senescent cells.** *Ann N Y Acad Sci* 2007, **1100:**250-263.
54. Sanger JW, Sanger JM, Kreis TE, Jockusch BM: **Reversible translocation of cytoplasmic actin into the nucleus caused by dimethyl sulfoxide.** *Proc Natl Acad Sci USA* 1980, **77:**5268-5272.
55. Starr DA: **A nuclear-envelope bridge positions nuclei and moves chromosomes.** *J Cell Sci* 2009, **122:**577-586.
56. Haque F, Lloyd DJ, Smallwood DT, Dent CL, Shanahan CM, Fry AM, Trembath RC, Shackleton S: **SUN1 interacts with nuclear lamin A and cytoplasmic nesprins to provide a physical connection between the nuclear lamina and the cytoskeleton.** *Mol Cell Biol* 2006, **26:**3738-3751.
57. Mehta IS, Elcock LS, Amira M, Kill IR, Bridger JM: **Nuclear motors and nuclear structures containing A-type lamins and emerin: Is there a functional link?** *Biochem Soc Trans* 2008, **36:**1384-1388.
58. Bridger JM, Kill IR, O'Farrell M, Hutchison CJ: **Internal lamin structures within G_1 nuclei of human dermal fibroblasts.** *J Cell Sci* 1993, **104:**297-306.
59. Senol M, Ozerol IH, Patel AV, Skoner DP: **The effect of Na+-K+ ATPase inhibition by ouabain on histamine release from human cutaneous mast cells.** *Mol Cell Biochem* 2007, **294:**25-29.
60. Moriya M, Linder MC: **Vesicular transport and apotransferrin in intestinal iron absorption, as shown in the Caco-2 cell model.** *Am J Physiol Gastrointest Liver Physiol* 2006, **290:**G301-G309.
61. Soltoff SP: **Evidence that tyrphostins AG10 and AG18 are mitochondrial uncouplers that alter phosphorylation-dependent cell signaling.** *J Biol Chem* 2004, **279:**10910-10918.
62. Munter S, Enninga J, Vazquez-Martinez R, Delbarre E, David-Watine B, Nehrbass U, Shorte SL: **Actin polymerisation at the cytoplasmic face of eukaryotic nuclei.** *BMC Cell Biol* 2006, **7:**23.
63. Schoenenberger CA, Buchmeier S, Boerries M, Sutterlin R, Aebi U, Jockusch BM: **Conformation-specific antibodies reveal distinct actin structures in the nucleus and the cytoplasm.** *J Struct Biol* 2005, **152:**157-168.
64. Laudadio RE, Millet EJ, Fabry B, An SS, Butler JP, Fredberg JJ: **Rat airway smooth muscle cell during actin modulation: rheology and glassy dynamics.** *Am J Physiol Cell Physiol* 2005, **289:**C1388-C1395.
65. Cramer LP, Mitchison TJ: **Myosin is involved in postmitotic cell spreading.** *J Cell Biol* 1995, **131:**179-189.
66. Fabian L, Troscianczuk J, Forer A: **Calyculin A, an enhancer of myosin, speeds up anaphase chromosome movement.** *Cell Chromosome* 2007, **6:**1.
67. Soeno Y, Shimada Y, Obinata T: **BDM (2,3-butanedione monoxime), an inhibitor of myosin-actin interaction, suppresses myofibrillogenesis in skeletal muscle cells in culture.** *Cell Tissue Res* 1999, **295:**307-316.
68. McDonald D, Carrero G, Andrin C, de Vries G, Hendzel MJ: **Nucleoplasmic beta-actin exists in a dynamic equilibrium between low-mobility polymeric species and rapidly diffusing populations.** *J Cell Biol* 2006, **172:**541-552.
69. Telenius H, Pelmear AH, Tunnacliffe A, Carter NP, Behmel A, Ferguson-Smith MA, Nordenskjold M, Pfragner R, Ponder BA: **Cytogenetic analysis by chromosome painting using DOP-PCR amplified flow-sorted chromosomes.** *Genes Chromosomes Cancer* 1992, **4:**257-263.

doi: 10.1186/gb-2010-11-1-r5
Cite this article as: Mehta *et al.*, Rapid chromosome territory relocation by nuclear motor activity in response to serum removal in primary human fibroblasts *Genome Biology* 2010, **11**:R5